

Joint mAsTer of Mediterranean Initiatives on renewabLe and sustainAble energy

Palestine Polytechnic University

Deanship of Graduate Studies and Scientific Research

Master Program of Renewable Energy and Sustainability

Assessment, Modeling, Simulation and Integration of Medium Temperature CSP With Food Processing Factory: Al Qasrawy Co. For Industries and Trading

By

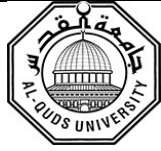
Majed Yousef Mohamad Sayed Ahmad

Supervisor

Dr. Khaled Tamizi

*Thesis submitted in partial fulfillment of requirements of the degree
Master of Science in Renewable Energy & Sustainability*

January, 2021



Joint mAsTer of Mediterranean Initiatives on renewabLe and sustainAble energy

The undersigned hereby certify that they have read, examined and recommended to the Deanship of Graduate Studies and Scientific Research at Palestine Polytechnic University and the Faculty of Science at Al-Quds University the approval of a thesis entitled:

**Assessment, Modeling, Simulation and Integration of Medium Temperature CSP
With Food Processing Factory: Al Qasrawy Co.**

Submitted by

Majed Yousef Mohamad Sayed Ahmad

in partial fulfillment of the requirements for the degree of Master in Renewable Energy & Sustainability.

Graduate Advisory Committee:

Prof./Dr.,

(Supervisor), University (typed)

Signature: _____

Date: _____

Prof./ Dr.,

(Co-supervisor), University (typed)

Signature: _____

Date: _____

Prof./Dr.....

(Internal committee member), University (typed).

Signature: _____

Date: _____

Prof./Dr.,

(External committee member), University (typed).

Signature: _____

Date: _____

Thesis Approved by:

Name: _____

Name: _____

Dean of Graduate Studies & Scientific Research
Palestine Polytechnic University

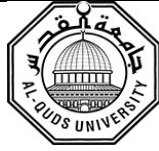
Dean of Faculty of Graduate Studies
Al-Quds University

Signature:.....

Signature:.....

Date:.....

Date:.....



Assessment, Modeling, Simulation and Integration of Medium Temperature CSP With Food Processing Factory: Al Qasrawy Co.

Submitted by

Majed Yousef Mohamad Sayed Ahmad

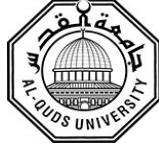
The state of Palestine is a developing occupied country, with a plentiful of renewable energy resources, solar irradiation reaches to $5.4 \text{ kWh/m}^2 \cdot \text{day}$, sun hours 3000 yearly, wind reach an average of 6 m/s in some locations (Ouda, 2001). which gives strong indication about the potentials of energy amounts that can be harvested annually.

The aim of this thesis is to create a reliable estimation of the thermal energy being consumed in an industrial facility that produces beverage and snacks, namely AlQasrawi Company for Industries and Trading. The methodology used is based on the thermodynamics first and second laws. The production sections were studied and the thermal loads that are being consumed were evaluated, the accumulative load required is $270 \text{ kW}_{\text{th}}$.

The solar potential in the area of the factory was studied, based on that selection of the suitable solar thermal collector is chosen to be LF-11 from Solar Industries, a German brand. An integration between the solar collector and the plant production section was studied based on the load profile of the factory. The above main three objectives were simulated using Matlab (MATLAB, 2015), to test the effects of different system sizes on the economic parameters.

In addition to the above, the economic analysis and environmental impacts for using solar thermal energy compared to the traditional power sources that is being used in the facility currently was carried out, and a levelized Cost Of Energy LCOE was in the range of $0.15\text{-}0.2 \text{ NIS/kWh}$. The Payback Period on discounted bases was calculated and found to range from 4-7 years.

Keywords: Solar Heating Industrial Process SHIP, Energy Intensity, Unit Operation, Heat Transfer Fluid HTF, Thermal Storage TS, Concentrated Solar Power CSP, Linear Fresnel LF, Levelized Cost Of Energy LCOE, Discounted PayBack Period DPBP.



تقييم، نمذجة، محاكاة وتكامل الطاقة الشمسية المركزة ذات درجة الحرارة المتوسطة مع مصنع تجهيز الأغذية: شركة القصر اوي

عمل الطالب

ماجد يوسف محمد سيد احمد

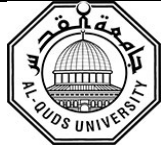
تعتبر فلسطين دولة تحت الاحتلال في طور التطور، تتمتع بمناطقها بوفرة من الإشعاع الشمسي يصل الى 5.4 كيلو واط/متر مربع في اليوم، مع ساعات اشعاع شمسي يصل الى 3000 ساعة في السنة، ومعدل سرعة رياح يصل الى 6 متر/ث في بعض المناطق، مما يعطي مؤشرا قويا على إمكانية الطاقة الممكن حصادها خلال السنة.

الهدف من رسالة الماجستير هذه هو عمل تقييم موثوق للأحمال الحرارية المستهلكة من قبل عمليات التصنيع في مصنع مرطبات وتسالي، تحديدا شركة القصر اوي للصناعة والتجارة. مع إمكانية استبدال النظام التقليدي المزود للحرارة بنظام شمسي من الألواح المركزة. تعتمد منهجية العمل في تقييم الاحمال المستهلكة على القانون الأول والثاني في الديناميكا الحرارية، وقد تم حساب هذه القيم ووجد انها مجتمعه للمصنع كاملا تصل الى 270 كيلو واط حراري.

لقد تم أيضا دراسة الطاقة الشمسية المتاحة في منطقة المصنع، وتم اختيار التكنولوجيا المناسبة من الألواح الشمسية المركزة من نوع LF-11 from Solar Industries الألمانية. بعد دراسة نمط الاحمال الحرارية اليومية في المصنع تم وضع تصور لطريقة الربط بين المحطة الشمسية والأنظمة المزودة للحرارة الحالية في المصنع.

لقد تم محاكاة الخطوات السابقة باستخدام برنامج ماتلاب الإصدار 2015، حيث تم بحث تأثير حجم النظام واجزاءه على بعض المؤشرات الاقتصادية الأولية. حيث وجد ان سعر الطاقة الممكن الحصول عليها من النظام مقارنة بالطاقة الكهربائية يتراوح بين 0.15-0.2 شيكل/كيلو واط.ساعة، وكانت فترة الاسترداد للمشروع تتراوح بين 4-7 سنوات اخذين بعين الاعتبار تناقص القيمة المالية عبر السنوات.

الكلمات المفتاحية: الحرارة الشمسية في العمليات الصناعية، كثافة الطاقة، وحدة العمليات، السائل الناقل للحرارة، التخزين الحراري، الطاقة الشمسية المركزة، المرايا المسطحة الخطية، سعر الطاقة مقارنة بسعر الطاقة الكهربائية، فترة الاسترداد للمشروع تحت تأثير عوامل تناقص قيمة العملة عبر فترة المشروع .



Joint mAster of Mediterranean Initiatives on renewabLe and sustainAble energy

DECLARATION

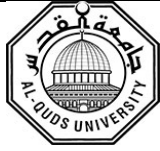
I declare that the Master Thesis entitled “ **Assessment, Modeling, Simulation and Integration of Medium Temperature CSP With Food Processing Factory: Al Qasrawy Co. For Industries and Trading.**

” is my own original work, and herby certify that unless stated, all work contained within this thesis is my own independent research and has not been submitted for the award of any other degree at any institution, except where due acknowledgement is made in the text.

Student Name Majed Yousef Mohamad Sayed Ahmad

Signature: _____

Date: _____



Joint mASter of Mediterranean Initiatives on renewabLe and sustainAble energy

STATEMENT OF PERMISSION TO USE

In presenting this thesis in partial fulfillment of the requirements for the joint Master's degree in Renewable Energy & Sustainability at Palestine Polytechnic University and Al-Quds University, I agree that the library shall make it available to borrowers under rules of the library.

Brief quotations from this thesis are allowable without special permission, provided that accurate acknowledgement of the source is made.

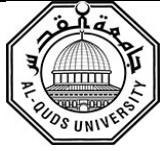
Permission for extensive quotation from, reproduction, or publication of this thesis may be granted by my main supervisor, or in [his/her] absence, by the Dean of Graduate Studies and Scientific Research [or Dean of Faculty of Graduate Studies] when, in the opinion of either, the proposed use of the material is for scholarly purposes.

Any copying or use of the material in this thesis for financial gain shall not be allowed without my written permission.

Student Name: Majed Yousef Mohamad Sayed Ahmad

Signature: _____

Date: _____



Joint mAsTer of Mediterranean Initiatives on renewabLe and sustainAble energy

DEDICATION

To...

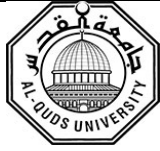
MY PARENTS

MY WIFE & KIDS

MY FAMILY

MY FRIENDS AND COLLEAGUES

Thank You...



Joint mAster of Mediterranean Initiatives on renewabLe and sustainAble energy

ACKNOWLEDGEMENT

I would like to thank

My Supervisor **Dr. Khaled Tamizi** for his support and guidance throughout the thesis expedition which enabled the dream come true....

JAMILA Master Program supervisor **Prof. Sameer Khader** for his care and dedication during the past two years that qualified me to reach this moment...

All Professors and Instructors in **Palestine Polytechnic University and Al- Quds University** who pushed us to our maximum limits....

AL QASRAWI COMPANY FOR INDUSTRIES AND TRADING

for opening their doors, and facilitating the accomplishment of this thesis.... Wishing them a prosperous future...

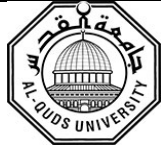


Table of Content

Chapter-1	Introduction	1
1.1	Geographical and energy statistics in Palestine	1
1.2	Literature Review.....	4
1.2.1	Current State of Heat Consumption in Industrial Sector Worldwide.....	5
1.2.2	State of Art Technology	7
1.2.3	Similar Studies.....	10
Chapter-2	Problem and Framework of the Thesis.....	12
2.1	Problem description	12
2.2	Objectives	13
2.3	Methodology	13
2.4	Time table	15
Chapter-3	Thermal Load Assessment Case Study; Al Qasrawi Factory.....	16
3.1	Introduction.....	16
3.2	Modeling of energy requirements in the Besly frying section.....	18
3.2.1	Energy in the solid content	20
3.2.2	Energy to evaporate the water	21
3.2.3	Energy in the evaporated oil.....	23
3.2.4	Energy released due to air flow	23
3.2.5	Energy released by heat transfer.....	24
3.2.6	Total energy required by the fryer.....	24

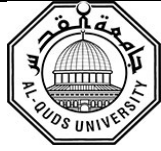


3.3	The energy required by the raw material section	25
3.3.1	Introduction	25
3.3.2	Energy required to evaporate the water in first station.....	27
3.3.3	Energy consumed by solid flour.....	28
3.3.4	Heat consumed to evaporate water in first dryer	28
3.3.5	Heat to exhaust air	29
3.3.6	The energy transfer through walls of dryer	29
3.4	Energy consumed by second drying station.....	30
3.4.1	Energy consumed by solid flour.....	31
3.4.2	Heat consumed to evaporate water in second dryer	31
3.4.3	Heat to exhaust air	32
3.4.4	The energy transfer through walls of dryer	32
3.5	Energy required in the general frying section	33
3.5.1	Energy in the solid content	34
3.5.2	Energy to evaporate the water	35
3.5.3	Energy in the evaporated oil.....	37
3.5.4	Energy released due to air flow	37
3.5.5	Energy released by heat transfer.....	38
3.5.6	Total energy required by the fryer.....	38
3.6	Energy required in the corn chips section	38
3.6.1	Energy required to evaporate the water	40



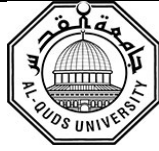
Joint mAster of Mediterranean Initiatives on renewabLe and sustainAble energy

3.6.2	Energy consumed by air	40
3.6.3	Energy consumed by flour and oil during drying operation.....	41
3.6.4	The energy transfer through walls of dryer	41
3.7	Summarization of thermal power needed in each section.....	42
Chapter-4	Consternated Solar Power (CSP) Analysis.....	43
4.1	Introduction.....	43
4.2	Solar potential in the factory location	43
4.3	Solar thermal collector selection.....	48
4.4	Simulation of the solar collector	59
Chapter-5	Integration of Solar Plant with Factory Thermal Loads	63
5.1	Solar collector LF-11 surface area	63
5.2	Integration scheme	67
5.3	The Thermal Storage tank size.....	71
Chapter-6	Economic Analysis and Environmental Impacts.....	75
Chapter-7	Conclusion and Future Recommendations	85
References.....		86
Appendix A.....		1
Appendix B.....		2



List of Abbreviations

a	Discount Rate
CSP	Concentrated Solar Power
DPBP	Discounted PayBack Period
EE	Energy Efficiency
EPA	Environmental Protection Agency
GDP	Gross Domestic Product
GHG	Green House Gases
GHGRP	Greenhouse Gas Reporting Program
HTF	Heat Transfer Fluid
IEA	International Energy Agency
inr	Inflation Rate
ir	Interest Rate
IRR	Internal Rate of Return
LCOE	Levelized Cost Of Energy
LF	Linear Fresnel
NPV	Net Present Value
O&M	Operations and Maintenance
P.V	Photo Voltaic
PT	Parabolic Trough
rr	Risk Rate
SHC	Solar Heating and Cooling
SHIP	Solar Heat in Industrial Processes
STC	Solar Thermal Collector
TS	Thermal Storage



List of Figures

Figure 1-1 Energy Intensity distribution around the world.....	2
Figure 1-2 Global Horizontal Irradiation.....	5
Figure 1-3 Total global energy consumption for heat (left) in 2015 and modern renewable	7
Figure 1-4 Stationary and tracking solar collector technologies related to operation temperature and process temperature range in different industrial branches.....	9
Figure 2-1 Thesis Schedule.....	15
Figure 3-1 Schematic diagram of general process flow in Al Qasrawi factory	17
Figure 3-2 Process diagram- Deep Frying; Besly chips	18
Figure 3-3 Mass flow and energy flow diagram- frying station	19
Figure 3-4 Drying section process flow diagram.....	25
Figure 3-5 Multi pass drying machine	26
Figure 3-6 A typical cross section of dryer, air circulation.....	27
Figure 3-7 First drying station energy and mass flow	28
Figure 3-8 Second drying station energy and mass flow	31
Figure 3-9 General chips frying station	34
Figure 3-10 Corn ships buffing section.....	39
Figure 4-1 Al Qasrawi Factory location map.....	44
Figure 4-2 The incidence angle θ between a normal to the collector face and the incoming solar beam radiation.....	45
Figure 4-3 Illustrating the collector azimuth angle ϕ_C and tilt angle Σ along with the solar azimuth angle ϕ_S and altitude angle β	46
Figure 4-4 Sun path diagram from a) PVSyst software b) for the facility location	47
Figure 4-5 I_B that reach earth surface over a year	47
Figure 4-6 Beam radiation on horizontal surface collector.....	48

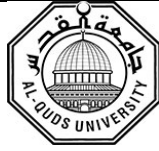


Figure 4-7 PTC 1800 50

Figure 4-8 LF-11 module..... 50

Figure 4-9 Industrial Solar LF-11 working principle..... 52

Figure 4-10 Extraterrestrial solar radiation for $\Sigma = 45^\circ$ on a stationary collector at $L = 45^\circ$ on north-south (N-S) and east-west (E-W) single-axis tracking collectors. The three dotted curves are for the winter solstice and the three solid curves are for the summer solstice..... 53

Figure 4-11 Zenith angle θ_z related to sun altitude angle α_s , 54

Figure 4-12 beam irradiation that can be harvested by single axis tracking CSP 55

Figure 4-13 Angles associated with the optical performance of the LFR technology, including transversal incidence θ_T , longitudinal incidence θ_L , solar zenith θ_z , and solar azimuth γ_s 56

Figure 4-14 Characteristic collector curve..... 57

Figure 4-15 Beam irradiation comparison based on the collector technology used 60

Figure 4-16 Efficiency of flat plate collector at mean temperatur of 150°C 60

Figure 4-17 Heat gain relevant to available heat over a year :a)Fixed solar collector b) Single axis tracking CSP 61

Figure 4-18 Comparison between technology in terms of efficiency 62

Figure 5-1 Hourly load profile of plant sections (a) Summer profile (b) winter profile..... 64

Figure 5-2 LF-11 module size, (1) supporting structure, (2) primary reflector, (3) receiver, consisting of secondary reflectors..... 65

Figure 5-3 Comparison of load profile and 2 standard LF-11 modules (area of 1080 m^2) heat gain in day= 180 (summer) and day = 355 (winter) 66

Figure 5-4 Difference between load demands of the factory and LF-11 standard modules heat gained over a year 67

Figure 5-5 Percentage of load satisfaction by the chosen LF-11 area over the year course 67

Figure 5-6 Possible integration points for solar heat, A is for supply level, B for process level... 68

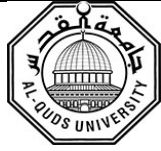
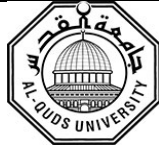


Figure 5-7 SHIP system for pre-heating with five subsections supplying an industrial heat consumer. The integration concept exemplary shown is PL_E_PM, i.e. on process level an external heat exchanger heats a process medium 69

Figure 5-8 Integration scheme depending on processes in the factory and the traditional heat sources. 71

Figure 6-1 Daily useful energy for area 975 m² and tank size 1.88..... 78



List of Tables

Table 1-1 Selected Energy Performance Indicators in Palestine, 2014-2017	2
Table 1-2 Energy Balance of Palestine in Physical Units, 2017	3
Table 1-3 Potential energy savings in GWh	4
Table 1-4 Thermal energy conversion technologies	6
Table 2-1 Production sections that utilise thermal loads in the studied factory.....	13
Table 3-1 Parameters used to evaluate the energy required for frying of Besly chips	20
Table 3-2 Summarization of thermal load from plant production sections	42
Table 4-1 Summary of clear-sky solar insolation terminology.....	44
Table 4-2 Incidence angle modifier for LF-11 module.....	58
Table 4-3 Prescribed conditions for testing of LF-11	58
Table 4-4 Average ambient temperature.....	59
Table 5-1 Comparison between the load power and heat gain in day 55	72
Table 5-2 Comparison between the load power and heat gain in day 255	73
Table 6-1 parameters values used in the eq. 6-1 to eq. 6-6.....	79
Table 6-2 The simulation results for different LF_11 areas and TS sizes, DPBP: Discounted Pay-Back Period, S.F: Solar Fraction.....	80
Table 6-3 Approximate Investment cost for selected system 975m ² and tank size factor 1.88, reference to overall system configuration.....	81
Table 6-4 Variables values used in eq. 6-7	83

Chapter-1

Introduction

1.1 Geographical and energy statistics in Palestine

The energy in Palestine is a critical issue. The energy intensity (amount of energy needed to produce one Gross Domestic Product GDP) is about 5.7 MJ/\$ (PCBS, 2017). It is considered relatively high when compared to Europe with 3.7 MJ/\$ (Intensity, 2018). See Figure 1-1 (countryeconomy.com, 2018) for the GDP distribution around the world. Adding to this the fact that 90% of final energy supply is being imported (PCBS, 2017). This will increase the prices of final products compared to neighboring countries eventually leading to low investments.

The energy that is consumed by the industrial sector in Palestine relevant to another sector is about 5.4%. It is given in general without segregation up to the end use by the activity, see

Table 1-1 (PCBS, 2017).

However, the (PCBS, 2017) data gives a value for the consumption of the industrial sector in general relevant to the type of consumed fuel, Table 1-2. With simple calculation according to the prices of fuel also provided by (PCBS, 2017), the estimated average cost of energy is 538M NIS/year.

According to statistics (PCBS, 2017), there is a rapid increase in the electric energy demand in all forms. Electricity demand increase is about 24% between 2010-2017.

From another perspective, a study was conducted by (PENRA, 2012) aimed at “promotion of energy efficiency & renewable energy in strategic sectors in Palestine”. The overall target for the national plan is to achieve cumulative electric energy savings of 384 GWh between 2012 and 2020, with individual goals for three phases among three main energy consuming sectors as shown in

Table 1-3

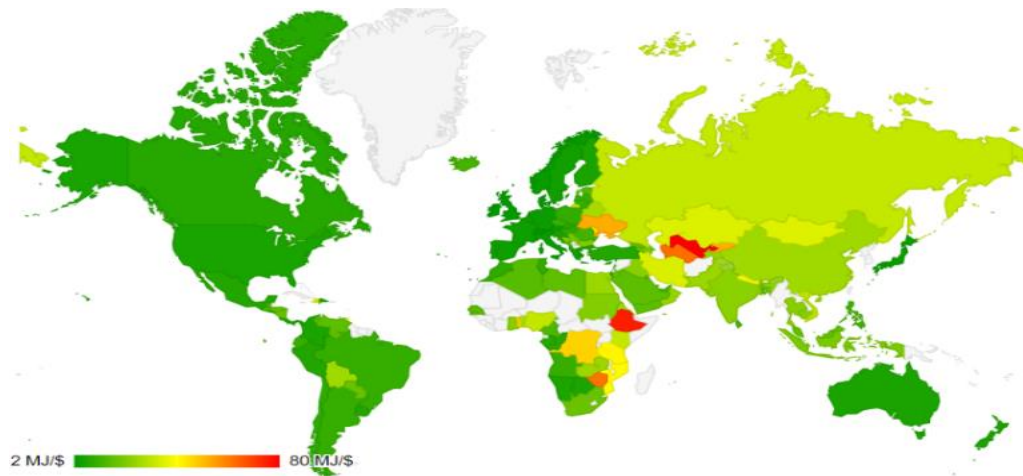


Figure 1-1 Energy Intensity distribution around the world

The focus of this thesis is to evaluate the thermal loads in the AlQasrawi Company for Industries and Trading, with proper definition of the thermal needs of each section within the plant. In addition to that, simulation for the facility while utilizing proper ‘Solar Heat in Industrial Process’ SHIP technology is going to be done, including integration structure between the sections and the Solar Thermal Collector STC.

Table 1-1 Selected Energy Performance Indicators in Palestine, 2014-2017

Indicator	Year			
	2014	2015	2016	2017
Renewable energy share in the total final energy consumption (%)	13.3	13.2	12.9	9.7
Energy Dependency Rate (%)	80.3	84.8	84.7	87.3
The Energy Consumption of the Transport Sector to the total Energy Consumption (%)	48.7	43.6	45.6	46.6
The Energy Consumption of the Household Sector to the total Energy Consumption (%)	38.4	41.4	39.7	38.4
The Energy Consumption of the Service Sector to the total Energy Consumption (%)	7.6	8.5	8.8	8.8
The Energy Consumption of the Industry Sector to the total Energy Consumption (%)	4.2	5.2	4.8	5.4
Energy Intensity (MJ/USD)	5.8	5.9	6.0	5.7
Annual Electricity Consumption Per Capita (kWh/Capita)	1,048.0	1,151.4	1,141.9	1,138.3

Table 1-2 Energy Balance of Palestine in Physical Units, 2017

Consumed by Industry	Total energy supply	Exports	Imports	Primary production	Energy Products
-	1,564,532	-	-	1,564,532	Solar Energy (MWh)
6,770	217,842	530	3,407	214,965	Wood and Charcoal (Ton)
8,780	35,120	-	-	35,120	Olive Cake (Ton)
-	23,583	-	23,583	-	Bitumen (Ton)
-	1,469	85	1,554	-	Oils and Lubricants (Ton)
12,248	189,537	-	189,537	-	LPG (Tons)
2,719	5,440	-	5,440	-	Fuel Oil (1000 Liter)
126	1,391	-	1,391	-	Kerosene (1000 Liters)
476	314,765	-	314,765	-	Gasoline (1000 Liters)
9,514	730,645	-	730,645	-	Diesel (1000 Liters)
647,988	5,621,864	-	5,576,864	45,000	Electricity (MWh)

Table 1-3 Potential energy savings in GWh

Sector	Phase I 2012-2014	Phase II 2015-2017	Phase III 2018-2020	Total Energy savings
Industrial	5	6	8	19
Buildings	38	130	195	363
Water Pumping	-	1	1	2
Total	43	17	204	384

1.2 Literature Review

Several researchers over the last 15 years have presented the solar energy potential in Palestine. There is a report (Bank., 2016), that is focused on Energy Efficiency EE usage rather than satisfying demands from additional resources. However, it is targeted toward the electricity as part of the energy mix and studied only on the residential sector, as 60% of electricity is being consumed in that sector. The aim of the report is to set targets for 2020-2030 timeframe, and gave recommendations about how it can be achieved.

Another study (Palestinian Environmental NGOs Network, 2016), is directed toward studying the electric energy generation from solar energy P.V. The frame of this study is in the theoretical picture, i.e., how much is possible to produce under current metrological position of Palestine (Temperature, humidity, wind and sky clearance effects on the P.V performance).

(Juaidi *et al.*, 2016), presented the potential of renewable energy resources in Palestine under current conditions. The conclusion is that due to 3000 sun hours/ year, and irradiation of 5.4 kWh/m².day, in addition to the wide spread of rural areas, it would be favorable to use Photo Voltaic PV technology to produce electricity. Especially if it is combined with wind technologies as a hybrid energy producing system. The study also pointed out to the wide spread of solar collectors to satisfy domestic water heating, which is about 62% (PCBS, 2017) of total population in west bank. However, 50% of this number is not used. Hence the people depend on other forms of energy to heat the water like electricity and gas, mainly.

Comparing this amount of energy to global picture Figure 1-2, it is noticed that Palestine has huge solar potential compared to other countries around the world(*Global Solar Atlas, 2019*)

In a recent review study of the solar energy prospects in Palestine (Ajjlouni and Alsamamra, 2019), the researcher presented the situation about the possibilities of the solar energy according to several studies reviewed. And gave recommendations toward using the solar thermal energy to produce power in areas like Jordan valley where PV technology efficiency is affected by high temperatures. Furthermore, the researcher recommended presenting more advance researches that utilize heating and cooling for space requirements and industrial processes needs.

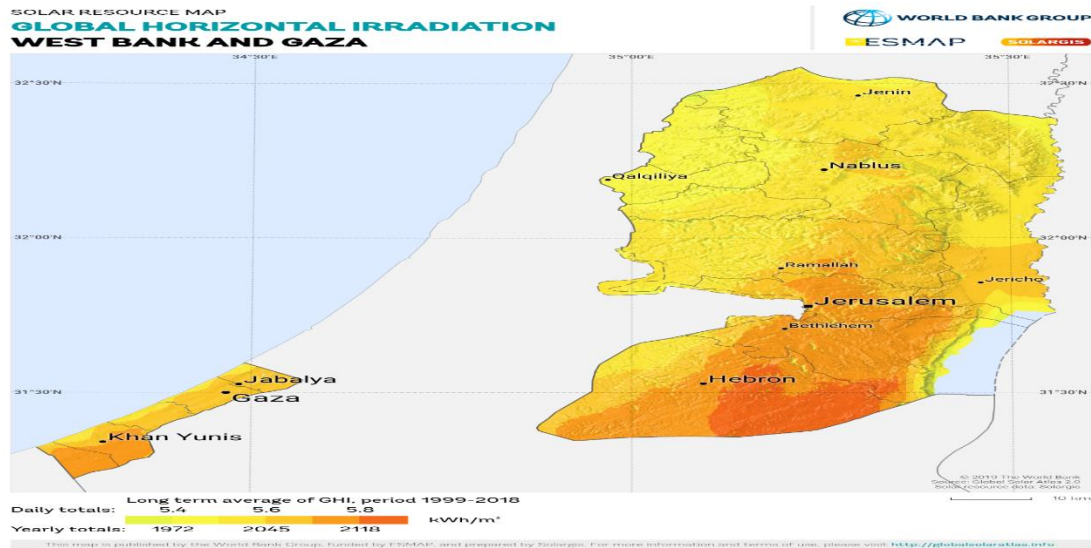


Figure 1-2 Global Horizontal Irradiation

1.2.1 Current State of Heat Consumption in Industrial Sector Worldwide

In terms of the heat generation in the industrial sector, the conventional systems are widely spreaded. The main factor that affects the design of such systems is the Heat Transfer Fluid HTF (e.g., thermal oil, superheated steam, saturated steam, pressurized hot water, air). “The primary

energy source depends on the access of the country to the fuel type. For example, India uses biomass, while USA uses Liquefied Petroleum Gas LPG, and other countries use coal”. See Table 1-4 (Ben Hassine *et al.*, 2014).

Table 1-4 Thermal energy conversion technologies

Conversion Technology	Fuel	Heat Transfer Fluid
Boiler	Gas, LPG, oil, coal, biomass, biogas (also in combination with natural gas)	Steam, hot water, thermal oil
Cogeneration systems	Gas, LPG, oil, coal, biomass, biogas (also in combination with natural gas)	Steam, hot water, thermal oil
Burner	Gas, LPG, oil, coal, biomass, biogas (also in combination with natural gas)	Hot air
Heat pump	Electricity	Hot water, hot air, thermal oil

SHIP is not widely spreaded, with only 160 operating solar thermal systems for process heat are reported worldwide (as of 2015). A total capacity of about 100 MWth (140,600 m²) (Schmitt *et al.*, 2015).

“The global Heat accounts for more than 50% of total final energy consumption but is mostly produced by fossil fuels Figure 1-3. In 2015, renewable heat consumption represented 9% of total global heat consumption and reached 18.5 EJ.

Over 2008-15, global renewable heat consumption increased by 20% from 15.4 EJ to 18.5 EJ Figure 1-3, Solar thermal grew fastest and doubled from 0.5 EJ to 1.2 EJ, reaching 7% of renewable heat consumption in 2015” (*Market Report Series Renewables 2017, Analysis and forecasts to 2022*, 2017).

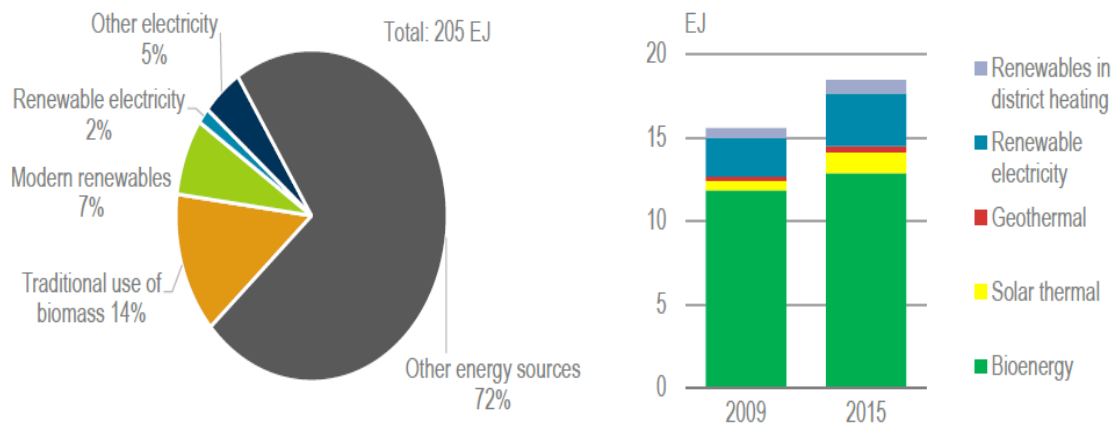


Figure 1-3 Total global energy consumption for heat (left) in 2015 and modern renewable

A world online database was developed by (AEE- INTEC, 2019), that contains an overview on existing solar thermal plants which provides thermal energy for production processes for different industry sectors. Each plant description contains a number of information about e.g. the size of the collector field, collector technology or integration point in the production process.

1.2.2 State of Art Technology

To be able to study the SHIP, it is essential to have knowledge about temperature levels in the process as this will facilitate the selection of proper technology Figure 1-4 (Horta, 2016)

Worldwide, in 1977, 22 countries initiated a multilateral agreement by establishing The Solar Heating and Cooling SHC Technology Collaboration Program, under the umbrella of International Energy Agency IEA. The IEA SHC mission was “To enhance collective knowledge and application of solar heating and cooling through international collaboration to reach the goal set in the vision of solar thermal energy meeting 50% of low temperature heating and cooling demand by 2050”.(Horta, 2016)

The members of IEA SHC agreed to perform “tasks” related to “research, development, demonstration, and test methods of solar thermal energy and solar buildings”. Task 49 is the one having Subtasks (IEA SHC || Task Publications, 2019):

Subtask A: Process heat collector development and process heat collector testing

Subtask B: Process integration and Process Intensification combined with solar process heat

Subtask C: Design Guidelines, Case Studies and Dissemination

This thesis will relay theoretically upon the technical fundamentals provided by this task 49 deliverables.

Finally, an old concept of unit of operation was introduced back in 1905 by Arthur D. Little. The basic idea of the concept is to classify operation steps with similar physical laws into one “unit operation” (Gavhane, 2014)

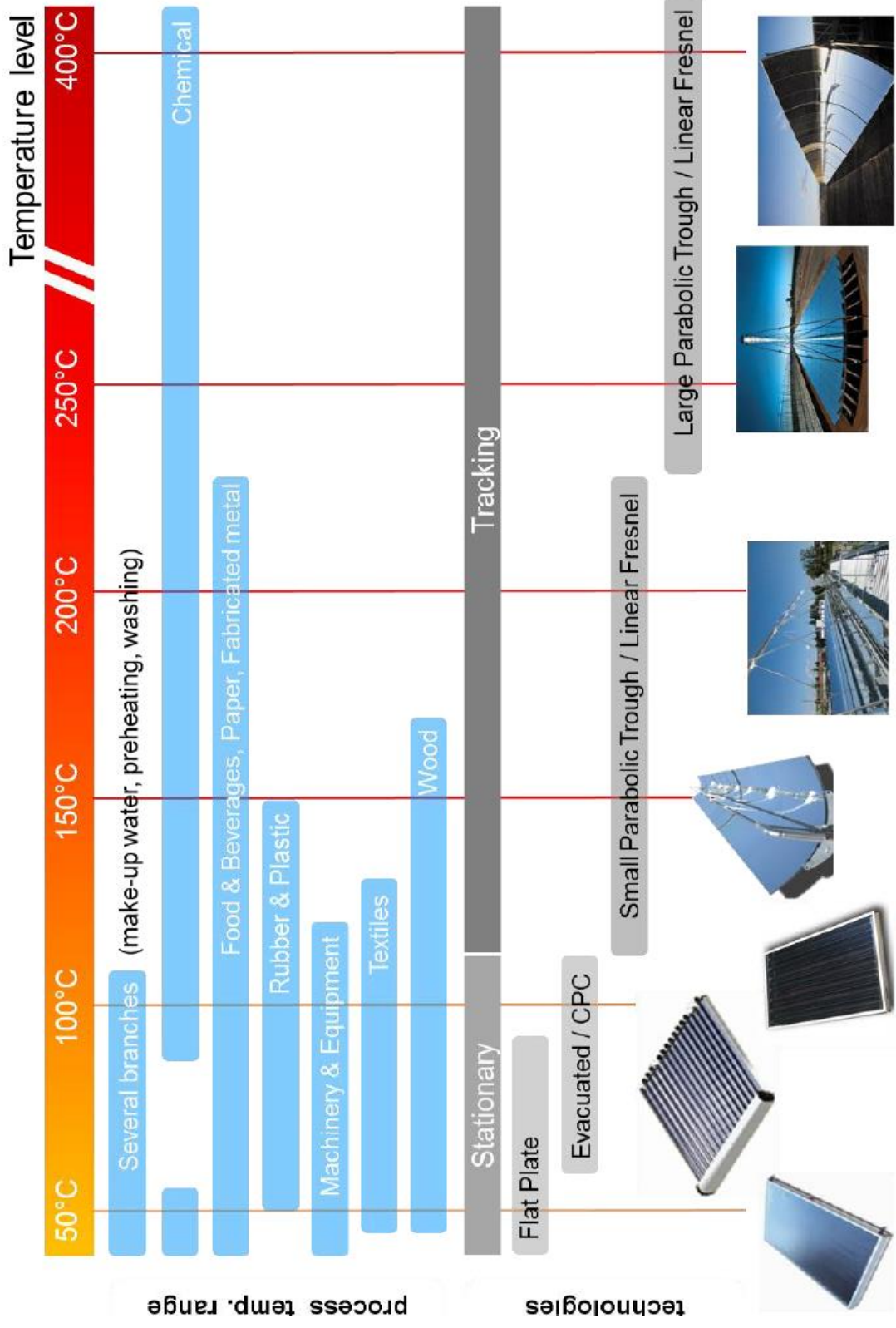


Figure 1-4 Stationary and tracking solar collector technologies related to operation temperature and process temperature range in different industrial branches

1.2.3 Similar Studies

The snacks industry that is going to be studied is classified under the Drying unit operation (Mujumdar and Hall, 2006a), the factory includes two sections that performs drying by conduction with hot oil which is named industrially as Frying, and another two sections that perform convection drying which is named industrially as Roasting or Drying.

According to (Mujumdar and Hall, 2006a), the model of the conveyor dryer is simple, however, modeling can never replace actual data, as the results of actual draying depends on many factors, like the surface area of the single pieces and water content in each piece hardening, product clumping, and product quality to name few. Nevertheless, conveyor dryer manufacturers depend on the simple modes to manufacture in addition to laboratory test results to specify the temperature limit that affect the quality of the produced products.

(Wu *et al.*, 2012) have modeled the energy flow using simple model equation relying on the first law of thermodynamics, he obtained an overall process efficiency of 70%, and gave recommendations for usage of exhaust gas in the gas burner as one suggestion to improve the process efficiency.

In order to simulate the sun path relative to latitude and longitude (Jazayeri, Uysal and Jazayeri, 2013) have developed a Simulink model that can track the sun at any hour of the year. In this thesis the M-file programming technique is used instead as it will be easier to link the tracking values to other thesis branches.

A similar study in Jordan was conducted by (Hiary, 2014), It estimated the technical potential to be 7.8% of the total thermal energy consumed in the industrial sector in 2012. A questionnaire and site visits were conducted, and a case study using linear Fresnel solar collector mounted in different orientations.

In 2016, (McMillan *et al.*, 2016) conducted a survey about the thermal energy consumption in the industrial sector in USA, the target was to estimate the Green House Gases. Relying on the mandatory regulations Greenhouse Gas Reporting Program (GHGRP), set by Environmental Protection Agency (EPA), they had initial estimate of factories that can be assessed, beside the environmental related figures, the study recommended the study of SHIP as alternated for some industries depending on the available area and location near HTF storage tanks.

Chapter-2

Problem and Framework of the Thesis

2.1 Problem description

After reviewing the literature and PCBS website, the thermal loads consumption across the industrial sector in Palestine is not available, and so, the possibility to introduce new green technologies to generate heat and examine the cost and environmental savings is not possible on a national level. In order to estimate such thermal energy consumption a questionnaire must be prepared and distributed, however, the frame of such a study and samples to be chosen are of unique type and assumptions. Due to the political situation and difficulties imposed on investment, facilities may have to have distributed locations, which would make decision to invest in SHIP very costly.

Adding to that the qualifications of the technical maintenance teams who could answer the questionnaire also forms an obstacle, as most of the big facilities are of the family type. The sensitivity parameters related to energy prices and its fluctuation can cause huge impacts on the decision wither to adopt or not the new green technology. All the previously mentioned challenges prevent the formation of such database, hence prevent investment on a national level.

However, investment on individual level can be done if proper feasibility studies are available, and so, this thesis comes to provide a technoeconomic study for a snacks production facility chosen- Al Qasrawi Company for Industries and Trading, which is one of leaders in the snacks industry market in Palestine.

The thesis will present the economic benefits that could result if the traditional power resources used in the factory are replaced with STC. To produce this outcome, the thermal loads in each section will be studied, the solar thermal potential that can be produced per square meters will be studied, and the integration between the process and the STC based on the load profile of the factory will be studied.

2.2 Objectives

The main objective is to present a case study for a real facility that uses heating processes. Assess the thermal loads in factory. Simulate the impacts of using SHIP technology. Discuss the different schemes of integration between the thermal loads and the SHIP and choosing the proper scheme. Finally, the environmental impacts saving, combined with economic benefits over the life of the project are calculated.

2.3 Methodology

The approach that is going to be followed to achieve the thesis objectives is as follows: initially, conducting field visits to locate the thermal load areas in the factory and get the initial data from factory in charge related to production capacity and load profile during the year on average, the factory includes many sections, production, packaging and loading, however, not all are utilizing thermal energy in its production process, and so, there are 4 main sections to be studied and to be modeled Table 2-1,

Table 2-1 Production sections that utilise thermal loads in the studied factory

<i>Production section</i>	<i>Production capacity (average / hours)</i>	<i>Working hours</i>
<i>Besly chips</i>	1250 kg/16H	07:00-24:00
<i>Raw chips general preparation</i>	6000 kg/16h	07:00-24:00
<i>General chip</i>	4800 kg/16h	07:00-24:00
<i>Corn chips</i>	1250 kg/16h	07:00-24:00

The study of the thermal load will consider only the steady state situation, applying the first and second laws of thermodynamics. If some data is not available from factory, it will be assumed based on similar studies and reference will be mentioned. The analysis will calculate the thermal loads based on production capacity, because the data related to gas and electrical consumption in

the factory are not released for this study by factory management. Secondly, the solar analysis modeling using numerical equations from literature will be conducted and simulated using (MATLAB, 2015), additionally, the results will be compared to a commercially proven software to verify it.

After that, the solar thermal collector selection must be done, in order to model the heat gain using equations from literature, upon that the simulation using (MATLAB, 2015) will be carried out. Fourthly, the integration structure between the production sections calculated thermal loads and the selected solar thermal collector will be discussed and recommended, as per International Energy Agency IEA recommendations for utilization of SHIP technology.

Finally, the economic analysis and environmental impacts will be discussed, with emphasis only on CO₂ gas avoidance results, as most of world studies focus on this type of gas as it is the most abundant heat trapping gas in the atmosphere and requires more time than other gases to convert to other forms naturally (Union of Concerned Scientists, 2017).

MATLAB software is chosen as it is free. Other software that provides simulation of loads with thermal nature are very expensive. Additionally, MATLAB can be programmed according to the type of problem available, providing the possibility to calculate the sun irradiation and the thermal loads and the behavior of the SHIP being used.

2.4 Time table

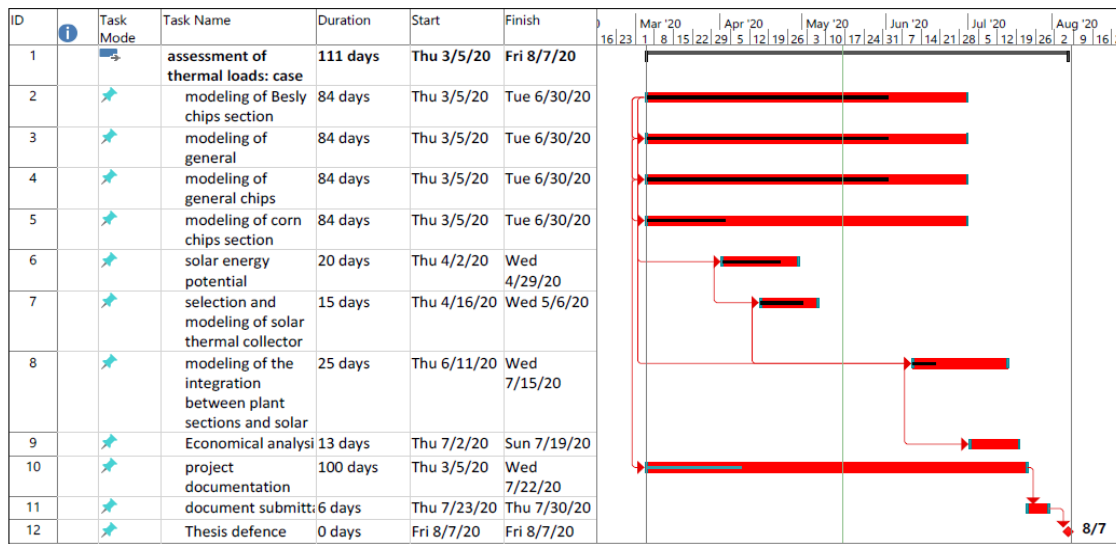


Figure 2-1 Thesis Schedule

Chapter-3

Thermal Load Assessment Case Study; Al Qasrawi Factory

3.1 Introduction

The case study that will be investigated in terms of thermal loads and satisfying the loads from thermal solar collector is Al Qasrawi Company for Trading and Industry. The factory produces several types of processed food, under the category of snacks and beverages to the local Palestinian market.

Out the factory products, three main types consume the major power of the factory, Corn chips, General chips and Besly chips. Each product is being produced in a separate section. Corn chips is roasted with hot air, the air is heated by electric heater production line or gas burner production line. General chips type is being prepared in a sub section that mixes flour and water, form the mixture to required shape and size, dry the formed products in air dryer heated by a water boiler, then the backs are transferred to the general chips station for frying according to production plans. The Besly production section is only dedicated for this type of chips, the section contains its own mixing station and frying production line.

The process flow diagram of the factory is shown in Figure 3-1, the average daily production from each section is about 1300 Kg/day. Each section consumes power to perform the production tasks, i.e., frying or roasting, that are classified under a common unit operation that is industrial drying, the source of heat to perform the drying operation is either electrical or gas. The purpose of this chapter is to evaluate the thermal loads consumed during the production from the three main sections and the subsection of preparation.

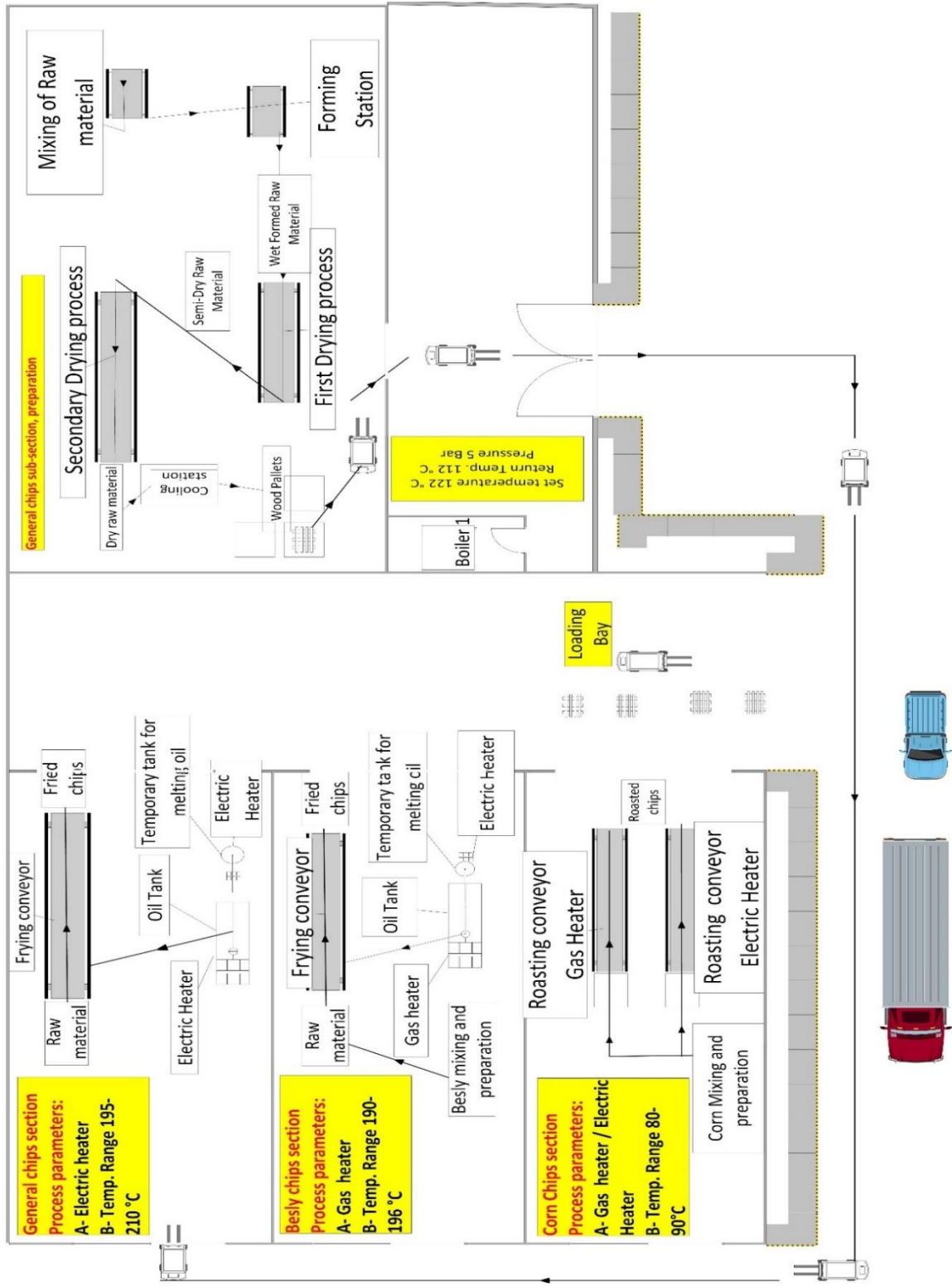


Figure 3-1 Schematic diagram of general process flow in Al Qasrawi factory

3.2 Modeling of energy requirements in the Besly frying section

The first section that will be studied is Besly Chips section, the material flow diagram is shown in Figure 3-2, the flour is being mixed with water in mixer and formed to required shape and size, then dropped into the fryer (point 7).

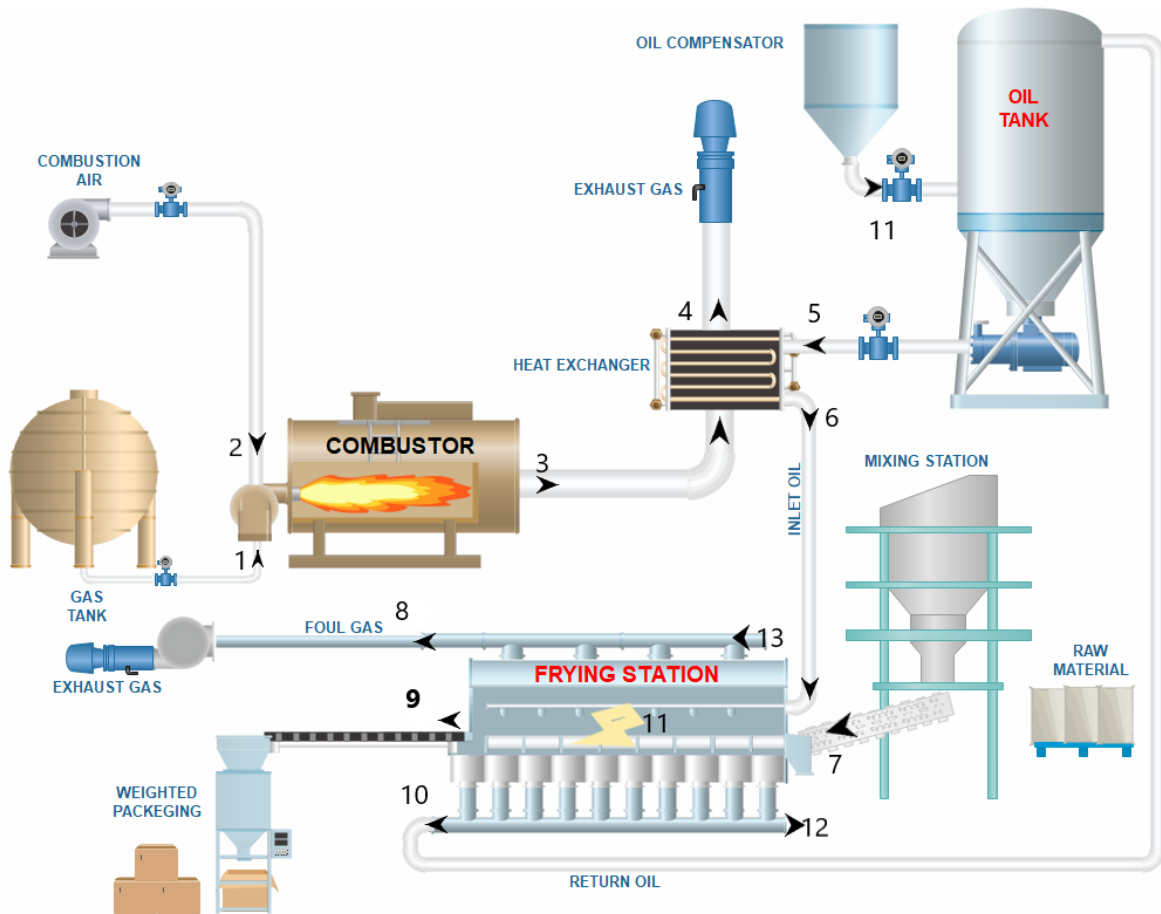


Figure 3-2 Process diagram- Deep Frying; Besly chips

The oil is pumped from the oil tank (point 5) through the heat exchanger into the frying station point 6. Heat is produced by burning the mixture of gas (point 1) and combustion air (point 2). The combustion gases go through the heat exchanger (point 3) to heat up the oil.

Finished product that contains flour, water and oil goes to the weighted packing station (point 9) after frying. Filtered foul gases (point 8) and hot air released to environment. Exhaust gases from

burner are filtered and discharged to environment (point 4). Some fine particles from oil are filtered and removed (point 12). Remaining oil returns to oil tank (point 10). Lost oil in the process is compensated by manual addition of fresh oil in the tank.

Studying the energy required to evaporate the water and give the chips the crispy taste, the fryer schematic diagram is shown in Figure 3-3

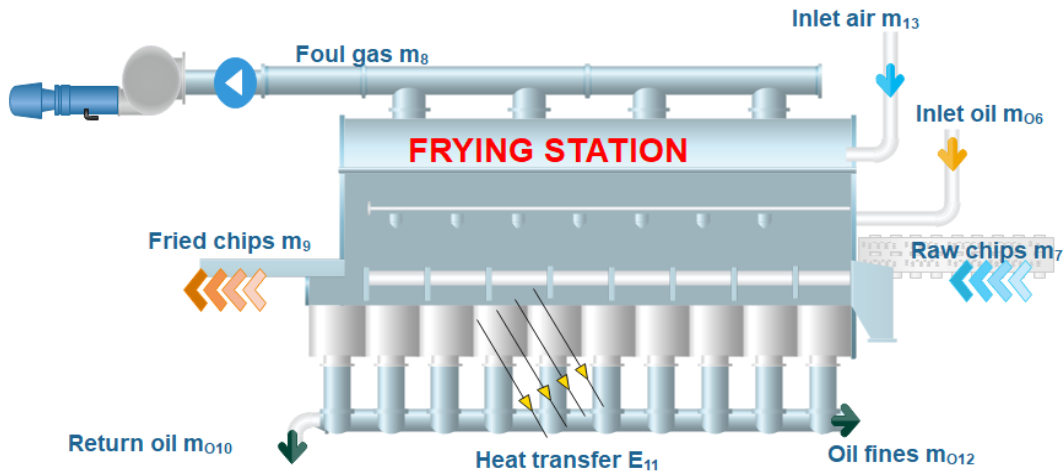


Figure 3-3 Mass flow and energy flow diagram- frying station

The first law of thermodynamic is dedicated conservation of the energy principle. The input energy to any system is equal to the output energy and the stored energy in the system (no stored energy in our case $E_{stored} = 0$) as shown in eq. 3-1

$$\dot{E} = \sum (E_{out} - E_{in}) \quad eq. 3-1$$

$$\dot{E}_{in} = \dot{E}_{fs} + \dot{E}_{fw} + \dot{E}_{ov} + \dot{E}_a + \dot{E}_{tr} \quad eq. 3-2$$

Where:

\dot{E}_{in} : Energy required by the frying station provided by heated oil m_6 .

\dot{E}_{fs} : Energy consumed to fry the solid flour.

\dot{E}_{fw} : Energy consumed to evaporate the water from the chips mixture.

\dot{E}_{ov} : Energy consumed by evaporation of some oil during the process.

\dot{E}_a : Energy consumed by the surrounding air that sucked by the foul gas.

\dot{E}_{tr} : Energy lost through the walls of fryer to surrounding

To evaluate the energy consumption in the Besly chips fryer, some data was given by the factory in charge, other data are estimated based on references, see Table 3-1.

Table 3-1 Parameters used to evaluate the energy required for frying of Besly chips

Parameter	Value or expression	Source
T_{fo}	468 K	Factory
T_9	453 K	(Wu <i>et al.</i> , 2012)
T_7	333 K	(Wu <i>et al.</i> , 2012)
T_6	473 K	(Wu <i>et al.</i> , 2012)
$T_{13} = T_{amb}$	298 K	Assumed
T_8	376 K	(Wu <i>et al.</i> , 2012)
T_b	373 K	Boiling temp.
\dot{m}_{s7}	0.0217 kg/s	Factory calculated
\dot{m}_{w7}	0.0144 kg/s	Calculated
\dot{m}_{s9}	0.0217 kg/s	Equal \dot{m}_{s7}
\dot{m}_{w9}	2.4×10^{-4} kg/s	Calculated
\dot{m}_{13}	0.01 kg/s	Calculated
\dot{m}_{012}	3.3×10^{-4} kg/s	Calculated
\dot{m}_{09}	0.0098 kg/s	Calculated
C_{fs}	1.662 kJ/ kg. K	internet
C_{fw}	4.18 kJ/ kg. K	(Çengel and Boles, 2010)
C_{pa}	1.006 kJ/ kg. K	(Çengel and Boles, 2010)
U	1.4×10^{-3} kW/ m ² . K	(Wu <i>et al.</i> , 2012)
A	20 m ²	Assumed
h_{fgo}	300 kJ/kg	(Wu <i>et al.</i> , 2012)
h_{fgw}	2256.7 kJ/kg	(Wu <i>et al.</i> , 2012)
X_{w7}	35 %	(Zhang <i>et al.</i> , 2006)
X_{w9}	2 %	(Mujumdar and Hall, 2006b)
X_{s9}	Equal X_{s7}	Calculated
X_{O9}	33.2 %	Calculated

3.2.1 Energy in the solid content

To evaluate the energy consumed in frying the solid content of the chips \dot{E}_{fs} , the solid content that is filtered through \dot{m}_{12} is considered negligible, hence the solid content is considered constant,

$$\dot{m}_{s7} = \dot{m}_{s9} \quad eq. 3-3$$

and the sensible heat energy can be calculated using

$$\dot{E}_{fs} = C_{fs} \dot{m}_{s7} (T_9 - T_7) \quad eq. 3-4$$

To evaluate the solid content, from factory given data, the section makes a mix of 1250 kg in a daily 16 hrs shifts, and so,

$$\dot{m}_{s7} = \frac{1250}{16 * 3600} = 0.0217 \frac{kg}{s} \quad eq. 3-5$$

The heat capacity of Wheat flour is 1.662 kJ/kg. K, (Engineers, 2008), and the temperature at 7 and 9 points from Table 3-1 are 333 K, and 453 K respectively, applying the numbers into eq. 3-4,

$$\dot{E}_{fs} = 1.662 \times 0.0217 \times (453 - 333) = 4.32 \frac{kJ}{s}$$

3.2.2 Energy to evaporate the water

\dot{E}_{fw} is the energy required to evaporate water \dot{m}_{wv} , that is energy required to bring water to boiling point (sensible heat), and then to evaporation (latent heat h_{fg}),

$$\dot{E}_{fw} = C_{pw} \cdot (T_b - T_7) \cdot \dot{m}_{wv} + h_{fg} \cdot \dot{m}_{wv} \quad eq. 3-6$$

$$\dot{m}_{wv} = \dot{m}_{w7} - \dot{m}_{w9} \quad eq. 3-7$$

Its worth noting that although the solid content is assumed constant, however, the mixture at point 7 is different from point 9, wherein 9 it contains oil with huge percentage by mass,

$$\dot{m}_7 = \dot{m}_{w7} + \dot{m}_{s7} \quad eq. 3-8$$

$$\dot{m}_9 = \dot{m}_{w9} + \dot{m}_{s9} + \dot{m}_{o9} \quad eq. 3-9$$

In order to evaluate the water content at point 7, the mixture of flour and water should be 1kg flour : 0.6 kg water, (Zhang *et al.*, 2006)

$$\dot{m}_{w7} = \frac{1250 * 0.6}{16 * 3600} = \frac{750}{57600} = 0.013 \frac{kg}{s}$$

To calculate the water content in the final product \dot{m}_{w9} , depending on given data from factory, the oil makeup is 36 units*18 kg = 648 kg, this amount is being added manually over the

course of the day, this amount of oil is to replace the oil being sucked in the final mixture \dot{m}_{o9} , the oil evaporated \dot{m}_{o8} , and the oil removed as fines at point \dot{m}_{o12} ,

$$\dot{m}_{oil\ make-up} = \dot{m}_{o9} + \dot{m}_{o8} + \dot{m}_{o12} \quad eq. 3-10$$

The oil make-up flow rate assuming constant supply

$$\dot{m}_{oil\ make-up} = \frac{36 * 18}{16 * 3600} = \frac{648}{57600} = 0.01125 \frac{kg}{s}$$

Assuming 3% of oil fines is removed

$$\dot{m}_{o12} = 0.003 \times 0.01125 = 3.3 \times 10^{-4} \frac{kg}{s}$$

Assuming 10% of oil is removed within foul gas

$$\dot{m}_{o8} = 0.1 \times 0.01125 = 1.125 \times 10^{-3} \frac{kg}{s}$$

This gives the oil amount absorbed in the final product

$$\dot{m}_{o9} = 0.01125 - 3.3 \times 10^{-4} - 1.125 \times 10^{-3} = 0.0098 \frac{kg}{s}$$

According to literature (Mujumdar and Hall, 2006b), oil should have 40 % by mass and water 2% by mass in order to get long shelf life, accordingly eq. 3-9 becomes

$$\dot{m}_9 = 58\%solid + 40\%oil + 2\%water \quad eq. 3-11$$

And so, the water flow rate in the final product is

$$\dot{m}_{w9} = \left(\frac{\dot{m}_{s9} + \dot{m}_{o9}}{0.98} \right) \times 0.02$$

$$\dot{m}_{w9} = \left(\frac{2.17 \times 10^{-2} + 9.8 \times 10^{-3}}{0.98} \right) \times 0.02 = 2.4 \times 10^{-4} \frac{kg}{s}$$

Substituting the values in eq. 3-7

$$\dot{m}_{wv} = 0.13 - 2.4 \times 10^{-4} = 0.0127 \frac{kg}{s} \quad eq. 3-12$$

Substituting the obtained values in eq. 3-6

$$\dot{E}_{fw} = C_{pw} \cdot (T_b - T_7) \cdot \dot{m}_{wv} + h_{fg} \cdot \dot{m}_{wv} \quad eq. 3-13$$

$$\dot{E}_{fw} = 4.18 \times (373 - 333) \times 0.0127 + 2256.7 \times 0.0127$$

$$\dot{E}_{fw} = 30.75 \frac{kJ}{s}$$

3.2.3 Energy in the evaporated oil

The energy that is consumed during the evaporation of oil which is released to the environment with foul gas at point 8 is equal to

$$\dot{E}_{ov} = h_{fgo} \times \dot{m}_{ov} \quad eq. 3-14$$

We have assumed earlier that $\dot{m}_{ov} = 1.125 \times 10^{-3} \frac{kg}{s}$, and the heat capacity of oil is 2.76 kJ/kg.K (Carlos and Santos, no date), and the enthalpy of oil $h_{fgo} = 300 \frac{kJ}{kg}$ (Wu *et al.*, 2012), based on that the energy consumed in oil evaporation

$$\dot{E}_{ov} = 300 \times 1.125 \times 10^{-3} = 0.3375 \frac{kJ}{s}$$

3.2.4 Energy released due to air flow

The energy caught by the air entering the fryer and released to surrounding through foul gas is given by

$$\dot{E}_a = C_{pa} \dot{m}_{13} (T_8 - T_{13}) \quad eq. 3-15$$

The heat capacity of air $C_{pa} = 1.006 \frac{kJ}{kgK}$, and the mass flow rate of the air $\dot{m}_{13} = 0.01 \frac{kg}{s}$ (Wu *et al.*, 2012), then

$$\dot{E}_a = 1.006 \times 0.01 \times (376 - 298) = 0.784 \frac{kJ}{s}$$

3.2.5 Energy released by heat transfer

The energy that is lost through the walls of the fryer \dot{E}_{tr} is considered based on steady state calculations, hence

$$\dot{E}_{tr} = U A (T_{fo} - T_{amb}) \quad eq. 3-16$$

Where $U = 1.4 \times 10^{-3} \text{ kW/m}^2 \cdot \text{K}$ (Bidwell, 1940) is the thermal conductivity of stainless steel grade 304, and the area of the fryer is measured to be $A = 20 \text{ m}^2$, with process parameters from Table 3-1,

$$\dot{E}_{tr} = 1.4 \times 10^{-3} \times 20 \times (468 - 298) = 4.76 \frac{\text{kJ}}{\text{s}}$$

3.2.6 Total energy required by the fryer

Finally summing all energy values obtained and substituting in eq. 3-2 gives the total thermal energy demand by the fryer to perform the process of frying

$$\dot{E}_{in} = \dot{E}_{fs} + \dot{E}_{fw} + \dot{E}_{ov} + \dot{E}_a + \dot{E}_{tr} \quad eq. 3-17$$

$$\dot{E}_{in} = 4.32 + 30.75 + 0.3375 + 0.784 + 4.76 = 37.9 \frac{\text{kJ}}{\text{s}} = \mathbf{40.95 \text{ kW}_{th}}$$

Other form of energy involved in the process like conveyors and blowers are not in the frame of study of this thesis.

3.3 The energy required by the raw material section

3.3.1 Introduction

In this section, the several shape and sizes of chips are prepared. The mixture of flour and water is formed, then dried in a drying process, after that it is cooled to room temperature, then packing in preliminary bags is done in order to send it to general chip frying section.

The process diagram for the drying process is shown in Figure 3-4. The flour is mixed with water at (point 1), then it goes to the formation station at (point 2) to be formed in the required shape and size.

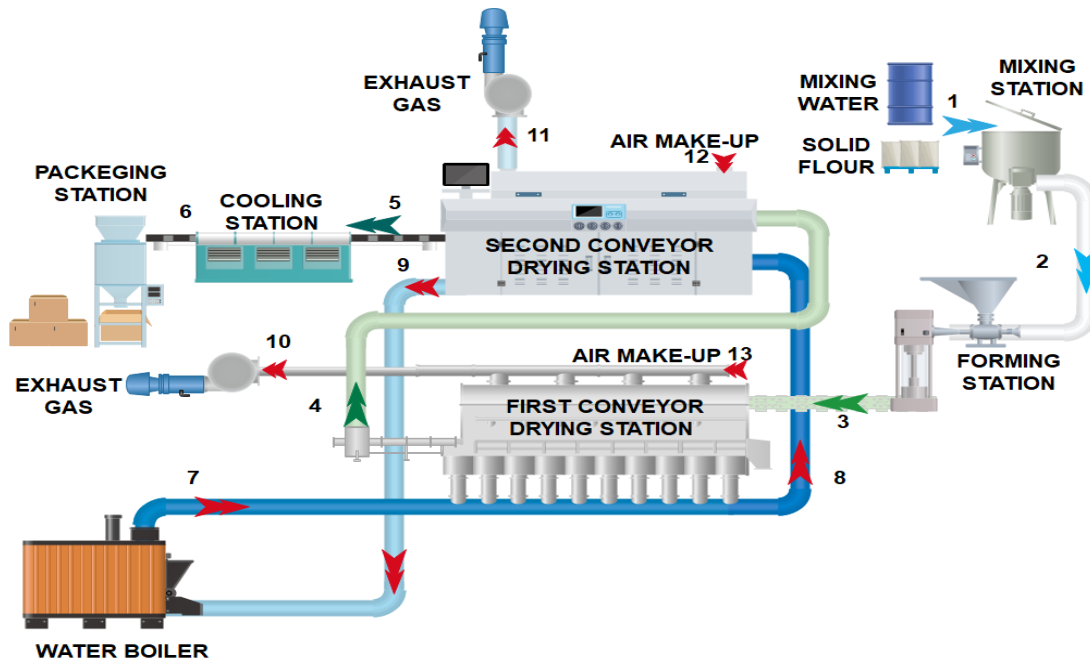


Figure 3-4 Drying section process flow diagram

Then the mixture goes through feeder/ spreader onto a conveyor which carries the raw chips at (point 3) into the first drying station. The first drying station is a multi-pass dryer type with 7 rounds Figure 3-5. (*Belt Type Fruit&vegetable Drying Machine/ Vegetable Dehydrator Supplier*, 2020). The raw chips lose some water percentage in this station.

The raw chips pumped to the second drying station at (point 4). The second dryer is a multi-pass conveyor dryer type with 9 rounds. The raw chips lose water percentage and go out to the cooling station at (point 5). After that, the raw chips are cooled to the ambient temperature by air in the cooling station. Finally, they go to the packing station in after which it will be dispatched to the general frying section.

The heat comes from a water boiler at (point 7) with 122°C temperature. It flows through a heat exchanger inside the dryer, where the air is blown through the heat exchanger fins, the air temperature reaches 70 °C. The hot water goes to second dryer at (point 8), where it goes another time through a heat exchanger and the air is blown again through exchanger fins. After that water returns back to the boiler at (point 9) with 110 °C temperature.

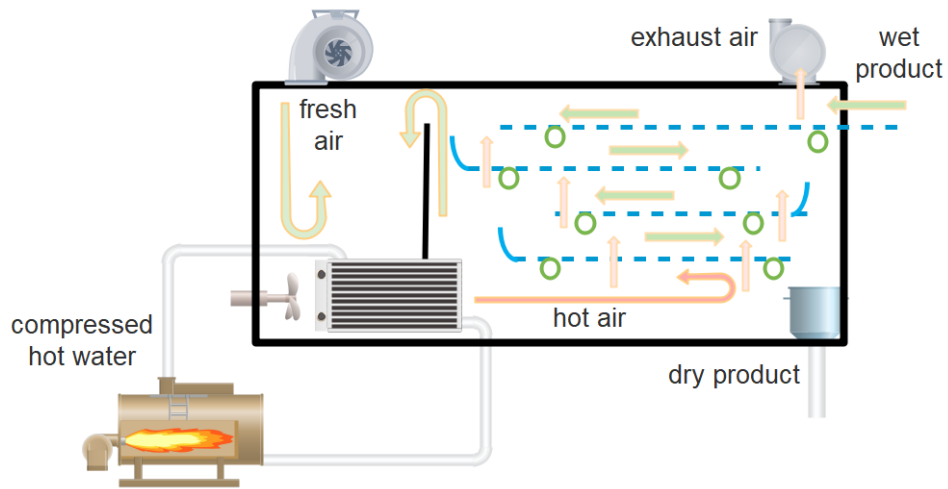


Figure 3-5 Multi pass drying machine

The air circulates several times inside the dryer. The air make up is open to the surrounding (points 12 and 13). The exhaust gases contain air and vapor water mainly. They go through (points 10 and 11). Figure 3-6 (Mujumdar and Hall, 2006b) presents the typical cross section of the dryer, it explains what happens inside the dryer of air circulation.

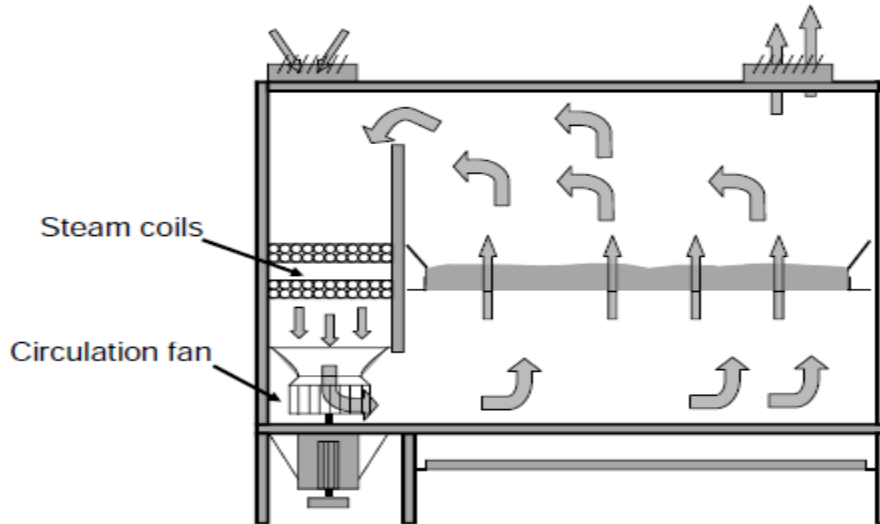


Figure 3-6 A typical cross section of dryer, air circulation

3.3.2 Energy required to evaporate the water in first station

Following the same approach of thermodynamics first law, and applying heat and mass conservation principles on the Figure 3-7. The energy transferred to the product between points 4 and 3 will be calculated. Then the energy required to evaporate the water from the product between 4 and 3, in addition, the air absorbed energy will be calculated. Finally, the heat transfer from the walls of the dryer will be calculated.

$$\dot{E}_{total-1} = \dot{E}_{s3} + \dot{E}_{wv} + \dot{E}_a + \dot{E}_{tr} \quad eq. 3-18$$

Where:

$\dot{E}_{total-1}$: Energy required by the first drying station provided by heated water \dot{m}_7 .

\dot{E}_{s3} : Energy consumed to dry the solid flour.

\dot{E}_{wv} : Energy consumed to evaporate the water from the chips mixture.

\dot{E}_a : Energy consumed by the surrounding air that sucked by the foul gas .

\dot{E}_{tr} : Energy lost through the walls of fryer to surrounding

To evaluate the energy consumption in the Besly chips fryer some data was given by the factory in charge, the other data are estimated based on references, see (Wu *et al.*, 2012)

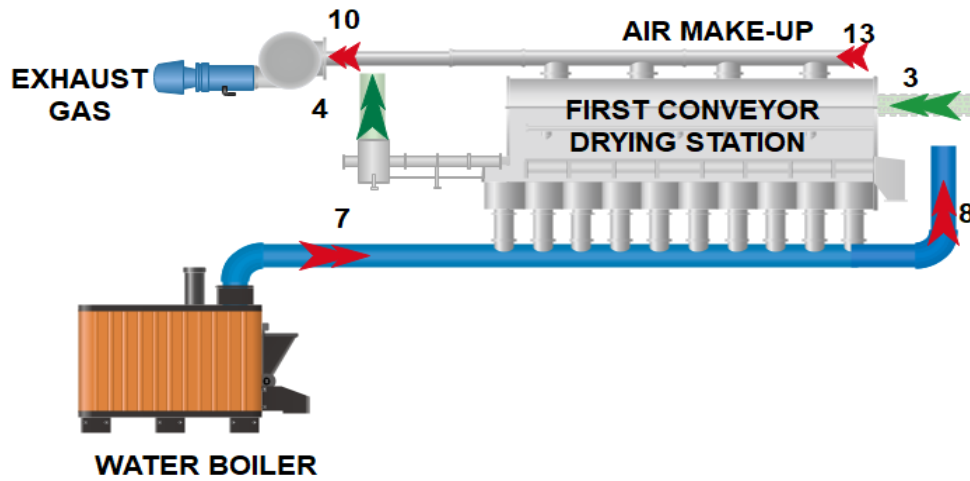


Figure 3-7 First drying station energy and mass flow

3.3.3 Energy consumed by solid flour

Starting with energy consumed by the solid content of the product \dot{E}_{s3}

$$\dot{E}_{s3} = C_{fs} \dot{m}_3 (T_4 - T_3) \quad \text{eq. 3-19}$$

From the given data of factory, the section mix around 6000 kg of flour in a 16 hrs shift, then the mass flow rate \dot{m}_{s3} of the flour equals

$$\dot{m}_{s3} = \frac{6000}{16 \times 3600} = 0.104 \frac{kg}{s}$$

The heat capacity of flour is 1.662 kJ/kg. K, (Engineers, 2008). The temperature inside the dryer reach 70 °C, and $T_3=25$ °C, substituting the values in eq. 3-19 will result the total energy consumed by the solid content of the product \dot{E}_{s3} ,

$$\dot{E}_{s3} = 0.104 \times 1.662 \times (343 - 298) = 7.8 \frac{kJ}{s}$$

3.3.4 Heat consumed to evaporate water in first dryer

The heat required to evaporate water in the first drying station \dot{E}_{wv} equals,

$$\dot{E}_{wv} = \dot{m}_{wv}(h_g @_{70} - h_f @_{25}) \quad \text{eq. 3-20}$$

In order to evaluate the water content at point 3, the mixture of flour and water should be 1kg flour : 0.6 kg water, (Zhang *et al.*, 2006), and the water is reduced by 15 % as per factory data, hence,

$$\dot{m}_{wv} = \dot{m}_{s3} \times 0.15 \quad \text{eq. 3-21}$$

$$\dot{m}_{wv} = 0.104 \times 0.15 = 0.0156 \frac{\text{kg}}{\text{s}}$$

From (Çengel and Boles, 2010), the $h_g @_{70} = 2626 \frac{\text{kJ}}{\text{kg K}}$, and $h_f @_{25} = 105 \frac{\text{kJ}}{\text{kg K}}$, substituting the values in eq. 3-20 to find the total heat required to evaporate water in the first drying station \dot{E}_{wv} ,

$$\dot{E}_{wv} = 0.0156 \times (2626 - 105) = 39.3 \frac{\text{kJ}}{\text{s}}$$

3.3.5 Heat to exhaust air

The energy absorbed by recycled air inside the dryer \dot{E}_a equals,

$$\dot{E}_a = \dot{m}_a C_{pa}(T_{10} - T_{13}) \quad \text{eq. 3-22}$$

As per (Mujumdar and Hall, 2006a), the $\dot{m}_a = 1461.3 \text{ kg/h}$, and $C_{pa} = 1.006 \frac{\text{kJ}}{\text{kg.K}}$ (Çengel and Boles, 2010), substituting the values in eq. 3-22 to find the total energy absorbed by recycled air inside the dryer \dot{E}_a

$$\dot{E}_a = \frac{1461.3}{3600} \times 1.006 \times (70 - 25) = 18.37 \frac{\text{kJ}}{\text{s}}$$

3.3.6 The energy transfer through walls of dryer

The energy lost through the walls of the dryer \dot{E}_{tr} equals

$$\dot{E}_{tr} = UA\Delta T \quad \text{eq. 3-23}$$

The dryer walls are from stainless steel grade 304 with $U = 1.4 \times 10^{-3} \text{ kW/m}^2 \cdot \text{K}$ (Bidwell, 1940), the area A of dryer is 93.6 m^2 , substituting the values in eq. 3-23

$$\dot{E}_{tr} = 1.4 \times 10^{-3} \times 93.6 \times 45 = 5.9 \frac{\text{kJ}}{\text{s}}$$

Substituting the energy values in eq. 3-18 yields the total energy required by the first drying station

$$\begin{aligned} \dot{E}_{total} &= \dot{E}_{s3} + \dot{E}_{wv} + \dot{E}_a + \dot{E}_{tr} && \text{eq. 3-24} \\ \dot{E}_{total-1} &= 7.8 + 39.3 + 18.37 + 5.9 = \mathbf{71.37 \text{ kW}_{th}} \end{aligned}$$

3.4 Energy consumed by second drying station

Applying heat and mass conservation principles Figure 3-8, we will calculate the energy transferred to the product between (points 5 and 4), after that the energy required to evaporate the water from the product between (point 5 and 4), in addition, the air absorbed energy will be calculated. Finally, the heat transfer from the walls of the dryer will be calculated.

$$\dot{E}_{total-2} = \dot{E}_{s4} + \dot{E}_{wv} + \dot{E}_a + \dot{E}_{tr} \quad \text{eq. 3-25}$$

Where:

$\dot{E}_{total-2}$: Energy required by the second drying station provided by heated water \dot{m}_8 .

\dot{E}_{s4} : Energy consumed to dry the solid flour.

\dot{E}_{wv} : Energy consumed to evaporate the water from the chips mixture.

\dot{E}_a : Energy consumed by the surrounding air that sucked by the foul gas.

\dot{E}_{tr} : Energy lost through the walls of fryer to surrounding

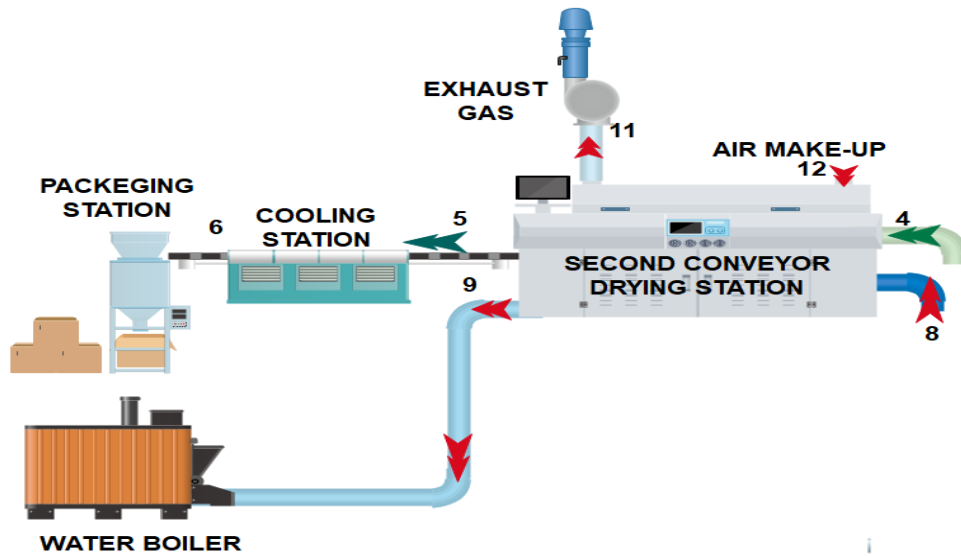


Figure 3-8 Second drying station energy and mass flow

3.4.1 Energy consumed by solid flour

The energy consumed by the solid content of the product \dot{E}_{s4} is

$$\dot{E}_{s3} = C_{fs} \dot{m}_3 (T_5 - T_4) \quad \text{eq. 3-26}$$

The solid content of flour is constant, $\dot{m}_{s3} = \dot{m}_{s4} = 0.104 \text{ kg/s}$. The heat capacity of flour is $1.662 \text{ kJ/kg} \cdot \text{K}$, (Engineers, 2008), and the temperature inside the dryer reaches $80 \text{ }^\circ\text{C}$ (T_5), and $T_4 = 70 \text{ }^\circ\text{C}$, substituting these values in eq. 3-19 to find the total energy consumed by the solid content of the product \dot{E}_{s4} in second dryer.

$$\dot{E}_{s4} = 0.104 \times 1.662 \times (353 - 343) = 1.73 \frac{\text{kJ}}{\text{s}}$$

3.4.2 Heat consumed to evaporate water in second dryer

The heat required to evaporate water in the second drying station \dot{E}_{wv} equals,

$$\dot{E}_{wv} = \dot{m}_{wv}(h_{g@80} - h_{f@70}) \quad eq. 3-27$$

In order to evaluate the water content at (point 4), the mixture of flour and water should be 1kg flour : 0.6 kg water, (Zhang *et al.*, 2006), and the water is reduced by 15 % as per factory data, hence,

$$\dot{m}_{wv} = \dot{m}_{s4} \times 0.15 \quad eq. 3-28$$

$$\dot{m}_{wv} = 0.104 \times 0.15 = 0.0156 \frac{kg}{s}$$

From (Çengel and Boles, 2010), the $h_{g@80} = 2643 \frac{kJ}{kg K}$, and $h_{f@70} = 293 \frac{kJ}{kg K}$, substituting the values in eq. 3-27 to find the total heat required to evaporate water in the second drying station \dot{E}_{wv} ,

$$\dot{E}_{wv} = 0.0156 \times (2643 - 293) = 36.66 \frac{kJ}{s}$$

3.4.3 Heat to exhaust air

The energy absorbed by recycled air inside the dryer \dot{E}_a equals,

$$\dot{E}_a = \dot{m}_a C_{pa}(T_{11} - T_{12}) \quad eq. 3-29$$

As per (Mujumdar and Hall, 2006a), the $\dot{m}_a = 1461.3$ kg/h, and $C_{pa} = 1.006 \frac{kJ}{kg.K}$ (Çengel and Boles, 2010), substituting the values in eq. 3-29

$$\dot{E}_a = \frac{1461.3}{3600} \times 1.006 \times (353 - 298) = 22.46 \frac{kJ}{s}$$

3.4.4 The energy transfer through walls of dryer

The energy lost through the walls of the dryer \dot{E}_{tr} equals to

$$\dot{E}_{tr} = UA\Delta T \quad eq. 3-30$$

The dryer walls are from stainless steel grade 304 with $U = 1.4 \times 10^{-3} \text{ kW/m}^2 \cdot \text{K}$ (Bidwell, 1940), the area A of dryer is 111.6 m², substituting the values in eq. 3-30

$$\dot{E}_{tr} = 1.4 \times 10^{-3} \times 111.6 \times 45 = 7 \frac{kJ}{s}$$

Substituting the energy values in eq. 3-31 yields to find the total energy required by the second drying station.

$$\begin{aligned} \dot{E}_{total-2} &= \dot{E}_{s4} + \dot{E}_{wv} + \dot{E}_a + \dot{E}_{tr} & \text{eq. 3-31} \\ \dot{E}_{total-2} &= 1.7 + 36.66 + 22.46 + 7 = 67.82 \frac{kJ}{s} \end{aligned}$$

3.5 Energy required in the general frying section

The general frying section is almost identical to the Besly chips frying section. The main difference is the heat source is an electrical heater for the oil rather than the gas burner. The other parameters are almost the same as in both sections.

The raw chips material comes from the drying section and filled inside a silo. Then it is fed in by using a feeder/ spreader over a conveyor that runs inside the deep-frying station.

Figure 3-9 shows the general chips frying station. The oil is pumped from the oil tank through the heat exchanger into the frying station (point 2). The finished product that contains flour, water, and oil goes to the weighted packing station (point 4) after frying. Filtered foul gases (point 3) and hot air released to the environment. Some fine particles from oil are filtered and removed (point 6). Remaining oil returns to oil tank (point 6). Lost oil in the process is compensated by the manual addition of fresh oil in the tank.

Again applying the thermodynamics principle in steady state conditions. The input energy to any system is equal to the output energy and the stored energy in the system (no stored energy in our case $E_{stored} = 0$) once again as shown in eq. 3-1

$$\dot{E} = \sum (E_{out} - E_{in}) \quad \text{eq. 3-32}$$

$$\dot{E}_{inG} = \dot{E}_{fs} + \dot{E}_{fw} + \dot{E}_{ov} + \dot{E}_a + \dot{E}_{tr} \quad \text{eq. 3-33}$$

Where:

\dot{E}_{inG} : Energy required by the frying station in the General chips section provided by heated oil m_{o2} .

\dot{E}_{fs} : Energy consumed to fry the solid flour.

\dot{E}_{fw} : Energy consumed to evaporate the water from the chips mixture.

\dot{E}_{ov} : Energy consumed by evaporation of some oil during the process.

\dot{E}_a : Energy consumed by the surrounding air that sucked by the foul gas.

\dot{E}_{tr} : Energy lost through the walls of fryer to surrounding

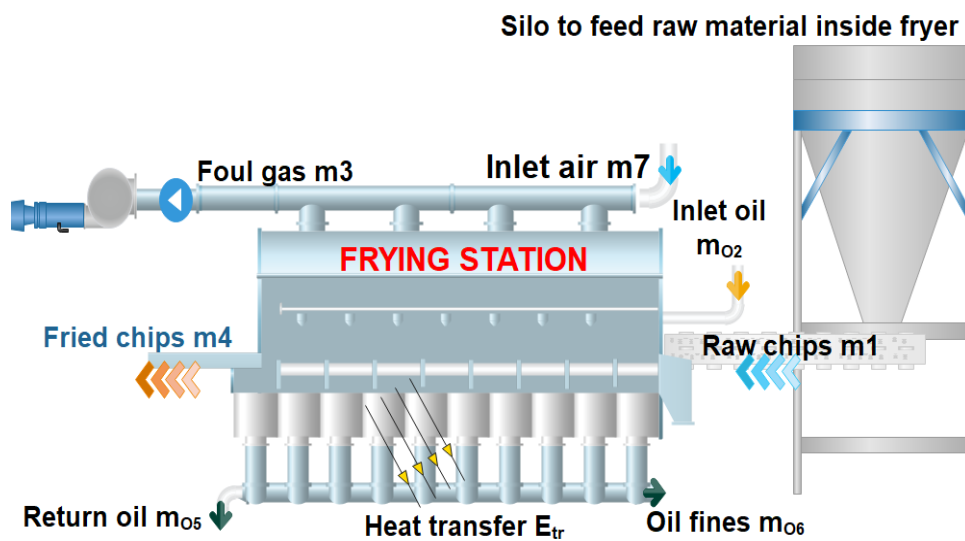


Figure 3-9 General chips frying station

To evaluate the energy consumption in the Besly chips fryer, some data was given by the factory in charge, other data are estimated based on references as will be pointed out in calculations

3.5.1 Energy in the solid content

To evaluate the energy consumed in frying the solid content of the chips \dot{E}_{fs} , the solid content that is filtered through \dot{m}_6 is considered negligible, hence the solid content is considered constant,

$$\dot{m}_{s1} = \dot{m}_{s4} \quad \text{eq. 3-34}$$

And the sensible heat energy can be calculated using

$$\dot{E}_{fs} = C_{fs} \dot{m}_{s1} (T_4 - T_1) \quad \text{eq. 3-35}$$

To evaluate the solid content, from factory given data, the section makes a mix of 4800 kg in a daily 16 hrs shifts, and so,

$$\dot{m}_{s1} = \frac{4800}{16 * 3600} = 0.0833 \frac{kg}{s}$$

The heat capacity of Wheat flour is 1.662 kJ/kg. K, (Engineers, 2008), and the temperature at $T_1 = 298$ K is the ambient temperature, and $T_4 = 473$ K is the frying temperature, substituting the numbers into eq. 3-35,

$$\dot{E}_{fs} = 1.662 \times 0.0833 \times (473 - 298) = 24.3 \frac{kJ}{s}$$

3.5.2 Energy to evaporate the water

\dot{E}_{fw} is the energy required to evaporate water \dot{m}_{wv} , that is the energy required to bring water to boiling point (T_b) (sensible heat), and then to evaporation (latent heat h_{fg}),

$$\dot{E}_{fw} = C_{pw} \cdot (T_b - T_1) \cdot \dot{m}_{wv} + h_{fg} \cdot \dot{m}_{wv} \quad \text{eq. 3-36}$$

$$\dot{m}_{wv} = \dot{m}_{w1} - \dot{m}_{w4} \quad \text{eq. 3-37}$$

In order to evaluate the water content at (point 1), the mixture of flour and water should be 1kg flour : 0.6 kg water, (Zhang *et al.*, 2006), however, this ready mixed chips had already been dried to 10% water content, accordingly

$$\dot{m}_{w1} = \frac{4800 * 0.1}{16 * 3600} = 0.00833 \frac{kg}{s}$$

The given data from the factory is used to calculate the water content in the final product \dot{m}_{w4} . The oil make up is 1200 kg, this amount is being added manually over the course of the day.

The added oil is to compensate the oil being sucked in the final mixture \dot{m}_{o4} , the oil evaporated \dot{m}_{o3} , and the oil removed as fines at point \dot{m}_{o6} ,

$$\dot{m}_{oil\ make-up} = \dot{m}_{o4} + \dot{m}_{o3} + \dot{m}_{o6} \quad eq. 3-38$$

The oil make-up flow rate assuming constant supply and is equal to

$$\dot{m}_{oil\ make-up} = \frac{1200}{16 * 3600} = 0.0208 \frac{kg}{s}$$

Assuming 5% of oil fines is removed

$$\dot{m}_{o6} = 0.05 \times 0.0208 = 1.04 \times 10^{-3} \frac{kg}{s}$$

Assuming 10% of oil is removed within foul gas

$$\dot{m}_{o3} = 0.1 \times 0.0208 = 2.08 \times 10^{-3} \frac{kg}{s}$$

This gives the oil amount absorbed in the final product

$$\dot{m}_{o4} = 0.0208 - 1.04 \times 10^{-3} - 2.08 \times 10^{-3} = 0.0177 \frac{kg}{s}$$

Applying the same principle about oil percentage in the final product (Mujumdar and Hall, 2006b). The oil should have 40 % by mass and water 2% by mass in order to get long shelf life, accordingly

$$\dot{m}_4 = 58\%solid + 40\%oil + 2\%water \quad eq. 3-39$$

And so, the water flow rate in the final product is

$$\begin{aligned} \dot{m}_{w4} &= \left(\frac{\dot{m}_{s9} + \dot{m}_{o9}}{0.98} \right) \times 0.02 \\ \dot{m}_{w4} &= \left(\frac{8.33 \times 10^{-2} + 1.7 \times 10^{-2}}{0.98} \right) \times 0.02 \\ \dot{m}_{w4} &= 2.06 \times 10^{-3} \frac{kg}{s} \end{aligned}$$

Substituting the values in eq. 3-37

$$\dot{m}_{wv} = 8.33 \times 10^{-3} - 2.06 \times 10^{-3} = 6.26 \times 10^{-3} \frac{kg}{s}$$

Substituting the obtained values in eq. 3-36 to find the energy consumed to evaporate the water from the chips mixture

$$\dot{E}_{fw} = C_{pw} \cdot (T_b - T_1) \cdot \dot{m}_{wv} + h_{fg} \cdot \dot{m}_{wv} \quad eq. 3-36$$

$$\dot{E}_{fw} = 4.18 \times (373 - 298) \times 6.26 \times 10^{-3} + 2256.7 \times 6.26 \times 10^{-3}$$

$$\dot{E}_{fw} = 16.1 \frac{kJ}{s}$$

3.5.3 Energy in the evaporated oil

The energy that is consumed during the evaporation of oil which is released to the environment with foul gas at point 8 is equal to

$$\dot{E}_{ov} = h_{fgo} \times \dot{m}_{ov3} \quad eq. 3-40$$

We have assumed earlier that $\dot{m}_{ov} = 2.08 \times 10^{-3} \frac{kg}{s}$, and the enthalpy of oil $h_{fgo} = 300 \frac{kJ}{kg} K$ (Wu *et al.*, 2012), based on that the energy consumed in oil evaporation

$$\dot{E}_{ov} = 300 \times 2.08 \times 10^{-3} = 0.624 \frac{kJ}{s}$$

3.5.4 Energy released due to air flow

The energy caught by the air entering the fryer and released to surrounding through foul gas is given by

$$\dot{E}_a = C_{pa} \dot{m}_2 (T_3 - T_7) \quad eq. 3-41$$

The heat capacity of air $C_{pa} = 1.006 \frac{kJ}{kg}$, and the mass flow rate of the air $\dot{m}_7 = 0.02 \frac{kg}{s}$ (Wu *et al.*, 2012), then

$$\dot{E}_a = 1.006 \times 0.02 \times (376 - 298) = 1.57 \frac{kJ}{s}$$

3.5.5 Energy released by heat transfer

The energy that is lost through the walls of the fryer \dot{E}_{tr} is considered based on steady state calculations, hence

$$\dot{E}_{tr} = U A (T_{fo} - T_{amb}) \quad \text{eq. 3-42}$$

The thermal conductivity of stainless steel grade 304 is $U = 1.4 \times 10^{-3} \text{ kW/m}^2 \cdot \text{K}$ (Bidwell, 1940), and the area of the fryer is measured to be $A = 23 \text{ m}^2$,

$$\dot{E}_{tr} = 1.4 \times 10^{-3} \times 23 \times (473 - 298) = 5.635 \frac{kJ}{s}$$

3.5.6 Total energy required by the fryer

Finally summing all energy values obtained and substituting in eq. 3-31 gives the total thermal energy demand by the fryer to perform the process of frying

$$\dot{E}_{inG} = \dot{E}_{fs} + \dot{E}_{fw} + \dot{E}_{ov} + \dot{E}_a + \dot{E}_{tr} \quad \text{eq. 3-32}$$

$$\begin{aligned} \dot{E}_{inG} &= 24.3 + 16.1 + 0.624 + 1.57 + 5.635 = 37.9 \frac{kJ}{s} \\ &= \mathbf{48.22 \text{ kW}_{th}} \end{aligned}$$

3.6 Energy required in the corn chips section

This section is relatively simple in operation and modeling compared to previous sections, as the oil is being mixed with corn flour and water initially. A drying operation occurs without the addition of more oil, this is known industrially as buffing.

The oil is mixed with corn flour and water in a ratio of 40%:40%:20% respectively. Figure 3-10 illustrates the basic principle behind the puffing operation. The mixed flour gets into a cutter that cuts the mixture to the required shape and size (point 1). The mixture goes into a conveyor dryer with a high temperature above the saturation point to force the water to be evaporated suddenly,

which is causing the puffing shape of the chips. After that the chips go into another stage near atmospheric pressure, where the remaining water is forced to evaporate and the chips to get its crunchy texture. The oil remains in the chips and the water percentage drops to 1% (point 4)(Matz, 1984).

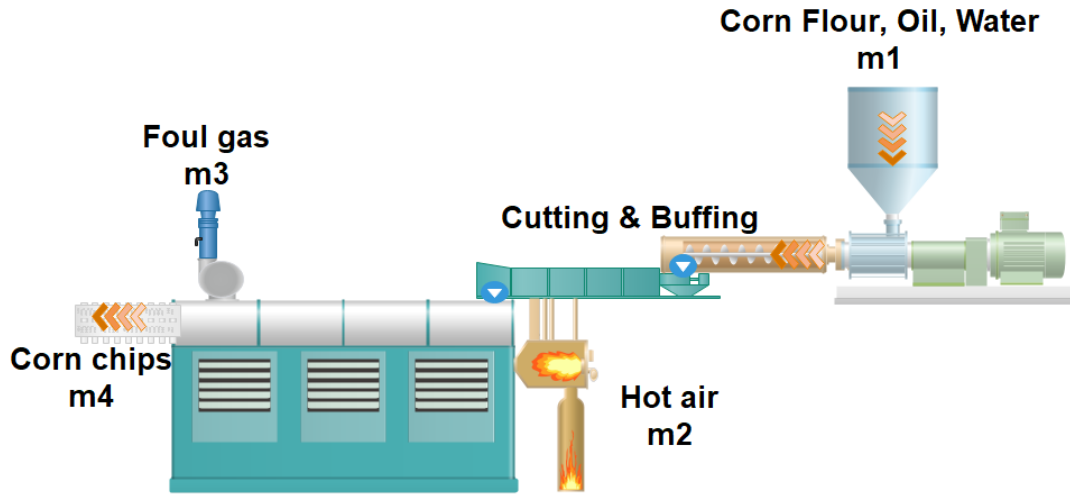


Figure 3-10 Corn chips buffing section

In order to model the puffing drying operation, (Lusas and Rooney, 2001) suggested dealing with it as a closed block to simplify the equation, as in the manufacturing of dryers. The manufacturers deal with the machine to provide one goal, which is removing the water content.

Applying the basic principles of mass and energy conservation, from thermodynamics classical point of view, the water that is mixed with corn flour and oil at (point 1) evaporates and goes out at (point 3). The oil relatively is unchanged and the solid mass of corn flour is constant between (points 1 and 4). Hot air is blown at (point 2) which has a high capacity to absorb vapor at temperature of 80 °C. The energy required to evaporate the water is equal to

$$\dot{E}_{inC} = \dot{E}_w + \dot{E}_a + \dot{E}_{F\&O} + \dot{E}_{tr} \quad \text{eq. 3-43}$$

Where:

\dot{E}_{inC} : The energy required to dry the corn chips provided by electric heater or gas burner

\dot{E}_w : The energy required to evaporate the water from the mixture

\dot{E}_a : Energy consumed by air that leaves with exhaust gas
 $\dot{E}_{F\&O}$: Energy absorbed by the flour and oil during the drying operation
 \dot{E}_{tr} : Energy transfer from the walls of the dryer

3.6.1 Energy required to evaporate the water

The water mass available in the mixture is 20% (Zhang *et al.*, 2006) and 40% oil the remaining is 40% corn flour. From the factory data the production capacity is 1250 kg/16 hours,

$$\dot{m}_{F1} = \frac{1250}{16 * 3600} = 0.0217 \text{ kg/s}$$

$$\text{Hence} \quad \dot{m}_{O1} = 0.0217 \text{ kg/s}$$

$$\text{And} \quad \dot{m}_{w1} = 0.0108 \text{ kg/s}$$

The water content at the final product (point 4) is 1%, the oil and flour masses remain constant, hence

$$\dot{m}_{w4} = \frac{0.0217 + 0.0217}{0.99} - (0.0217 + 0.0217) = 4.38 \times 10^{-4} \text{ kg/s}$$

$$\dot{m}_{wv} = \dot{m}_{w1} - \dot{m}_{w4} = 0.0103 \text{ kg/s}$$

$h_{g@80} = 2643 \text{ kJ/kg K}$, $h_{f@25} = 104.83 \text{ kJ/kg K}$ (Çengel and Boles, 2010). The energy required to evaporate the water \dot{E}_w

$$\dot{E}_w = (h_{g@80} - h_{f@25}) \cdot \dot{m}_{wv} \quad \text{eq. 3-44}$$

$$\dot{E}_w = (2643 - 104.83) \times 0.0103$$

$$\dot{E}_w = 26.14 \text{ kJ/s}$$

3.6.2 Energy consumed by air

The energy consumed by air \dot{E}_a is

$$\dot{E}_a = \dot{m}_{a2} C_{pa} (T_2 - T_{amb}) \quad \text{eq. 3-45}$$

The mass flow rate of air $\dot{m}_{a2} = 0.02 \frac{\text{kg}}{\text{s}}$ (Wu *et al.*, 2012), and the heat capacity of air $C_{pa} = 1.006 \frac{\text{kJ}}{\text{kg.K}}$, then

$$\dot{E}_a = 0.02 \times 1.006 \times (353 - 298) = 1.11 \text{ kJ/s}$$

3.6.3 Energy consumed by flour and oil during drying operation

The energy consumed during the drying of mixture $\dot{E}_{F\&O}$ is

$$\dot{E}_{F\&O} = \dot{m}_{F\&O}(C_{PF} + C_{PO})(T_2 - T_4) \quad \text{eq. 3-46}$$

The specific heat for corn flour is $C_{PF} = 2.198 \text{ kJ/kg} \cdot \text{K}$ (Engineers, 2008), the specific heat of soybean oil $C_{PO} = 2.53 \text{ kJ/kg} \cdot \text{K}$ (Santos, 2005), we assume that $T_2 = 80 \text{ }^\circ\text{C}$ which is the highest temperature the mixture can reach before leaving at point 4, substituting the values in eq. 3-46

$$\begin{aligned} \dot{E}_{F\&O} &= (.0217 + .0217) \times (2.53 + 2.198) \times (353 - 313) \\ \dot{E}_{F\&O} &= 8.21 \text{ kJ/s} \end{aligned}$$

3.6.4 The energy transfer through walls of dryer

The energy that is lost through the walls of the fryer \dot{E}_{tr} is considered based on steady state calculations, hence

$$\dot{E}_{tr} = U A (T_2 - T_{amb}) \quad \text{eq. 3-47}$$

The thermal conductivity of stainless steel grade 304 is $U = 1.4 \times 10^{-3} \text{ kW/m}^2 \cdot \text{K}$ (Bidwell, 1940), and the area of the fryer is measured to be $A = 60 \text{ m}^2$,

$$\dot{E}_{tr} = 1.4 \times 10^{-3} \times 60 \times (353 - 298) = 6.72 \frac{\text{kJ}}{\text{s}}$$

The total energy required in the corn section \dot{E}_{inc} eq. 3-43 is

$$\dot{E}_{inc} = 26.14 + 1.11 + 8.21 + 6.72 = 42.18 \text{ kJ/s}$$

3.7 Summarization of thermal power needed in each section

In Table 3-2 the thermal power needed in each section is presented, where it is noted the variation between the energy consumption depending on the production load available

Table 3-2 Summarization of thermal load from plant production sections

Plant section	Calculated Thermal Load kW _{th}
Besly chips	40.95
First drying station- Preparation section	71.37
Second drying station- Preparation section	67.82
General chips frying section	48.22
Corn chips section	42.18
Total	270.54

Chapter-4

Consternated Solar Power (CSP) Analysis

4.1 Introduction

The factory under consideration is utilizing huge energy over the year from traditional power resources, gas and electrical. The main objective of this thesis is to present the renewable energy resources as a free clean and sustainable alternative that could satisfy the loads available.

This chapter is devoted to solar thermal analysis that will be used to feed the energy to plant sections according to the loads calculated in chapter 3. The work will be divided into 3 main sections, in the first section the calculation of the energy that can be harvested from the sun over the year on hourly basis based on factory location are done. In the second section the selection of the solar thermal collector and calculation of the energy that can be harvested per square meter is performed. The third section will be devoted to the simulation of the equations used in previous sections.

4.2 Solar potential in the factory location

Al Qasrawi factory under consideration is located in West bank-Hebron city Figure 4-1 (*31°30'23.0"N 35°01'25.4"E - Google Maps, no date*)

Hebron city lays over a mountain series with different topologies that have effects on the solar collection ability. However, those variations are considered minor if compared to technical factors like shading and tilt angle of the collectors.

The methodology that will be used to calculate the solar incidence radiation I_r is followed by almost all references. The methodology and nomenclature used in (Masters, 2004) will be followed. The theory behind the equations is left to reader to refer to, however, the equations that are used in the simulation in the final section of this chapter will be mentioned.



Figure 4-1 Al Qasrawi Factory location map

The Table 4-1 shows all the abbreviations that is used for solar radiation calculation in the succeeding equations.

Table 4-1 Summary of clear-sky solar insolation terminology

Abbreviation	Description	units
I_0	extraterrestrial solar insolation	W/m^2
m	air mass ratio	Dimensionless
I_B	beam insolation at earth's surface	W/m^2
A	apparent extraterrestrial solar insolation	W/m^2
k	atmospheric optical depth	Table 7.6 (Masters, 2004)
C	sky diffuse factor	Table 7.6 (Masters, 2004)
I_{BC}	beam insolation on collector	W/m^2
θ	incidence angle	Degree
Σ	collector tilt angle	Degree
I_H	insolation on a horizontal surface	W/m^2
I_{DH}	diffuse insolation on a horizontal surface	W/m^2
I_C	insolation on collector	W/m^2
n	day number	1-365 Dimensionless
β	solar altitude angle	Degree
δ	solar declination	Degree
ϕ_s	solar azimuth angle (+ = AM)	Degree
ϕ_c	collector azimuth angle (+ = SE)	Degree
L	latitude	Degree
H	hour angle	Degree

Reference to (Masters, 2004), the total beam insolation I_B at earth surface in clear sky day is defined by

$$I_B = Ae^{-km} \quad \text{eq. 4-1}$$

Where:

$$m = \frac{1}{\sin\beta} \quad \text{eq. 4-2}$$

$$A = 1160 + 75 \sin \left[\frac{360}{365} (n - 275) \right] \quad W/m^2 \quad \text{eq. 4-3}$$

$$k = 0.174 + 0.035 \sin \left[\frac{360}{365} (n - 100) \right] \quad \text{eq. 4-4}$$

In order to relate this radiation to the specific factory location, the approach followed by (Masters, 2004) will be used, in which the energy that can be harvested during the year sunlight hours will be calculated, starting with general situation of inclined solar collector, then adjust the equations to fit for horizontal plan collector. Figure 4-2 illustrates the clear sky insolation on tilt collector (Σ) surface which is equal to

$$I_{BC} = I_B \cos \theta \quad \text{eq. 4-5}$$

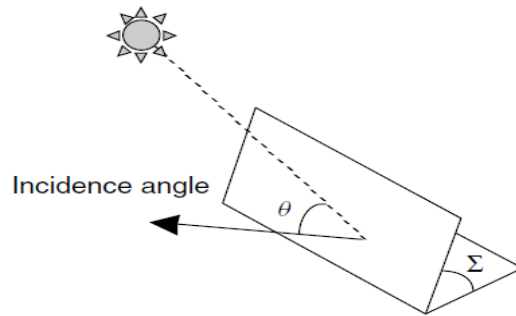


Figure 4-2 The incidence angle θ between a normal to the collector face and the incoming solar beam radiation

The incidence angle can be found as in with the help of Figure 4-3 with respect to the measured angles.

$$\cos \theta = \cos \beta \cos(\phi_S - \phi_C) \sin \Sigma + \sin \beta \cos \Sigma \quad \text{eq. 4-6}$$

$$\sin \beta = \cos L \cos \delta \cos H + \sin L \sin \delta \quad \text{eq. 4-7}$$

The sun altitude angle resulted is a function of the sun location in the sky at each hour of the day as shown in eq. 4-6 and eq. 4-7.

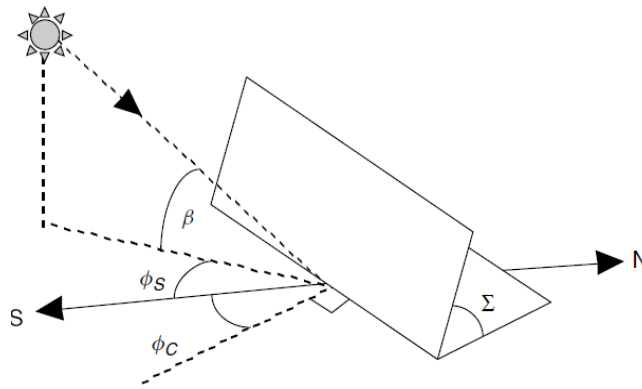


Figure 4-3 Illustrating the collector azimuth angle ϕ_C and tilt angle Σ along with the solar azimuth angle ϕ_S and altitude angle β .

Since we will be dealing with solar collectors with tracking capabilities (IRENA, 2012), and for comparison reasons the preceding equation (eq. 4-6) should be adjusted to fit the horizontal plan, i.e. tilt angle Σ equal to zero, this will modify the incidence angle to be equal

$$\cos \theta = \sin \beta \quad \text{eq. 4-8}$$

The above equations were programmed into a (MATLAB, 2015) M-file. To validate the code initially, it is compared with commercially proven software. PVSyst R6.7 (*PVSyst – Logiciel Photovoltaïque*, no date) is used for comparison. Figure 4-4 (a) presents the obtained sun path diagram from PVSyst, and Figure 4-4 (b) illustrates the programmed code sun path relevant to factory location, both are calculated based on solar hour basis.

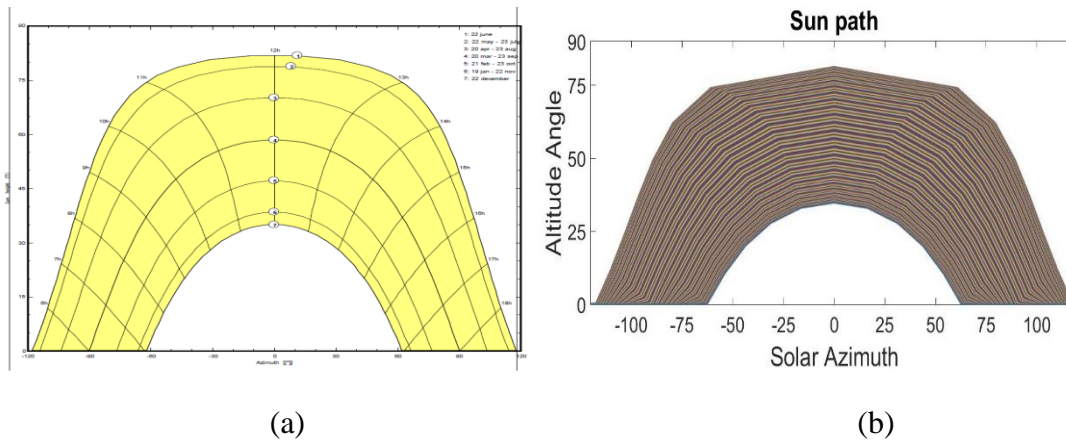


Figure 4-4 Sun path diagram from a) PVSyst software b) for the facility location

Figure 4-5 illustrates the beam radiation that can reach the facility location on clear sky day over a year, Figure 4-6 presents the amount of beam irradiation that can be collected each hour daily on horizontal surface.

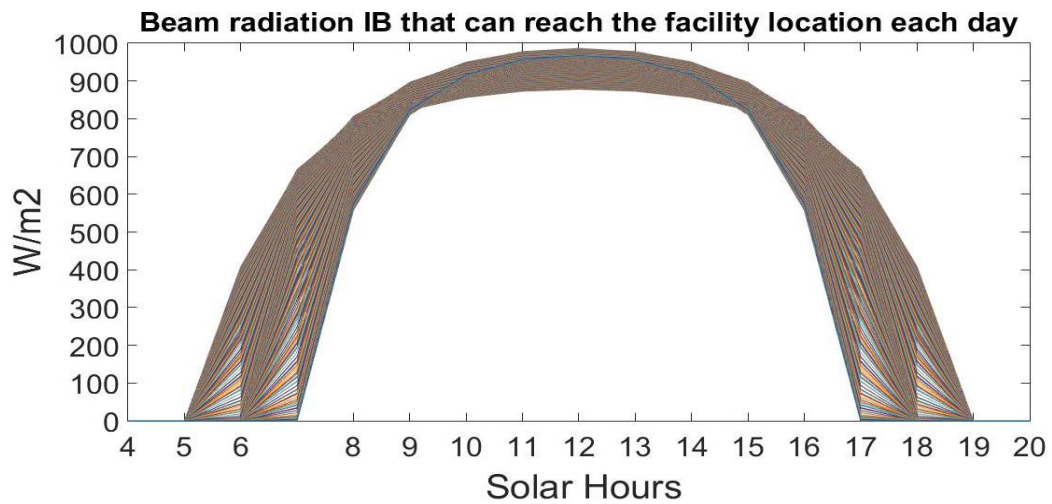


Figure 4-5 I_B that reach earth surface over a year

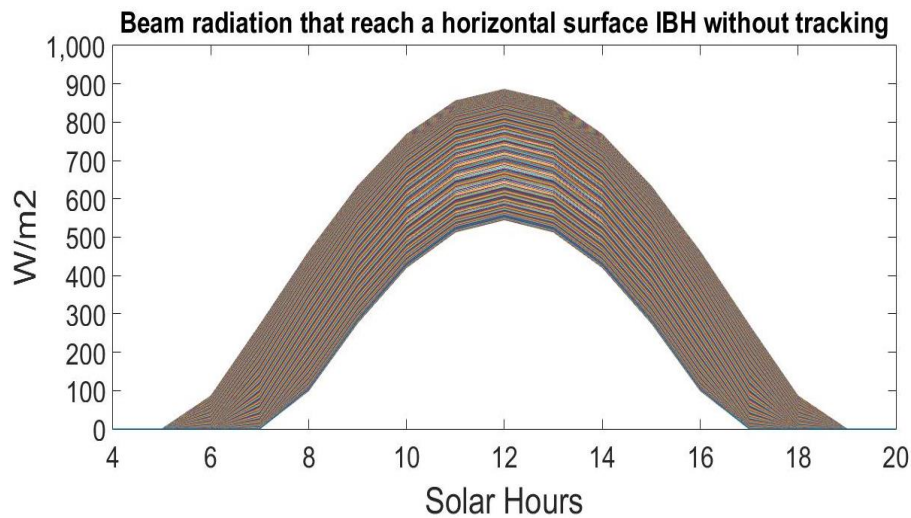


Figure 4-6 Beam radiation on horizontal surface collector

4.3 Solar thermal collector selection

Several solar thermal technological advancements occur every year, in terms of collector apparatus, collector receiver, and many other factors. However, since 1977 the International Energy Agency IEA have adopted an initiative to “to enhance collective knowledge and application of solar heating and cooling through international collaboration to reach the goal set in the vision of solar thermal energy meeting 50% of low temperature heating and cooling demand by 2050.” (Krummenacher and Muster, 2015). Under the category of Solar Heating and Cooling program SHC, the members of the IEA SHC projects (referred to as ‘task’) have developed in the field of research, development, demonstration (RD&D), and test methods for solar thermal energy and solar buildings over 50 tasks, 47 tasks had finished.

The methodology of this thesis will depend on the outcomes of IEA SCH task 49, which is dedicated to Solar Heating in Industrial Processes SHIP. Starting with the classification of use of solar thermal collectors depending on the commercially available technologies. Figure 1-4 (Horta, 2016) puts 2 technologies in our hands for selection that can work in the food and beverage industry within temperature range of $150\text{ }^{\circ}\text{C} < T < 250\text{ }^{\circ}\text{C}$. First, Parabolic Trough PT. Second, Linear Fresnel

LF. For details about construction and theoretical operation principle (Horta, 2016) is a good reference to start with.

“Parabolic Trough concentrator (PT): tracking line-focus concentrator designed after the parabola geometrical feature of reflecting any ray incident on its aperture parallel to its axis to the parabola focus; one-axis tracking around the longitudinal (absorber) axis; coupled with evacuated or non-evacuated (single-pass) absorber tubes; depending on the absorber and on the effective concentration factor is suitable to the medium temperature ranges ($100^{\circ}\text{C} < T < 250^{\circ}\text{C}$); Figure 4-7 (Group, 2015).

Linear Fresnel reflector (LF) Concentrator: tracking line-focus concentrator designed after the Fresnel principle of dividing a parabola into segments displaced in (or close to) a horizontal plane; individual mirror one-axis tracking around the longitudinal axis; coupled with evacuated or non-evacuated (single-pass) absorber tubes located at a vertical displacement related to its focal length; used with a secondary concentrator located around the absorber to enhance its optical behavior; depending on the absorber and on the effective concentration factor is suitable to the medium temperature ranges ($100^{\circ}\text{C} < T < 250^{\circ}\text{C}$)” Figure 4-8 (Industrial Solar GmbH, 2010). (Horta, 2016)



Figure 4-7 PTC 1800



Figure 4-8 LF-11 module

The linear Fresnel collector LF is selected for the following reasons (IRENA, 2012):

1. LFCs flat mirrors used are from the standard commercial type,
2. LFCs steel structure that holds the moving parts is easier to install and maintain,
3. The configuration of LFC reduces the wind loads on the apparatus, which results additionally in less thermal and optical losses, moreover reducing mirror damaging.
4. Although the concentration ratio in PTC is higher than in LFC, however, due to the flatness configuration in LFT it increases the acceptance angle.

From the commercially installed Concentrating Solar Power CSP worldwide, (GROUP, 2017), many projects were installed and successfully operate from pioneer companies. The world most commonly used LF is the module LF-11 from Industrial Solar- Germany, which is installed for the range of temperatures required in this thesis.

LF-11 module from (Industrial Solar GmbH, 2010) is “a solar thermal collector optimized for industrial applications. It can provide heat at up to 400°C and operate with pressures of up to 120 bars. Besides water, therminol or high-temperature glycol it can also generate steam directly. Due to its modular design, the system can be scaled up from a few hundred kW to several MW”. Complete data sheet of the selected CSP LF-11 is attached in appendix A.

In the previous section the modeling of irradiation on a fixed horizontal surface was presented. In terms of LF, the incidence angle $\cos \theta$ have to be adjusted, in order to minimize this angle hence maximize the direct beam irradiation harvested.

The difference between the two modeling processes depends on the working principle of the LF Figure 4-9. The LF has two main parts, a collector which is stationary flat mirrors, and a receiver which is evacuated or non-evacuated tube surrounded by a secondary reflector/ concentrator to enhance the optical performance of the module. The sun is reflected from the primary mirrors on to the absorber tube, some of the sun reflected rays hits the secondary reflector, which again reflects it back on the absorber.

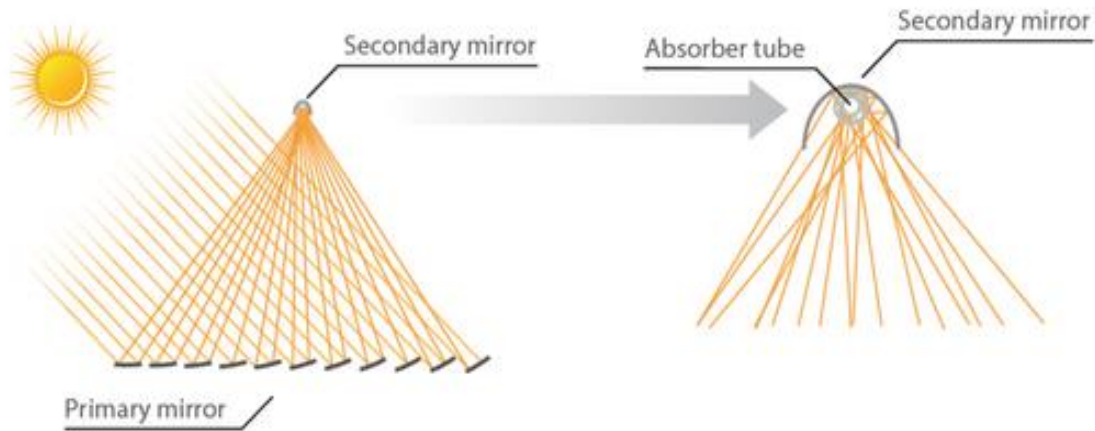


Figure 4-9 Industrial Solar LF-11 working principle

Based on (Duffie and Beckman, 2013), the incidence angle for a horizontal single axis tracking system rotated about north-south axis to minimize the angle of incidence is:

$$\cos\theta = \sqrt{(\cos^2 \theta_z + \cos^2 \delta \sin^2 H)} \quad \text{eq. 4-9}$$

Where:

θ_z : is the incidence angle between the sun beam and the normal on the surface, in this case of horizontal plane it is the zenith.

The irradiation that can be collected using eq. 4-9 is shown in Figure 4-10, it compares the summer and winter extraterrestrial solar radiation for slope equal to latitude =45° facing south, and on north-south (N-S) and east-west (E-W) horizontal single-axis tracking collectors. The comparison is on summer and winter solstice. The comparison shows that in winter the fixed system can collect more irradiation compared to traditionally mounted N-S single axis collectors, however in summer the time span for collection is wider and the amount is higher.

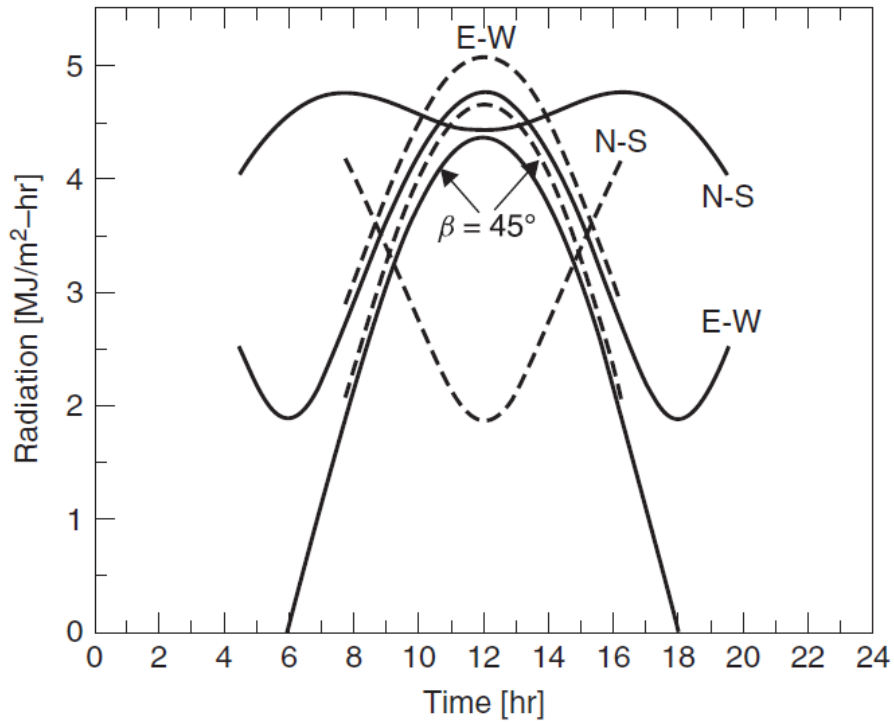


Figure 4-10 Extraterrestrial solar radiation for $\Sigma = 45^\circ$ on a stationary collector at $L = 45^\circ$ on north-south (N-S) and east-west (E-W) single-axis tracking collectors. The three dotted curves are for the winter solstice and the three solid curves are for the summer solstice

It is to be noted that according to geometry in Figure 4-11 (Duffie and Beckman, 2013) and in order not to introduce another variable,

$$\cos\theta_z = \sin\beta \quad \text{eq. 4-10}$$

Then substituting in eq. 4-9

$$\cos\theta = \sqrt{(\sin^2\beta + \cos^2\delta \sin^2H)} \quad \text{eq. 4-11}$$

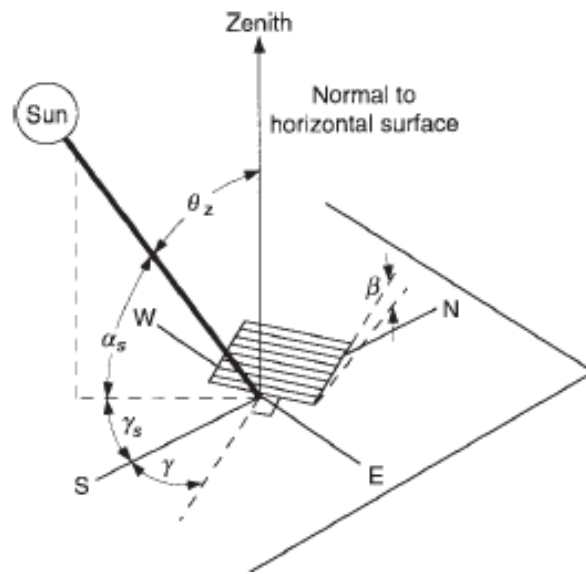


Figure 4-11 Zenith angle θ_z related to sun altitude angle α_s ,

After simulation of eq. 4-11 over a year course, the beam irradiation that can be harvested by horizontal single axis solar collector is shown in Figure 4-12

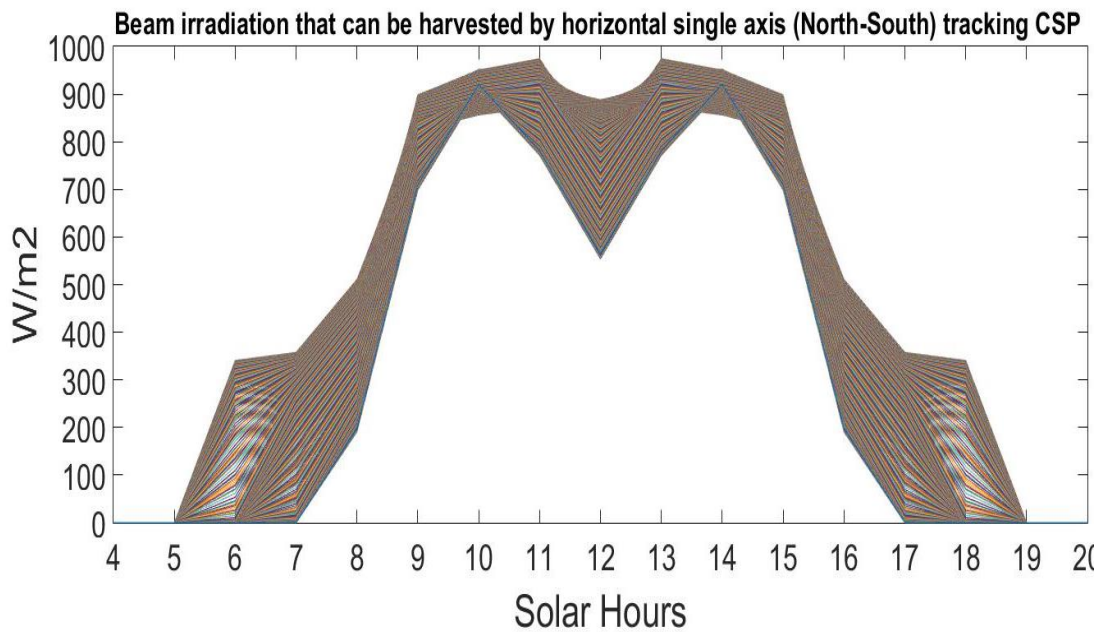


Figure 4-12 beam irradiation that can be harvested by single axis tracking CSP

Based on the geometry of the LF and the sun path, the reflected beam is analyzed into two main axis that constitute the portion of sun beam that reaches the absorber. The transversal axis normal to absorber tube (θ_T), and longitudinal axis parallel to the absorber tube (θ_L) as shown in Figure 4-13 (Wagner, 2012)

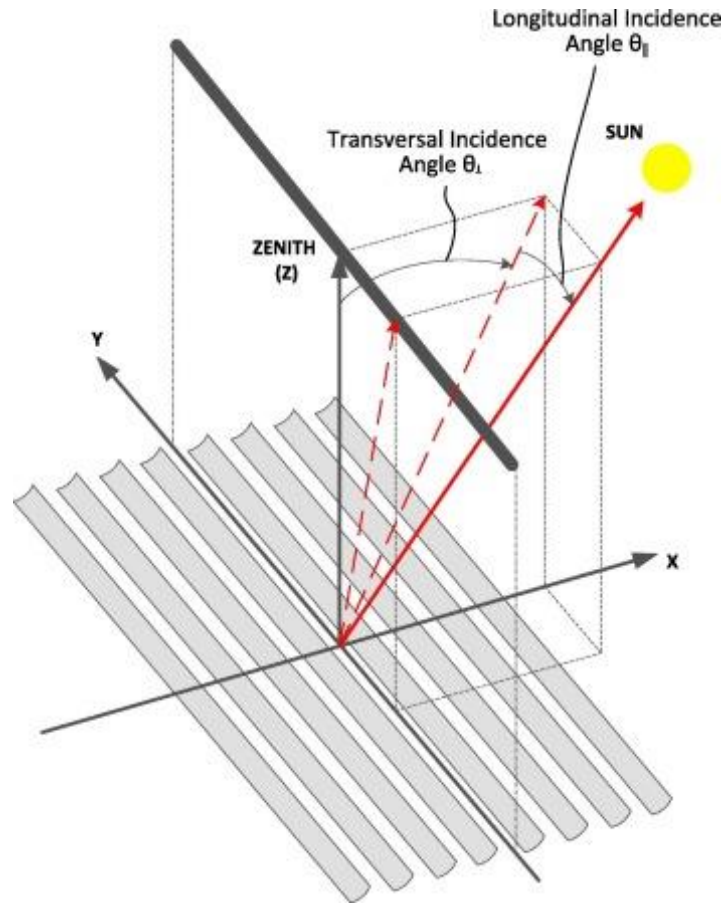


Figure 4-13 Angles associated with the optical performance of the LFR technology, including transversal incidence θ_T , longitudinal incidence θ_L , solar zenith ϑ_z , and solar azimuth γ_s .

According to (Giovannetti *et al.*, 2016), the steady states model that describes the specific heat gained \dot{Q} per gross area (A) of the CSP is equal to

$$\frac{\dot{Q}}{A} = I_{BC} \eta_{opt} \psi(\theta_T, \theta_L) - a_1(T_m - T_{amb}) - a_2(T_m - T_{amb})^2 \quad eq. 4-12$$

Where:

η_{opt} : optical or zero-loss efficiency that accounts for the loss between aperture area and absorber, in the chosen module LF-11 Figure 4-14 (INDUSTRIAL SOLAR, 2009), it is equal $\eta_{opt} = 0.635$

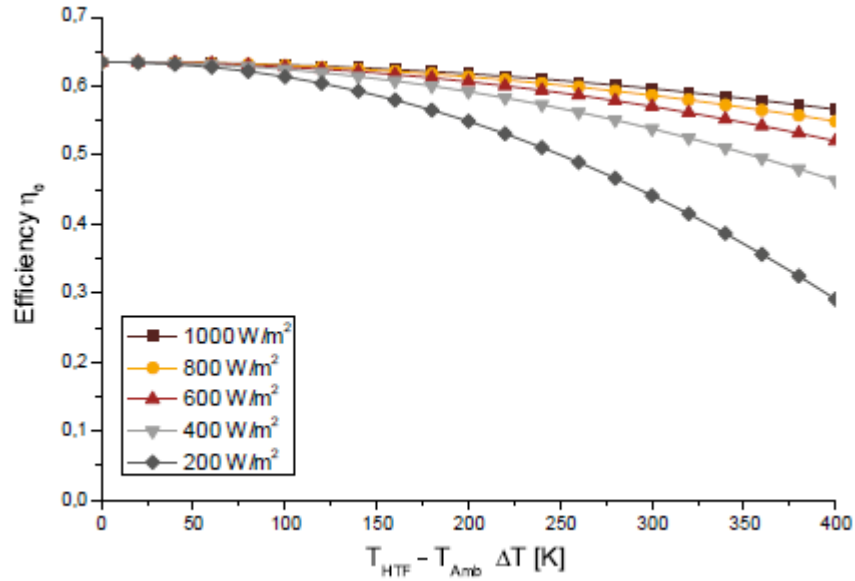


Figure 4-14 Characteristic collector curve

$\psi(\theta_T, \theta_L)$: Incidence Angle modifier under normal incidence, it accounts for the incidence conditions (both on the Longitudinal and Transversal directions) over the optical performance of the collector. In the chosen module LF-11, the incidence angle modifiers have to be interpolated as the data sheet gives for integer incidence angles the values of transvers and longitudinal Table 4-2 (INDUSTRIAL SOLAR, 2009). After finding the values corresponding to each incidence angle it has to be multiplied with the other variables in the equation.

$a_1(T_m - T_{amb})$: thermal loss coefficient depending on difference between ambient temperature and mean temperature of the absorber, in the chosen module LF-11, this value is not mentioned.

$a_2(T_m - T_{amb})^2$: thermal loss coefficient under prescribed conditions in Table 4-3 (INDUSTRIAL SOLAR, 2009). For the chosen module LF-11, $a_2 = 0.00043 W/(m^2K^2)$

The evaluation of the heat loss depends on the load profile of the factory, assuming the Heat Transfer Fluid HTF flowing in LF-11 is *Therminol 66* (Eastman Chemical Company, 2002), with a

flow rate of $\dot{m}_{TF} = 1 \text{ kg/s}$, the heat loss term $a_2(T_m - T_{amb})$ depends on the mean temperature of the receiver, and the heat capacity of the TF used C_{pTF} , based on the first law of thermodynamics,

$$\dot{Q}_{loss} = a_2(T_m - T_{amb})^2 = \dot{m}_{TF} C_{pTF} (T_m - T_{amb}) \quad \text{eq. 4-13}$$

The monthly average ambient temperature changes between January and July between 13°C and 27°C (*PVSyst – Logiciel Photovoltaïque*, no date) Table 4-4.

Table 4-2 Incidence angle modifier for LF-11 module

Angle	Transversal	Longitudinal
00	1.000	1.000
05	1.044	0.962
10	1.000	0.937
15	1.034	0.907
20	0.996	0.867
25	1.015	0.821
30	0.998	0.768
40	0.956	0.640
50	0.951	0.485
60	0.784	0.311
70	0.553	0.141
80	0.300	0.022
90	0.075	0.000

Table 4-3 Prescribed conditions for testing of LF-11

30°C ambient temperature	900 W/m ² direct normal radiation
160°C inflow temperature	Azimuth angle 90°
180°C outflow temperature	Zenith angle 30°

In a clear sky day, based on the hourly heat gained the HTF temperature will rise, and so the heat capacity C_{pTF} will change between 1.56 kJ/kg.K at 10°C up to 2.38 kJ/kg.K at 250°C, the data sheet of *Therminol 66* (Eastman Chemical Company, 2002) is attached in appendix B.

Utilizing the heat gained each hour $I_{BC} \eta_{opt} \psi(\theta_T, \theta_L)$ in eq. 4-12, and substituting in eq. 4-13 to calculate the final temperature at each hour and evaluate the heat loss. In order to simplify the calculations, the extreme heat loss is subtracted from the hourly heat gained,

$$\dot{Q}_{loss} = a_2(T_m - T_{amb})^2$$

$$\dot{Q}_{loss} = 0.00043 \times (523 - 286)^2 = 24.1 \text{ W/m}^2$$

eq. 4-14

Since the HTF can be heated up to 345°C (Eastman Chemical Company, 2002), and the process requires maximum 210°C of temperature, and assuming system losses like pipes and heat exchangers, from engineering point of view it would be logical to allow the HTF to reach 250°C, then the mirrors will defocus the radiation, this will avoid over estimation of the system and additional protection costs.

Table 4-4 Average ambient temperature

Definition of a geographical site

Geographical Site	Al qasrawi factory										Country	Palestinian Territory,		
	File al qasrawi factory_MN71.SIT of 15/05/20 16h42													
Situation	Latitude		31.51° N					Longitude		35.08° E				
Time defined as	Legal Time		Time zone UT+2					Altitude		0 m				
Monthly Meteo Values	Source: Meteonorm 7.1 (1990-2004), Sat=100%													
	Jan.	Feb.	Mar.	Apr.	May	June	July	Aug.	Sep.	Oct.	Nov.	Dec.	Year	
Hor. global	92.9	106.1	166.6	191.9	231.7	246.5	249.0	228.6	185.8	145.8	107.3	90.3	2042.5	kWh/m ² .mth
Hor. diffuse	44.7	47.3	62.0	72.8	71.7	52.7	55.1	54.4	52.0	49.7	38.4	38.2	639.0	kWh/m ² .mth
Extraterrestrial	176.7	198.4	268.2	305.2	344.5	344.0	350.2	327.5	277.7	236.6	182.3	164.0	3175.2	kWh/m ² .mth
Clearness Index	0.526	0.535	0.621	0.629	0.672	0.717	0.711	0.698	0.669	0.616	0.589	0.551	0.643	
Amb. temper.	13.1	13.8	16.4	19.2	22.4	25.1	27.6	27.9	26.1	23.6	18.9	15.1	20.8	°C
Wind velocity	3.3	3.4	3.2	3.2	3.2	3.3	3.4	3.2	3.2	2.8	2.7	2.9	3.1	m/s

4.4 Simulation of the solar collector

In the previous sections the models that describe the behavior of solar collectors either fixed or single axis tracking were presented. In this section the simulation of the previous equations will be presented.

For comparison purpose between the two collectors technologies and the impact of tracking system on the irradiation collected, Figure 4-15 presents the concept of single axis tracking as maximizing the radiation that can be gained by the collector (black colors), relevant to the available irradiation (red color), and comparing it to horizontal fixed collector (yellow colors)..

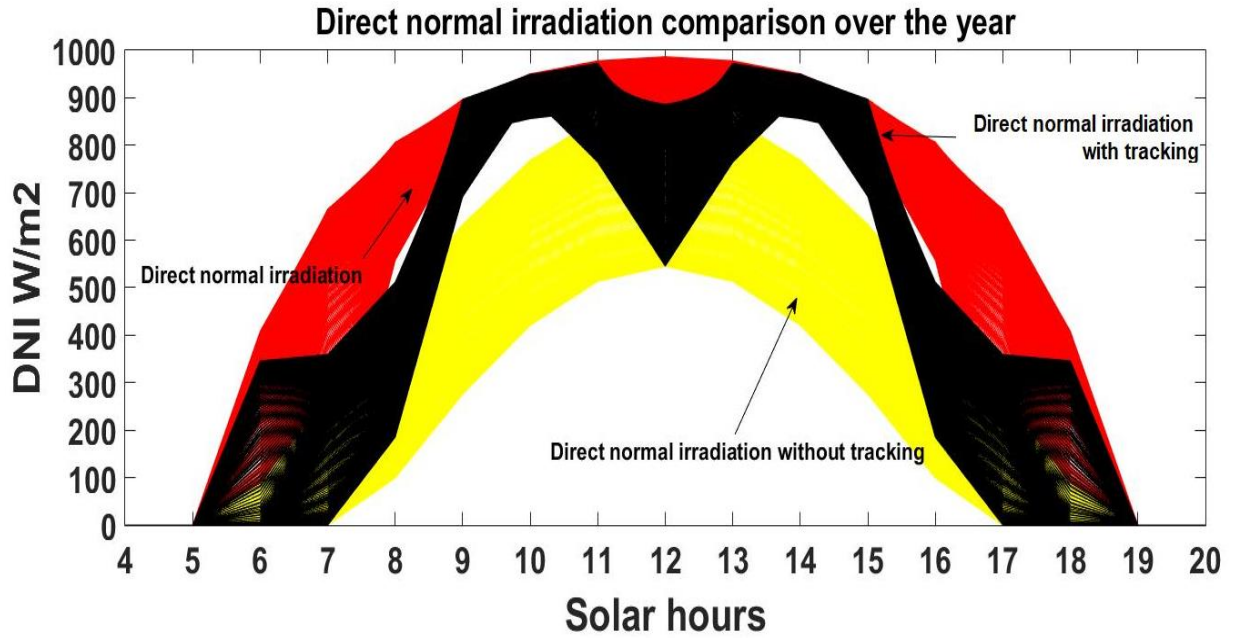


Figure 4-15 Beam irradiation comparison based on the collector technology used

In terms of the heat gained compared to available heat for fixed solar collector, the efficiency of the solar collector was assumed 25% at the operating temperature of the process 150°C Figure 4-16 (Moss *et al.*, 2018), Figure 4-17 (a) shows that the maximum heat gain is 1.74 kW/m².

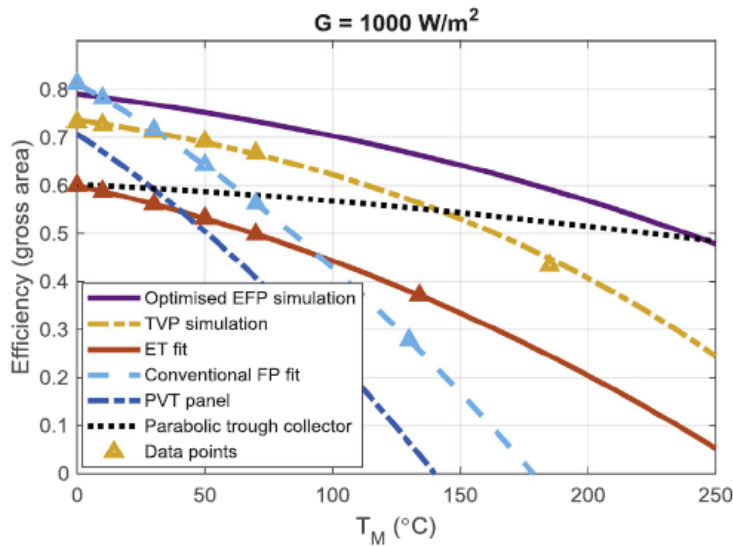


Figure 4-16 Efficiency of flat plate collector at mean temperature of 150 °C

Comparing this amount to what can be harvested by single axis tracking LF-11, Figure 4-17 (b) presents a huge difference of heat gained with tracking technology reaching up to 3.8 kW/m².

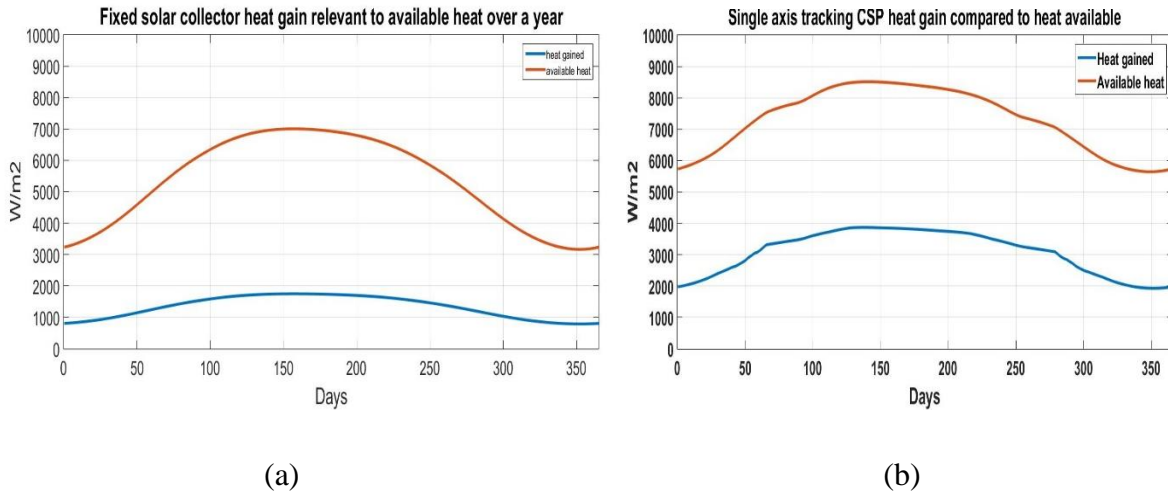


Figure 4-17 Heat gain relevant to available heat over a year :a)Fixed solar collector b) Single axis tracking CSP

Figure 4-18 illustrates that the LF-11 serves the purpose of collecting higher irradiation and eventually would serve the plant thermal load. In addition, the LF-11 have good efficiency most of the year, especially in summer, where the ambient temperature goes higher, still the Fresnel performs well.

It is to be noted that the calculations are based on steady state model, and the factors related to diffuse irradiation, wind speed, thermal losses under prescribed operation and ambient temperature conditions, and long wave irradiance time dependent thermal capacitance of the collector are all ignored in this simulation, as these factors are to be addressed in the testing facility under prescribed conditions. In addition, the data sheet of LF-11 provides the necessary parameters needed to calculate the heat gain using steady state model, subsequently the area and investment requirements that will be calculated in next chapters.

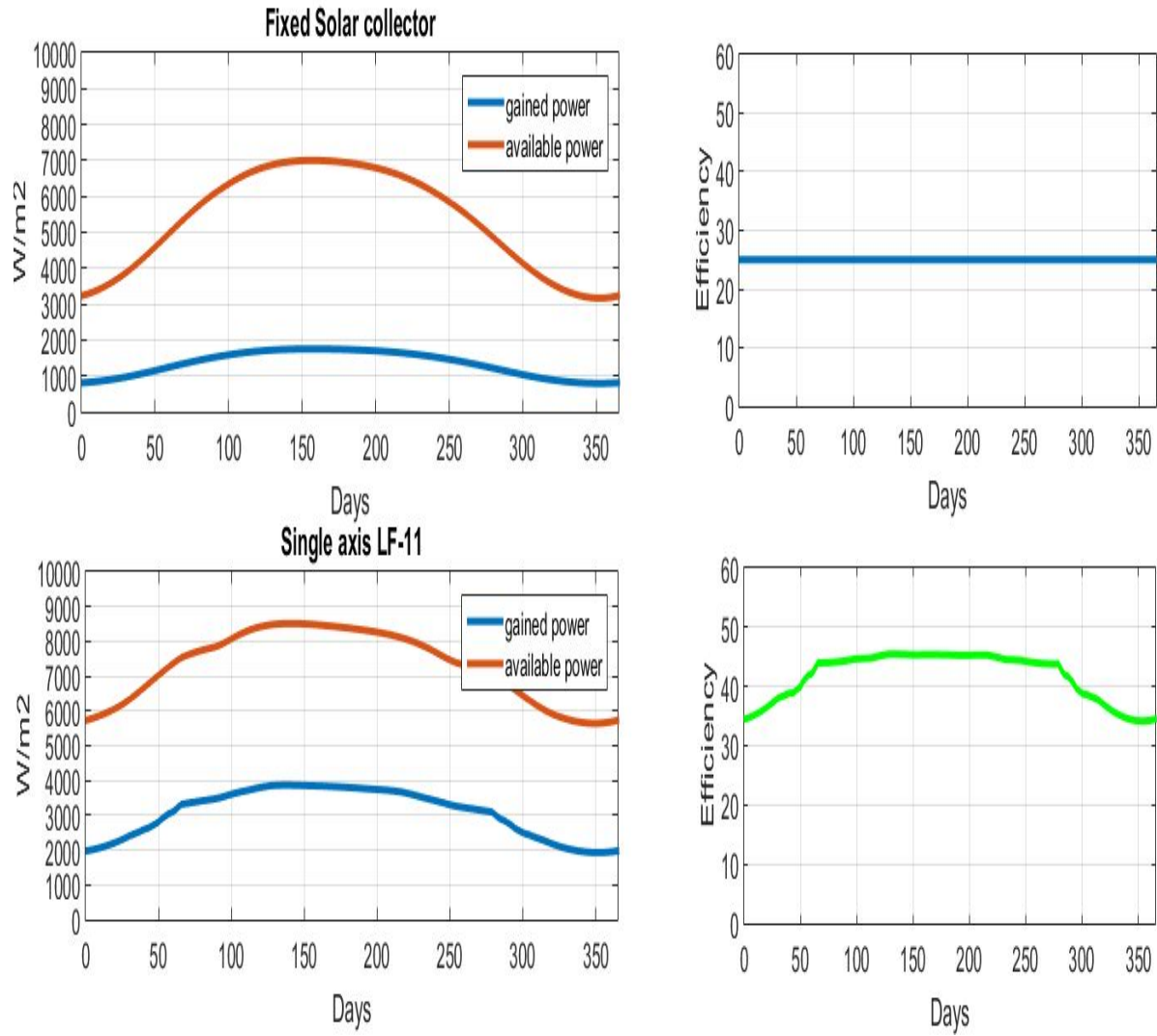


Figure 4-18 Comparison between technology in terms of efficiency

Chapter-5

Integration of Solar Plant with Factory Thermal Loads

This chapter is dedicated to integration scheme and calculations of the solar plant area, in addition to the thermal loads profile in the factory.

Using the previously calculated loads in Chapter 3 and heat gain per m² in chapter 4, the surface area of the LF-11 will be calculated. Then the integration scheme according to industrially adopted practices will be presented and discussed. After that, the Thermal Storage TS tank sizing will be estimated roughly.

5.1 Solar collector LF-11 surface area

Using the previously calculated thermal loads of the factory summarized in Table 3-2, and the heat gain of LF-11 per square meter Figure 4-17 (b), which ranges between 3.8 kW in summer peak 21st June and minimum of 1.9 kW in 21st Dec.

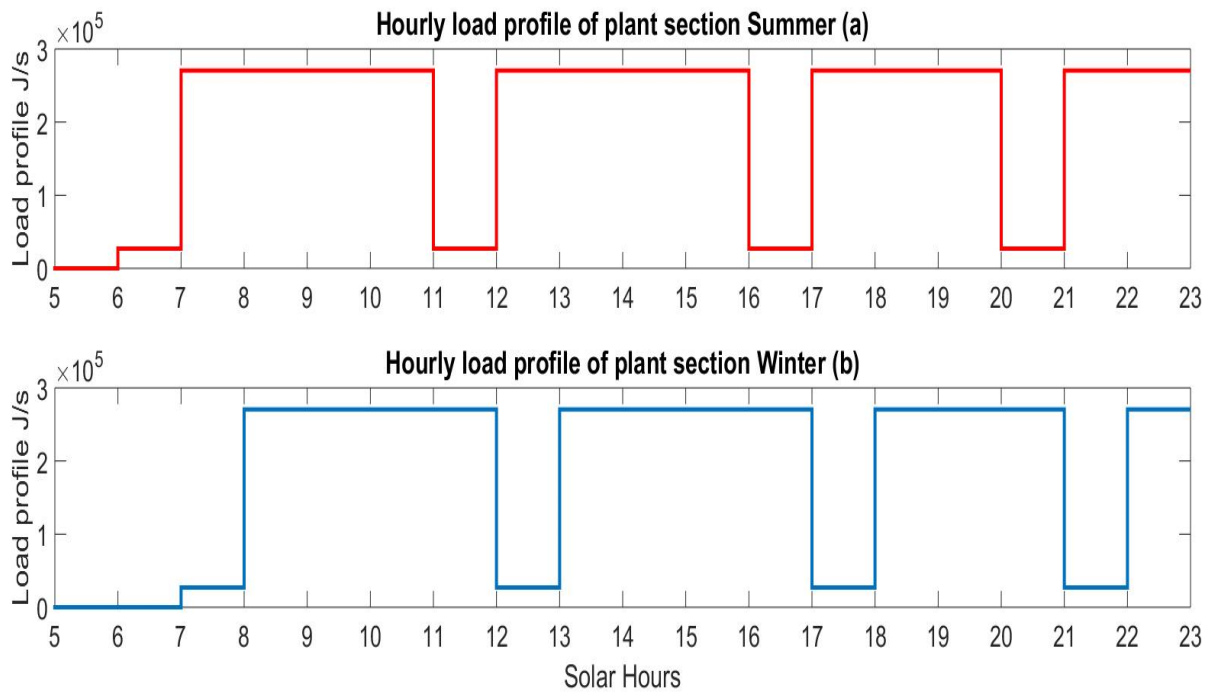


Figure 5-1 Hourly load profile of plant sections (a) Summer profile (b) winter profile

In order to evaluate the area needed by the collector, the load profile over a day course is needed. Loads of the factory follow a typical daily profile, where the day shift starts at 07:00 o'clock in the morning, and a break for prayer and lunch at 12:00 Pm. A shift change occurs at 17:00 Pm. Another break time at 20:00 and the night shift ends at 23:00 Pm. One day holiday on Friday. The plant sections' accumulative hourly load profile is shown in Figure 5-1.

The load starts with 10% of the energy required by each station, which is the amount needed to heat up the process medium. After that, the process starts working continuously with a 100% load assuming a steady flow of material to be dried. During the break times and shift change the load available is the one required to keep the process medium at the required temperature, which is approximately 10% of full load. During summer the solar hours are around one hour in advance of local time, and so the summer load profile is adjusted to account for this adjustment as shown in Figure 5-1 (a) and (b) for winter time. Solar hours are used to enable the calculations with heat gained by LF-11.

Depending on the manufacturer data that shown in Figure 5-2 (INDUSTRIAL SOLAR, 2009), the standard recommended module length is 65 m of LF-11. It has an area $7.5 \times 65 = 487.5 \text{ m}^2$. The available area of the roof is 3000 m^2 . If the chosen total area of the LF-11 is 1080 m^2 ($7.5 \text{ m} \times 4 \text{ m} \times 4 \text{ modules/row} \times 9 \text{ rows}$). Then the heat gain of solar collector compared to the load profile at summer and winter solstices would be as shown in Figure 5-3.

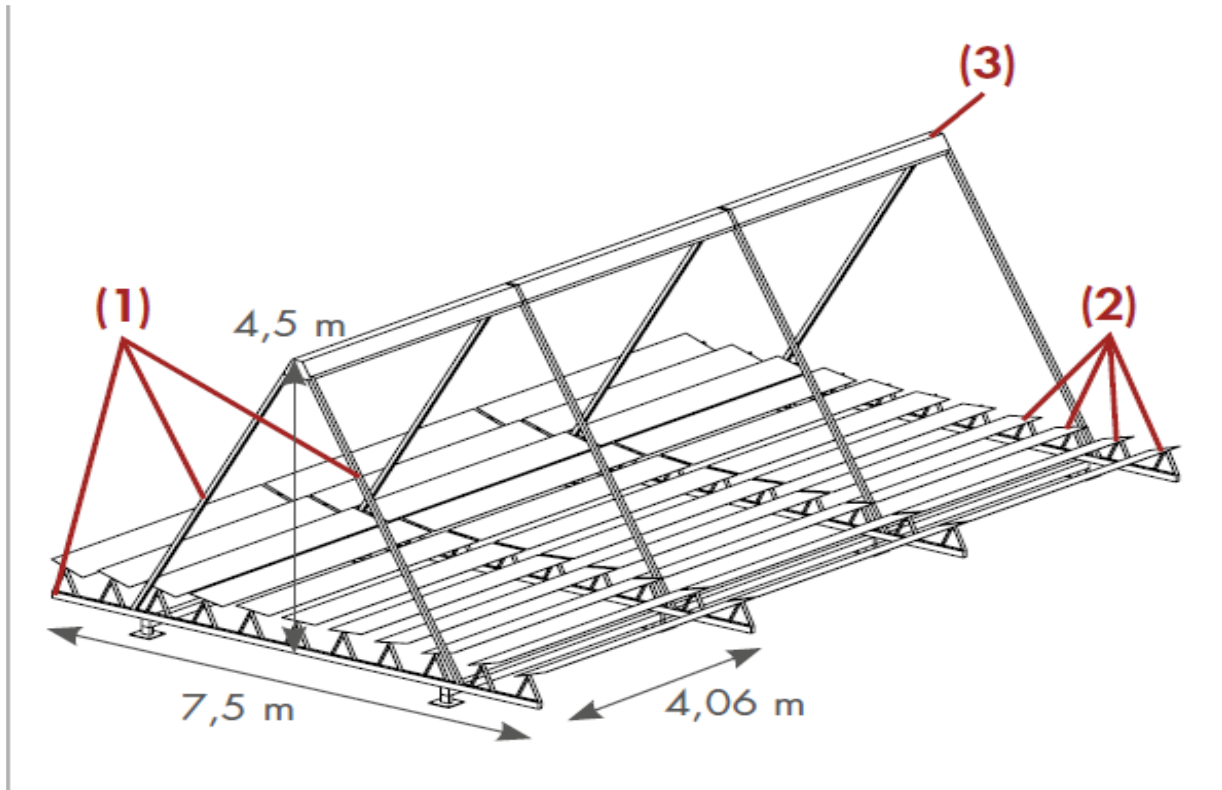


Figure 5-2 LF-11 module size, (1) supporting structure, (2) primary reflector, (3) receiver, consisting of secondary reflectors

It's clear that the solar collector can satisfy partial load requirement during summer and winter. The excess heat gained daily by LF-11 should be transferred to the night shift with Thermal Storage TS tank.

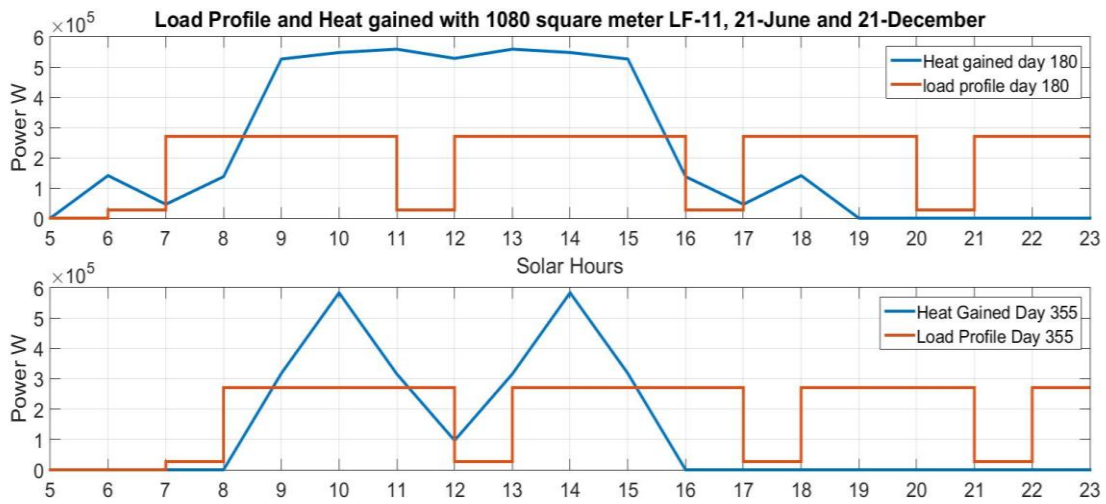


Figure 5-3 Comparison of load profile and 2 standard LF-11 modules (area of 1080 m²) heat gain in day=180(summer) and day =355(winter)

The deficiency of the chosen modules LF-11 heat gained compared to load profile over a year course is shown in Figure 5-4. In autumn and winter (from day 255 to day 55) (11th September- 24th February) it is clear that LF-11 can satisfy the load demand partially, and the heat gained cannot satisfy the two shifts thermal loads demands.

From (day 55 to day 255) (24th February- 11th September) there would be excess heat gain more than the thermal loads demand of the factory. Additionally, the drop in day 81 (21st March) and day 295 (21st October) is due to the beam radiation and incidence angle that described in eq. 4-9 (Duffie and Beckman, 2013) would give an abrupt change as was shown in Figure 4-10.

The choice of gross area of 1080 m² is clearly proving to be a good choice in terms of the heat gain, as more than half of the year the thermal load demand is satisfied with 15% excess. However, the contribution of the LF-11 for the remaining days in the year as shown in Figure 5-5. It is less than the demand requirements to about 30% shortage in December.

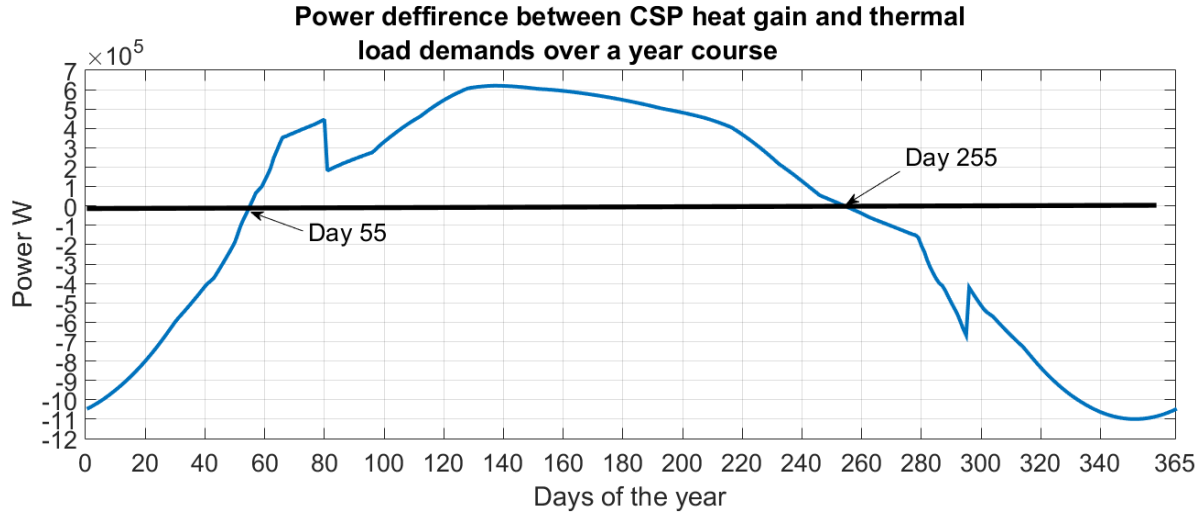


Figure 5-4 Difference between load demands of the factory and LF-11 standard modules heat gained over a year

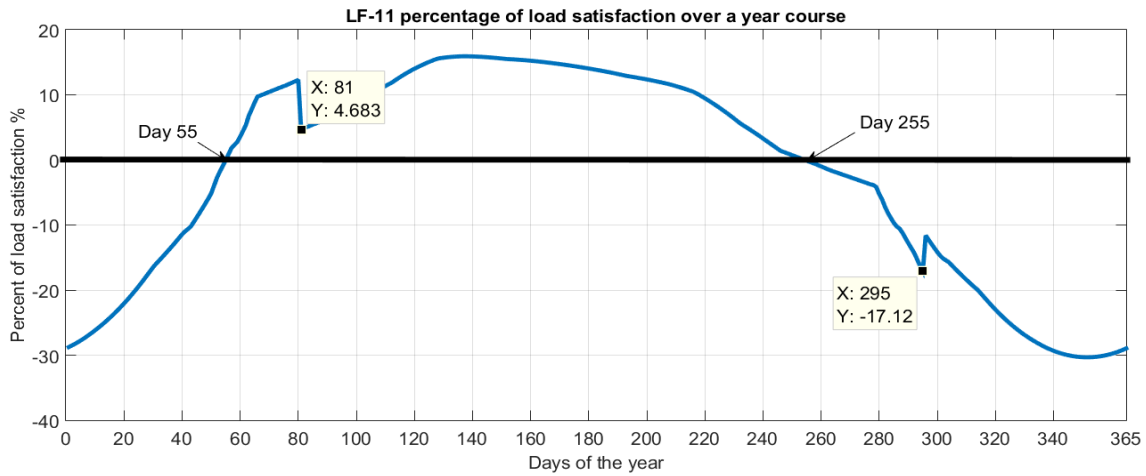


Figure 5-5 Percentage of load satisfaction by the chosen LF-11 area over the year course

5.2 Integration scheme

Referred to the standards of International Energy Agency IEA task 49 Figure 5-6 the integration of solar thermal plant depends on the intended usage and the nature of process available and on the possibility of investment (Muster-Slawitsch *et al.*, 2015).

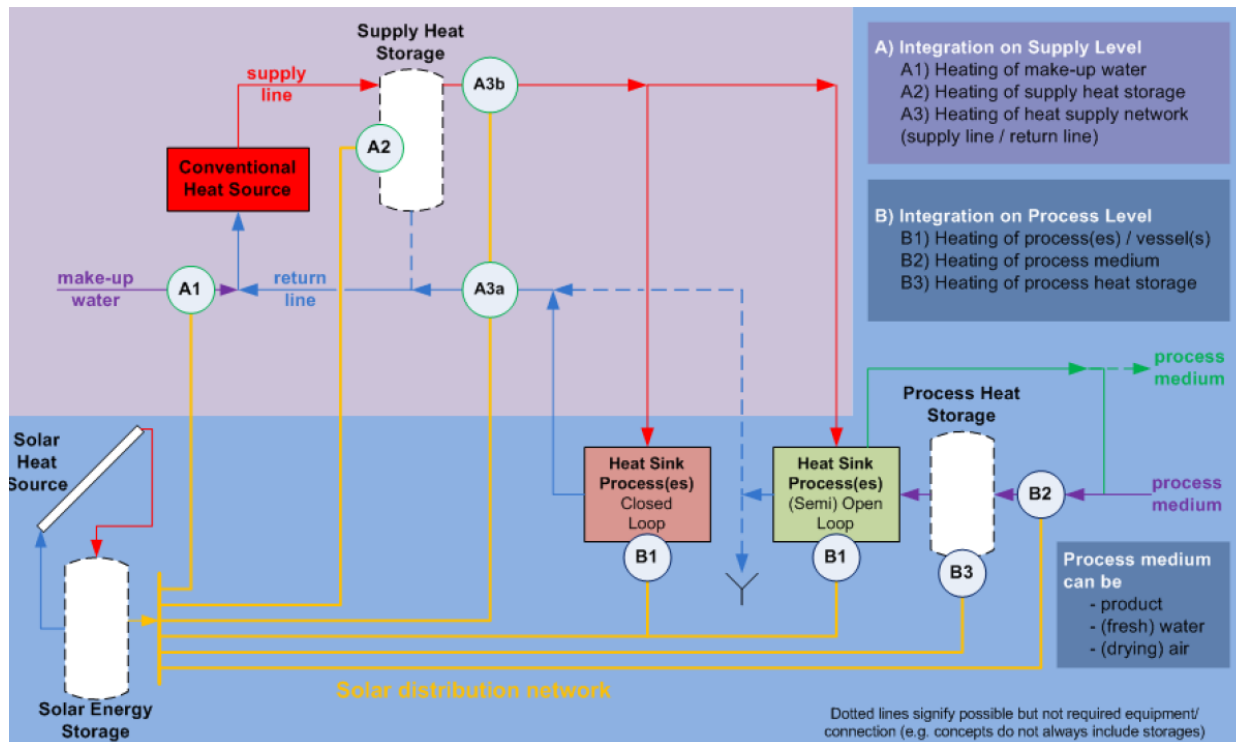


Figure 5-6 Possible integration points for solar heat, A is for supply level, B for process level

The choice of the integration scheme depends on the available process equipment, the burners or the conventional heat suppliers is heating the process medium (oil, air) through heat exchangers. In order to keep the current situation of the factory running specially in winter where the chosen system LF-11 with estimated area cannot meet the required loads, the scheme in Figure 5-7 (Muster-Slawitsch et al., 2015) is recommended.

The usage of the storage tank depends on the load profile available, since the factory runs a night shift, then it would be logical to store some of the excess heat gained by the collector to cover night shift demands. The choice of the size of the storage tank depends on investment and load profile to be covered.

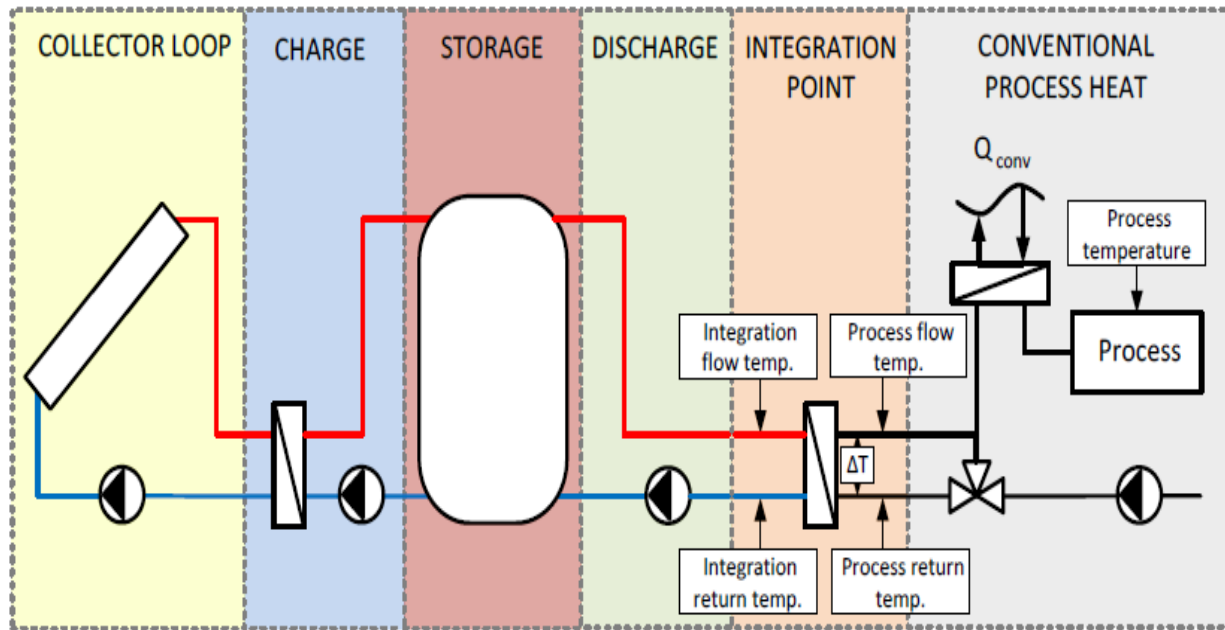


Figure 5-7 SHIP system for pre-heating with five subsections supplying an industrial heat consumer. The integration concept exemplary shown is PL_E_PM, i.e. on process level an external heat exchanger heats a process medium

The discharge section allows integration of many process with CSP through storage tank. The integration point could be a heat exchanger a valve or a T piece. The selection of integration point is depending on the process medium, and the flow from the storage tank (it can determine the temperature of the process medium and the heat to be transferred).

The process return temperature is a critical factor, when the return temperature is lower, the mean temperature of the solar collector is lower, enabling more heat gain. Accordingly, the load with lowest temperature level should be prioritized.

According to (TRNSYS, 2004) documentation for the design of Thermal Storage TS tanks, many configuration exists depending on the investment and loads available. It is worth noting that some tanks have many nodes (a node is a segment of the tank where thermal properties are same), this would enable the integration of different loads at different integration temperature. Utilizing

either passive (mass flow up and down due to density) or active (pump) stratification in order to maintain highest temperature required mainly during charging times.

The storage tanks have two major types (Muster-Slawitsch *et al.*, 2015), Sensible heat storage tank, where the storage medium is fluid (water, thermal oil, solid media, molten salt (Bauer *et al.*, 2012)), or latent heat storage tank, where the storage medium is (chemicals, Phase Change Material PCM).

The charging section is performing two major rules, if the heat gain can lift the temperature inside the TS, then it is allowing the HTF to exchange heat with tank storage fluid. If the CSP is not gaining heat due to shadows or night hours, the heat exchanger would isolate the TS from heating the CSP hence losing heat.

The collector loop pump is responsible for controlling the HTF temperature, where controlling the mass flow rate will control the temperature set point of the TS. Based on the above discussion, the same scheme is repeated in the factory section depending on temperature and heat needs, Figure 5-8 shows the integration points depending on the factory process. It is to be noted that in general drying section there are two drying stations. It was represented by one as only the return water which is one line to the boiler that is to be heated.

Additionally, there is an electric heater inside the corn chips machine which will not be replaced. Instead additional heat exchanger will be inserted in the machine to enable heating of air used in the process as was explained in section 3.6.

Moreover, the Besly chips and General Chips use oil as a process medium, hence the original heating system will not be changed, instead the oil supply from the oil tanks will be heated before continuing the original cycle, therefore the conventional system in all processes can adjust the process medium temperatures at any time the LF-11 couldn't fulfill the process requirements.

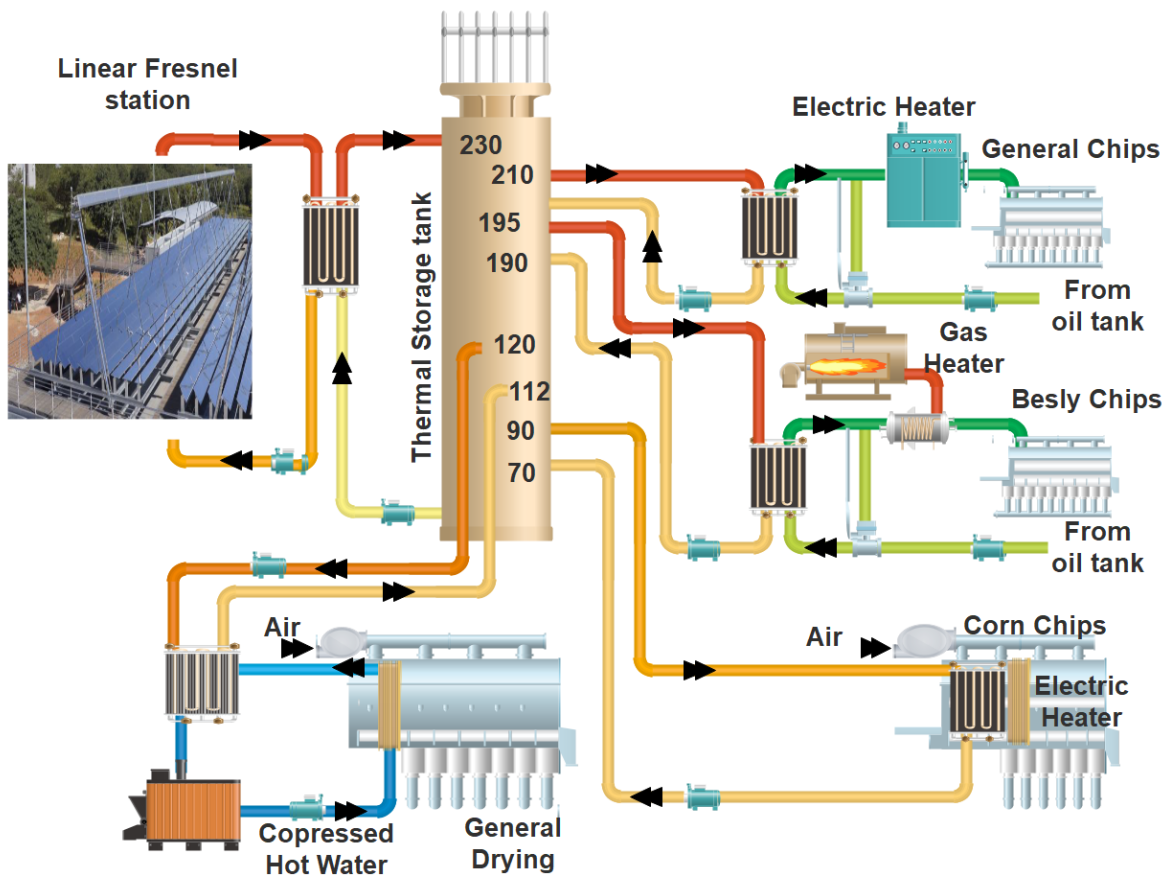


Figure 5-8 Integration scheme depending on processes in the factory and the traditional heat sources.

5.3 The Thermal Storage tank size

The size of the tank depends on the load profile of the plant. The main objective is to enable utilizing the heat of the sun during shading and night hours.

To calculate the size of the TS, referring to Figure 5-4, in the days 55 (24 February) and 255 (11 September), the load is being satisfied completely by solar heat with no excess or shortage, and so, the load profile and sun power of those two days to calculate the tank size is used.

The load profile of the factory and the heat gained by the LF-11 CSP for the date 55 and 255 are shown in Table 5-1 and Table 5-2 respectively. It can be noticed that when the load consumes

power more than what can be produced by the CSP LF-11, the difference will be negative. The total difference is approximately zero, which indicates that what is being charged is being consumed almost exactly.

Table 5-1 Comparison between the load power and heat gain in day 55

Solar Hour	Load Profile kW	Heat Gained LF-11 kW	Difference
7	27059	0	-27059*
8	270590	12531.31	-258059
9	270590	519443.9	248853.9
10	270590	610333.3	339743.3
11	270590	540988.7	270398.7
12	27059	257281.2	230222.2
13	270590	540988.7	270398.7
14	270590	610333.3	339743.3
15	270590	519443.9	248853.9
16	270590	12531.31	-258059
17	27059	0	-27059
18	270590	0	-270590
19	270590	0	-270590
20	270590	0	-270590
21	27059	0	-27059
22	270590	0	-270590
23	270590	0	-270590
		Total	-2030.37

* negative sign for heat discharge, positive sign is for the heat charging

Based on the above discussion the heat capacity size of the TS will be the sum of the negative differences, which is 1950244 kW in day 55, and 2146030 kW in day 255, and so, the TS heat capacity size should be approximately $2.2 \times 10^6 kW$.

The volume of the TS depends on the type of the heat storing material and technology, as the heat is being stored on temperatures of medium range $< 250 \text{ }^\circ\text{C}$, then from process complication point of view, water will be excluded, as the system will be pressurized and additional investment would be required.

Table 5-2 Comparison between the load power and heat gain in day 255

Solar Hour	Load Profile kW	Heat Gained LF-11 kW	Difference
6	27059	0	-27059*
7	270590	6618.889	-263971
8	270590	59570.37	-211020
9	270590	535873.6	265283.6
10	270590	566241.1	295651.1
11	27059	580984.6	553925.6
12	270590	400065	129475
13	270590	580984.6	310394.6
14	270590	566241.1	295651.1
15	270590	535873.6	265283.6
16	27059	59570.37	32511.37
17	270590	6618.889	-263971
18	270590	0	-270590
19	270590	0	-270590
20	27059	0	-27059
21	270590	0	-270590
22	270590	0	-270590
23	270590	0	-270590
		Total	2146.102

* negative sign for heat discharge, positive sign is for the heat charging

As the design of TS tank is not in the scope of this thesis, the same HTF *Therminol 66* (Eastman Chemical Company, 2002) will be used, which have the liquid density $\rho_{@ 210\text{ }^\circ\text{C}} = 878\text{ kg/m}^3$, and the enthalpy $h_{@ 210\text{ }^\circ\text{C}} = 416.1\text{kJ/kg}$. dividing the heat to be discharged by the tank over the enthalpy then by the density we get the volume of the tank,

$$Tank\ size = \frac{2.2 \times 10^6\ kJ}{\frac{416.1\text{kJ}}{kg} \times 878\frac{kg}{m^3}} = 6.022\ m^3$$

This tank size is only containing the heat required to satisfy the load in the day shift, however, in order to satisfy both working shifts, this size should be multiplied by a factor that accounts for the remaining working hours. This will be incorporated in the next chapter where the economical factor is a main concern that should be considered when evaluating system size.

The calculated tank size is an estimate that depends on the LF-11 heat gain which is originally depending on clear sky irradiation calculations. Hence, the tank size exact size depends on the investment and available space in the factory and the type of heat storing medium.

It should be emphasized that that all calculations are based on steady state equations, however, in real situations more complicated equations describing the models should be solved, this can be done using computerized software like TRNSYS, which is dedicated to simulate thermal processes and develop a deeper insight over the system.

Chapter-6

Economic Analysis and Environmental Impacts

This chapter is dedicated to the economic analysis, where the energy costs will be evaluated, the payback period will be calculated, and other indicators will be presented. The aim is to give the investor a broader perspective about the system size under different CSP LF-11 sizes, upon which the company should decide which size of the system it will adopt.

In addition to the economic analysis, environmental impacts will be evaluated under different scenarios, as one of the major objectives of this thesis.

6.1 Levelized Cost Of Energy LCOE

As the costs of renewable energy differ due to technology types, it was agreed by economists to bring it to a common energy unit “Electricity”, in order to enable investors to select the appropriate options for their investments based on the country and regulations available.

The LCOE is adopted worldwide (IRENA, 2012), to facilitate the consideration of different parameters affecting the technology adoption, such as energy resource, and fuel prices. However, one of the drawbacks of this method that it assumes constant discounted cash flow over the lifetime of the project, wherein the actual cases huge fuel price fluctuations might occur for example as in current times COVID 19. Similarly, interest and inflation rates might change dramatically due to economic crises, in addition to the political situation of the region in general.

The LCOE for a renewable system takes into account the discounted value of the money over the life time of the project, and based on the costs of the system from investment to operation and maintenance to annual useful energy produced. It calculates the costs of useful unit of energy converted to electricity.

The equations used to calculate the LCOE from (Castro, 2016) and (IRENA, 2012) are the same, however, I’m following the equations in (Castro, 2016) as it is more detailed and it was

adopted in a similar work like this thesis. However, it was for Parabolic Trough technology instead of Linear Fresnel as the CSP heat source.

$$LCOE = \frac{I_t * i + d_{om}}{E_{annual}} \quad eq. 6-1$$

Where:

I_t : total investment New Israeli Shekel NIS

i : discount rate factor

d_{om} : Operation and Maintenance costs, usually 2% of total investment (Kalogirou, 2003)

E_{annual} : annual useful energy converted to electric energy kWh.

$$i = \frac{a(1+a)^n}{a(1+a)^n - 1} \quad eq. 6-2$$

And

$$a = (1 + ir_1)(1 + rr_2)(1 + inr_3) - 1 \quad eq. 6-3$$

Where:

a : is discounted rate

ir_1 : is interest rate

rr_2 : risk rate

inr_3 : inflation rate

n : lifetime of the project

The total investment includes the fixed costs and variable costs. Fixed costs are irrelevant of solar field size, such as piping, pumps and heat exchangers. Variable costs are related to solar field cost per square meter and heat storage tank with its insulation, and the HTF volume needed.

As per (IEA-ETSAP and IRENA, 2015) the cost of LF ranges between 1200-1800 \$/kWp, as per email correspondence with the Solar Industries the manufacturer of LF-11, the cost for the 270 kWp system that was calculated in this thesis is from 300-350 k€ (the cost per kW is 1400 \$/kW), this falls within the range of 1200-1800\$/kWp indicated within the surveys of (IEA-ETSAP and IRENA, 2015).

The LCOE of traditionally generated electricity in Palestine is 0.57 NIS/kWh, comparing this value to the LCOE of CSP, this would seem normal, as the initial investment is high of CSP however, the operation and maintenance O&M expenses are relatively small.

In order to relate these costs to the specific area calculations that was adopted from the beginning, based on the average hourly production over the year is 300 w/m² Figure 4-15, it will be assumed that each kW will be produced by 3.3 m². The cost of LF_11 per square meter is 430 \$/m². Tacking a conversion price of 3.5 NIS/\$, then the system cost is 1500 NIS/m².

The Thermal Storage TS size was calculated in chapter 5. The same approach is adopted if we are reducing the storing hours, however the cost will be different. The cost of storage system is taken within the cost of the system priced above; but this storage system is to cover maximum of 4 hours without sun, which is equal to a fraction of 0.4 of daylight hours.

The size of tank will be changed to cover more hours as was assumed in chapter 5; hence the fraction is increased with one-hour increases until 8.8 hours coverage is reached, which stands for the 9 hours daylight and another 8.8 hours working without sun which occurs in winter. Figure 6-1 shows the useful energy that can be harnessed and stored under the case of 975 m² area and tank size factor 1.88, which is 9 hours day light and 8 hours from night.

To take the incremental cost resulting from tank size and insulation and HTF, it will be assumed that the cost will increase in the amount of 2.5% of total investment with 10,000 NIS as starting value of manufacturing

$$VI_t = 0.025 * tank * FI_t + 10000$$

eq. 6-4

Where:

VI_t: variable cost as function of tank size and fixed cost

FI_t: fixed cost related to area of collector and price of 1500 NIS/m²

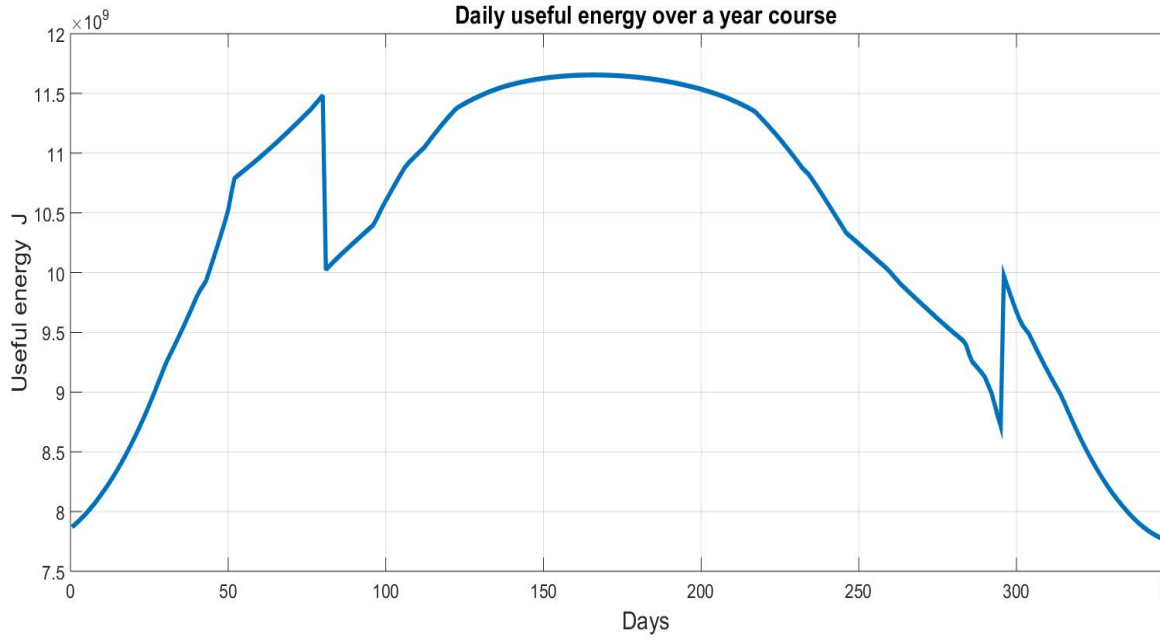


Figure 6-1 Daily useful energy for area 975 m² and tank size 1.88

$$FI_t = Price \left(\frac{NIS}{m^2} \right) * area(m^2)$$

eq. 6-5

Hence the total investment

$$I_t = FI_t + VI_t$$

eq. 6-6

Under the simplified model of the system and economic calculations, several areas and tank sizes were simulated to obtain the lowest LCOE, and the shortest payback period. Another factor is

also being studied which is the solar fraction; which indicates the percentage over the year the energy from sun will replace the conventional one.

In order to make the system consistent with the manufacturer data sheet (INDUSTRIAL SOLAR, 2009), the simulation chosen areas are: 244, 488, 731, 975,1080, 1218 m². The tank sizes factors were simulated as a multiple of accumulative load of the factory above which the CSP will defocus the mirrors, and under it will be the useful energy that can either feed the load or be stored to night shift. Based on the above equations the following variables parameters in Table 6-1 were used in the simulation,

Table 6-1 parameters values used in the eq. 6-1 to eq. 6-6

variable	value	reference
ir1	6.5%	(Palestine Lending interest rate - data, chart TheGlobalEconomy.com, no date)
rr2	-	
inr3	3.2%	(Palestine Inflation Rate 1998-2020 Data 2021-2022 Forecast Calendar Historical, no date)
n	25 years	Assumed
Price	1500 NIS/m ²	Email correspondence date July-2020
E_{annual}	Useful heat amount only	Calculated in simulation
d_{om}	2%	(Kalogirou, 2003)

The flowing Table 6-2, shows the results of simulations for the above scenarios. It can be noticed that the area of the LF-11 have huge effect over the tank size, causing the area 244 m² to be with lowest LCOE. From another technical perspective, the calculations made so far are based on clear sky calculations, shading of collectors was not considered too, this would affect the Solar Fraction S.F percentage, making the choice of first area with lowest cost very risky, hence it will be excluded from next discussions.

Comparing the next two area 488 and 731, it is clear the LCOE and Discounted Payback Period DPBP are slightly different, however, the S.F is 20% higher, and so, for the above same reasons with area 244, area 488 will be excluded from our choices.

Table 6-2 The simulation results for different LF_11 areas and TS sizes, DPBP: Discounted Pay-Back Period, S.F: Solar Fraction

Area m ²	Tank size factor	Total Investment NIS	LCOE NIS	DPBP Years	S.F
244	1.4	3.66E+05	0.165	4.7542	20.72%
	1.5	3.66E+05	0.1647	4.7457	20.76%
	1.6	3.66E+05	0.1643	4.7373	20.80%
	1.7	3.66E+05	0.164	4.7288	20.84%
	1.88	3.66E+05	0.1634	4.7138	20.91%
488	1.4	7.32E+05	0.1687	4.8624	40.50%
	1.5	7.32E+05	0.1684	4.8476	40.63%
	1.6	7.32E+05	0.168	4.8387	40.71%
	1.7	7.32E+05	0.1677	4.8287	40.80%
	1.88	7.32E+05	0.1671	4.8164	40.91%
731	1.4	1.10E+06	0.1736	4.9950	59.03%
	1.5	1.10E+06	0.1706	4.9095	60.08%
	1.6	1.10E+06	0.17	4.8940	60.28%
	1.7	1.10E+06	0.1698	4.8873	60.37%
	1.88	1.10E+06	0.1693	4.8743	60.54%
975	1.4	1.46E+06	0.2121	6.2257	64.50%
	1.5	1.46E+06	0.2012	5.8587	67.99%
	1.6	1.46E+06	0.1919	5.5644	71.29%
	1.7	1.46E+06	0.1836	5.3125	74.40%
	1.88	1.46E+06	0.1732	4.9866	78.90%
1080	1.4	1.62E+06	0.2299	5.8470	65.99%
	1.5	1.62E+06	0.2176	6.4161	69.68%
	1.6	1.62E+06	0.207	6.0466	73.22%
	1.7	1.62E+06	0.1978	5.7526	76.60%
	1.88	1.62E+06	0.1839	5.3161	82.37%
1218	1.4	1.83E+06	0.2537	7.7780	67.40%
	1.5	1.83E+06	0.2396	7.2138	71.41%
	1.6	1.83E+06	0.2274	6.7618	75.22%
	1.7	1.83E+06	0.2168	6.3878	78.89%
	1.88	1.83E+06	0.2007	5.8445	85.15%

Jumping to the last two areas, 1080 and 1218, it can be noticed that solar fraction S.F almost have the same value when changing the tank size factor, however, the initial investment is causing

the LCOE to be above 0.2 NIS/kWh, and the DPBP in the range of five years, and so, the choice of 1218 m² area is excluded also.

Comparing the remaining 3 area choices, 731 and 975 and 1080, it can be noticed that 975 can harness more energy than 731 and almost like the 1080 area. In addition, with big tank size factor; 1.88, the DPBP is near to the 731 area, which makes it the favorable among all choices.

But again, the final judgment in such case is to perform a deeper feasibility study which includes risk analysis. Additional parameters are Net Present Value NPV, and Internal Rate of Return IRR, were help deciding over the lifecycle of the project how much the project can gain from savings. It should be emphasized at this point that Co₂ saving amount is not considered within the potential future income, as there is no policy/ incentive for Co₂ offset is available in Palestine.

Based on the above comparisons and discussion, and from an engineering point of view, it is preferred to select the system with 975m² and tank size 1.88, in order to utilize the maximum possible solar fraction S.F with moderate investment and around 5 years of DPBP. Based on that the system size would be as in Table 6-3.

Table 6-3 Approximate Investment cost for selected system 975m² and tank size factor 1.88, reference to overall system configuration

Item Description	Size	Expected Investment(unit)
Linear Fresnel (Main apparatuses, piping to the tank, pump from Lf-11 to the storage tank)	975 m ²	$1.46 \times 10^6 \text{ NIS}$
Thermal Storage Tank, including tank insulation	$6 \times 1.88 = 12.4 \text{ m}^3$	$0.025 \times 1.88 \times 1.46 \times 10^6 + 10000 = 72156.25 \text{ NIS}$
HTF <i>Therminol 66</i> ⁽¹⁾	50 m ³	$\frac{150\$}{200\text{kg}} \times 3.5 \frac{\text{NIS}}{\$} \times 1002 \frac{\text{kg}}{\text{m}^3} \times 50 \text{ m}^3 = 3.9453 \times 10^4 \text{ NIS}$
Piping 2" Carbon steel Schedule 40 ⁽²⁾	300m	$5.4 \frac{\$}{\text{m}} \times 300 \text{ m} \times 3.5 \frac{\text{NIS}}{\$} = 5670 \text{ NIS}$

Insulation of piping Fiber Glass 25mm ⁽³⁾	70 m ²	$2 \frac{\$}{m^2} \times 3.5 \frac{NIS}{\$} \times 70 m^2$ $= 490 NIS$
High quality API 610 standard petroleum chemical process thermal oil centrifugal pump ⁽⁴⁾	6 pcs	$1500 \frac{\$}{pc} \times 3.5 \frac{NIS}{\$} \times 6 Pcs = 31500 NIS$
Approximate total		$1.46 \times 10^6 + 7.2 \times 10^4 + 3.9 \times 10^4 + 5670$ $+ 490 + 3.15 \times 10^4$ $= 1,608,660 NIS$
Discounted Pay Back Period		4.98 years
Levelized Cost Of Energy LCOE		0.1732 NIS/kWh
Internal Rate of Return IRR		0.1912 ⁽⁵⁾
Net Present Value		5.08×10^6 ⁽⁵⁾

⁽¹⁾(AliBaba.com, 2020c)

⁽²⁾(Global Technology & Engineering, 2020)

⁽³⁾(AliBaba.com, 2020b)

⁽⁴⁾(AliBaba.com, 2020a)

⁽⁵⁾ Calculated using Excel Function NPV, IRR

6.2 Environmental impacts

In this section, the CO₂ emissions are going to be evaluated. Assuming complete combustion in the conventional heating burner. The methodology to be followed is by estimating the amount of heat that is offset by CSP system, and converting this heat amount to the conventional Natural Gas NG used in the burners. Also, taking into account the already existing heat exchanger and burners efficiency.

The calculations are repeated for each CSP area scenario. If there would be incentives against amount of CO₂ offset, then it would be added to the cash flow income to the factory.

The useful heat amount produced by the system for a year course for 975m² and tank size 1.88 as an example is shown in Figure 6-1, the accumulative heat produced over the year is $4.97 \times 10^{12}J$.

Under the assumption of efficiency of 85% for the burner and its heat exchanger (Wu *et al.*, 2012), the amount of heat to be produced by the conventional heating system is $5.13 \times 10^{12}J$. Dividing this energy value by 3.6×10^6 gives the electric energy equivalent of $1.425 \times 10^6 kWh$.

According to (Engineering ToolBox, 2009) the CO₂ emission from burning a fuel is

$$q_{CO_2} = \frac{c_f}{h_f} \times \frac{M_{CO_2}}{M_C} \quad \text{eq. 6-7}$$

Where:

q_{CO_2} = specific CO₂ emission [kg_{CO_2}/kWh]

c_f = specific carbon content in the fuel [kgC/kg_{fuel}]

h_f = specific energy content in the fuel [kWh/kg_{fuel}]

M_C = Molecular weight Carbon [$kg/kmol$ Carbon]

M_{CO_2} = Molecular weight Carbon Dioxide [$kg/kmol$ CO₂]

The values of above variables eq. 6-7 (Engineering ToolBox, 2009) are:

Table 6-4 Variables values used in eq. 6-7

Variable	Value
c_f [kgC/kg_{fuel}]	0.75
h_f [kWh/kg_{fuel}]	15.4
M_{CO_2} [$kg/kmol$ CO₂]	44
M_C [$kg/kmol$ Carbon]	12

Based on the above eq. 6-7 the specific amount of CO₂ emissions is $0.18 \frac{kg_{CO_2}}{kWh}$, since the selected area have an electrical energy value of $1.425 \times 10^6 kWh$, then the amount of avoided CO₂ is

$$\begin{aligned}
 \text{amount of } CO_2 \text{ offset} & \qquad \qquad \qquad \text{eq. 6-8} \\
 & = \text{amount of energy (kWh)} \times q_{CO_2} \left(\frac{kg_{CO_2}}{kWh} \right) \\
 & = 0.18 * 1.425 \times 10^6 = 256,500 kg_{CO_2}
 \end{aligned}$$

If in a voluntary market the price of 1000 kgCO₂ ranges between 0.1\$ - 44.8\$ (Energysage, 2019), on average in 2016 it was 3.3 \$/ton_{CO₂}. Translating this price to our examples means that an amount of $3.3 \times 256 = 844.4$ \$ can be added as positive cash flow to the company.

In USA and Europe, companies are forced to naturalize their CO₂ footprint, either by enhancing their process efficiency or buying a CO₂ offset amounts as per yearly prices regulated by governments. These amounts of money are used in fighting GHG by planting trees or producing power from R.E projects.

Chapter-7

Conclusion and Future Recommendations

The industrial sector in Palestine consumes huge amount of traditional energy, which can be substituted with RE resources, especially the CSP and P.V technologies. Taking advantage from the geographical location of Palestine. Al-Qasrawi for trading and Industries Co. represents one of the leading companies in the food processing section in Palestine. It is noted that it consumes thermal loads from conventional sources. And a great potential for energy saving can be achieved.

The thermal loads at peak time was calculated for the factory production sections. It was evaluated to be $270 \text{ kW}_{\text{p-th}}$. The models were developed using basic thermodynamic laws. Assuming steady state raw material feed rate, the load profile was built.

The CSP technology was selected due to industrial and currently operating projects is Linear Fresnel LF-11, manufactured by Solar Industries. The output heat from LF-11 can satisfy 79% of the load demand over the year.

The winning case after comparison of different LF-11 areas and Thermal Storage sizes is 975 m^2 , tank size 12.4 m^3 . It has the LCOE 0.17 NIS/kWh accompanied with solar fraction of 79% and DPBP of 4.98 years. Also, the IRR is 0.1912 and the NPV is $5.08 \times 10^6 \text{ NIS}$.

The work of this thesis succeeded in developing the models for the thermal loads and the solar plant with the integration between both, however there is still a big room for:

1. Using specialized software to simulate the transient behavior of the system. Additionally, it will enable energy efficiency analysis prior to the RE study.
2. Investigating the control strategy that can be used to manage the loads satisfaction with the available heat from CSP. Moreover, the control strategy can expand the range of utilization of the system by adding offices and space cooling requirements to the plant thermal loads.
3. The HTF replacement with Latent heat material inside the TS, and the impact on the size and economic parameters of the system.
4. Generalization of this study methodology and results over the same industrial sector in Palestine.

References

31°30'23.0"N 35°01'25.4"E - Google Maps (no date). Available at: <https://www.google.com/maps/place/31°30'23.0%22N+35°01'25.4%22E/@31.506399,35.0215453,686m/data=!3m2!1e3!4b1!4m6!3m5!1s0x0:0x0!7e2!8m2!3d31.5063994!4d35.0237336> (Accessed: 6 November 2019).

AEE- INTEC (2019) *Home / Solar Heat for Industrial Processes (SHIP) Plants Database*. Available at: <http://ship-plants.info/> (Accessed: 28 November 2019).

Ajlouni, E. and Alsamamra, H. (2019) 'A Review of Solar Energy Prospects in Palestine', *American Journal of Modern Energy*, 5(3), pp. 49–62. doi: 10.11648/j.ajme.20190503.11.

AliBaba.com (2020a) *High Quality Api 610 Standard Petrochemical Process Thermal Oil Centrifugal Pump*. Available at: https://www.alibaba.com/product-detail/Api-610-Pump-Pumps-Pump-Centrifugal_60805452227.html?spm=a2700.7724857.normalList.1.4c745927DN7Mij&s=p (Accessed: 3 September 2020).

AliBaba.com (2020b) *High Temperature Insulation Fiberglass Wool Plat*. Available at: https://www.alibaba.com/product-detail/25mm-Thick-Insulation-Fiberglass-Fiberglass-Insulation_62067019220.html?spm=a2700.7724857.normalList.2.47bc5e1156gjC1&s=p (Accessed: 3 September 2020).

AliBaba.com (2020c) *Lh 66 Heat Transfer Fluid*. Available at: https://www.alibaba.com/product-detail/LH-66-Heat-Transfer-Fluid_60734307528.html?spm=a2700.7724857.normalList.15.6d7e634aBrxN1x (Accessed: 3 September 2020).

Bank., I. B. for R. and D. T. W. (2016) *WEST BANK & GAZA ENERGY EFFICIENCY ACTION PLAN 2020-2030 Final Report*. Available at: http://www.fmep.org/maps/west-bank/projection-of-israels-west-bank-partition-plan-may-2008/is_v18n3_map_west_bank_partition.gif/image_view_fullscreen.

Bauer, T. *et al.* (2012) 'Thermal Energy Storage Materials and Systems', *Annual Review of Heat Transfer*, 15(15), pp. 131–177. doi: 10.1615/annualrevheattransfer.2012004651.

Belt Type Fruit&vegetable Drying Machine/ Vegetable Dehydrator Supplier (no date). Available at: <https://www.food-machines.org/vegetable-processing-machinery/belt-type-fruit-vegetable-drying-machine.html> (Accessed: 12 May 2020).

Bidwell, C. C. (1940) 'Thermal conductivity of metals', *Physical Review*, 58(6), pp. 561–564. doi: 10.1103/PhysRev.58.561.

Carlos, J. and Santos, O. (no date) 'Specific Heat of Some Vegetable Oils By Differential Scanning Calorimetry and Microwave Oven 1 Introduction 2 Materials and Methods', pp. 610–614.

Castro, A. A. (2016) 'Integration of a concentrating solar thermal system in an expanded cork agglomerate production line November 2016', (November), p. 81.

Çengel, Y. A. and Boles, M. A. (2010) 'Thermodynamics: An Engineering Approach, 7th Edition (Appendix 1: Property Tables and Charts)'. McGraw-Hill Education, pp. 907–956.

countryeconomy.com (2018) *United States (USA) GDP - Gross Domestic Product 2018* / countryeconomy.com. Available at: <https://countryeconomy.com/gdp/palestine> (Accessed: 16 October 2019).

Duffie, J. A. and Beckman, W. A. (2013) *Wiley: Solar Engineering of Thermal Processes, 4th Edition* - John A. Duffie, William A. Beckman. Available at: <http://eu.wiley.com/WileyCDA/WileyTitle/productCd-0470873663.html>.

Eastman Chemical Company (2002) *Heat Transfer Fluids | Official Site | Therminol*. Available at: <https://www.therminol.com/> (Accessed: 27 May 2020).

Energysage (2019) *2019 Pros and Cons of Electric Cars | EnergySage, EnergySage*. Available at: <https://www.energysage.com/other-clean-options/carbon-offsets/costs-and-benefits-carbon-offsets/> (Accessed: 18 July 2020).

Engineering ToolBox (2009) *Combustion of Fuels - Carbon Dioxide Emission, 2009*. Available at: https://www.engineeringtoolbox.com/co2-emission-fuels-d_1085.html (Accessed: 2 June 2020).

Engineers, A. society of agricultural and biological (2008) 'Properties of Grain and Grain Products', *American society of agricultural and biological engineers*, ASAE D243.

Gavhane, K. (2014) *Unit Operations-ii Heat & Mass Transfer*. Nirali Prakashan. Available at: <https://books.google.com.my/books?id=cyKSIfJYfQC> (Accessed: 16 October 2019).

Giovannetti, F. *et al.* (2016) 'IEA SHC Task 49 - Solar Process Heat for Production and Advanced Applications - Comparison of process heat collectors with respect to technical and economic conditions - Deliverable A.2.1'.

Global Solar Atlas (2019). Available at: <https://globalsolaratlas.info/map?c=11.178402,8.525391,3> (Accessed: 28 November 2019).

Global Technology & Engineering (2020) *2" Schedule 40 Carbon Steel Pipe*. Available at: <https://www.globaltecheng.com/ProductCart/pc/2-Schedule-40-Carbon-Steel-Pipe-p4613.htm> (Accessed: 3 September 2020).

GROUP, M. T. W. (2017) 'DESCRIPTION OF BUSINESSES AND SHIP PROJECTS . SOLAR HEAT FOR INDUSTRIAL', p. 70. Available at: http://www.solarconcentra.org/wp-content/uploads/2017/07/Solar-Concentra.GT_.Media_.Temperatura.Situación-Mercado.SHIP_.v1.pdf.

Group, S. (2015) *Soliterm*. Available at: <http://solitermgroup.com/en/content.php?cat=2&content=2> (Accessed: 15 May 2020).

Ben Hassine, I. *et al.* (2014) *IEA SHC Task 49 Solar Process Heat for Production and Advanced Applications Deliverable B2, Integration Guideline*. Available at: <http://task49.iea-shc.org/publications> (Accessed: 16 October 2019).

Hiary, M. Al (2014) *THE POTENTIAL OF SOLAR PROCESS HEAT IN JORDAN*. Kassel University, Kassel, Germany.

Horta, P. (2016) 'Process Heat Collectors: State of the Art and available medium

temperature collectors’, p. 33.

IEA-ETSAP and IRENA (2015) ‘Solar heat for industrial processes -Technology Brief’, (January), p. 37. Available at: www.irena.org/Publications.

IEA SHC // Task Publications (2019). Available at: <https://www.iea-shc.org/publications-tasks> (Accessed: 28 November 2019).

INDUSTRIAL SOLAR, renewables onsite (2009) ‘Technical Data Industrial Solar LF-11 General description’.

Industrial Solar GmbH (2010) *Fresnel Collector - Industrial Solar - Renewables Onsite*. Available at: <https://www.industrial-solar.de/technologies/fresnel-collector/> (Accessed: 15 May 2020).

Intensity, J. M. K. C. D. et al. (2018). E. E.-E. (2018) *Energy intensity - Energy Education*. Available at: https://energyeducation.ca/encyclopedia/Energy_intensity (Accessed: 16 October 2019).

IRENA (2012) *Renewable Energy Cost Analysis - Concentrating Solar Power, IRENA working paper*. doi: 10.1063/1.2993731.

Jazayeri, K., Uysal, S. and Jazayeri, M. (2013) ‘MATLAB/simulink based simulation of solar incidence angle and the sun’s position in the sky with respect to observation points on the Earth’, *Proceedings of 2013 International Conference on Renewable Energy Research and Applications, ICRERA 2013*, (October), pp. 173–177. doi: 10.1109/ICRERA.2013.6749746.

Juaidi, A. et al. (2016) ‘An overview of renewable energy potential in Palestine’, *Renewable and Sustainable Energy Reviews*. Elsevier Ltd, pp. 943–960. doi: 10.1016/j.rser.2016.07.052.

Kalogirou, S. (2003) ‘The potential of solar industrial process heat applications’, *Applied Energy*, 76(4), pp. 337–361. doi: 10.1016/S0306-2619(02)00176-9.

Krummenacher, P. and Muster, B. (2015) ‘Solar process heat for production and advanced applications: Methodologies and software tools for integrating solar heat into industrial processes’, p. 27. Available at: http://task49.iea-shc.org/Data/Sites/1/publications/IEA_Task_49_Deliverable_B1_201502181.pdf.

Lusas, edmond w. and Rooney, L. W. (2001) *snack foods processing*. Technomic Pub. Co.
Market Report Series Renewables 2017, Analysis and forecasts to 2022 (2017). INTERNATIONAL ENERGY AGENCY. Available at: www.iea.org/publications/renewables2017.

Masters, G. M. (2004) *Renewable and Efficient Electric Power Systems, Renewable and Efficient Electric Power Systems*. doi: 10.1002/0471668826.

MATLAB (2015) *R2015a - MATLAB & Simulink*. Available at: <https://www.mathworks.com/help/matlab/release-notes-R2015a.html> (Accessed: 15 May 2020).

Matz, S. A. (1984) ‘Puffed Snacks’, in *Snack Food Technology*. Dordrecht: Springer Netherlands, pp. 150–165. doi: 10.1007/978-94-010-9778-9_13.

McMillan, C. *et al.* (2016) ‘Generation and Use of Thermal Energy in the US Industrial Sector and Opportunities to Reduce its Carbon Emissions’, *Contract*. Joint Institute for Strategic Energy Analysis. Available at: www.nrel.gov/publications.

Moss, R. W. *et al.* (2018) ‘Performance and operational effectiveness of evacuated flat plate solar collectors compared with conventional thermal, PVT and PV panels’, *Applied Energy*. Elsevier, 216(January), pp. 588–601. doi: 10.1016/j.apenergy.2018.01.001.

Mujumdar, A. S. and Hall, C. W. (2006a) *Conveyor Dryers, Handbook of Industrial Drying Foreword to the First Edition*.

Mujumdar, A. S. and Hall, C. W. (2006b) ‘Handbook of Industrial Drying Foreword to the First Edition’, pp. 1–1279.

Muster-Slawitsch, Bettina *et al.* (2015) ‘Solar Integrating Solar Heat into Industrial Processes (SHIP) Booklet on results of Task49/IV Subtask B’. Available at: <http://task49.iea-shc.org/>.

Ouda, D. M. (2001) ‘Prospects of Renewable Energy in Gaza Strip’, in *Net 2001*. Available at: http://site.iugaza.edu.ps/mouda/files/2010/02/NET2001_con_paper.pdf.

Palestine Inflation Rate | 1998-2020 Data | 2021-2022 Forecast | Calendar | Historical (no date). Available at: <https://tradingeconomics.com/palestine/inflation-cpi> (Accessed: 5 July 2020).

Palestine Lending interest rate - data, chart | TheGlobalEconomy.com (no date). Available at: https://www.theglobaleconomy.com/Palestine/lending_interest_rate/ (Accessed: 5 July 2020).

Palestinian Environmental NGOs Network (2016) ‘Pre Master Plan Solar Energy Production in Palestine: Opportunities and Challenges’. Available at: <http://www.pengon.org/uploads/articles/4.pdf>.

PCBS, P. C. B. of Statistics (2017) *Energy Balance of Palestine, 2017*. Available at: http://www.pcbs.gov.ps/Portals/_Rainbow/Documents/EnergyB-2017-1E.html.

PENRA, P. E. and N. R. A. (2012) ‘PROMOTION OF ENERGY EFFICIENCY & RENEWABLE ENERGY IN STRATEGIC SECTORS IN PALESTINE’. Available at: <http://www.penra.pna.ps/ar/Uploads/Files/Bookelt.pdf> (Accessed: 16 October 2019).

PVSyst – Logiciel Photovoltaïque (no date). Available at: <https://www.pvsyst.com/> (Accessed: 15 May 2020).

Santos, J. C. O. (2005) ‘Comparative study of specific heat capacities of some vegetable oils obtained by DSC and microwave oven COMPARATIVE STUDY OF SPECIFIC HEAT CAPACITIES OF SOME VEGETABLE OILS OBTAINED BY DSC AND MICROWAVE OVEN’, (January). doi: 10.1007/s10973-005-0050-x.

Schmitt, B. *et al.* (2015) *Solar IEA SHC Task 49 SolarPACES Annex IV Solar Process Heat for Production and Advanced Applications Potential studies on solar process heat worldwide Deliverable C5*. Available at: <http://task49.iea-shc.org/publications> (Accessed: 16 October 2019).

TRNSYS (2004) ‘Mathematical Reference - Volume 5’, *TRNSYS 16 Documentation*, 5, pp. 1–434.

Union of Concerned Scientists (2017) *Why Does CO2 get more attention than other gases?*, *Union of Concerned Scientists*. Available at: <https://www.ucsusa.org/resources/why-does-co2-get-more-attention-other-gases> (Accessed: 7 January 2021).

Wagner, M. J. (2012) 'WREF 2012: Results and comparison from the SAM linear fresnel technology performance model', *World Renewable Energy Forum, WREF 2012, Including World Renewable Energy Congress XII and Colorado Renewable Energy Society (CRES) Annual Conferen*, 4(April), pp. 2666–2673.

Wu, H. *et al.* (2012) 'Modelling of energy flows in potato crisp frying processes', *Applied Energy*, 89(1), pp. 81–88. doi: 10.1016/j.apenergy.2011.01.008.

Zhang, Y. *et al.* (2006) 'Technology for processing textured starch chips made from potato flour', *Nongye Gongcheng Xuebao/Transactions of the Chinese Society of Agricultural Engineering*, 22(8), pp. 267–269. Available at: https://www.researchgate.net/publication/298185893_Technology_for_processing_textured_starch_chips_made_from_potato_flour (Accessed: 6 May 2020).

Appendix A

LF-11 Data Sheet



Technical Data

Industrial Solar linear Fresnel collector LF-11

The Industrial Solar linear Fresnel collector LF-11 is a linear focussing solar system for generating process heat in the range of 100 kW to 10 MW at pressures up to 120 bar (standard 40 bar) and temperatures up to 400°C. Different heat transfer fluids can be used like pressurized water or thermal oil, but it is also possible to directly generate or even super-heat steam. The Industrial Solar LF-11 includes all necessary components for generating process heat.

The use of high quality safety glass mirrors and optimized row spacing results in a high thermal peak output of 562 W/m² (under reference conditions, see p.3) in terms of primary reflector aperture area, and 375 W/m² in terms of installation area usage.

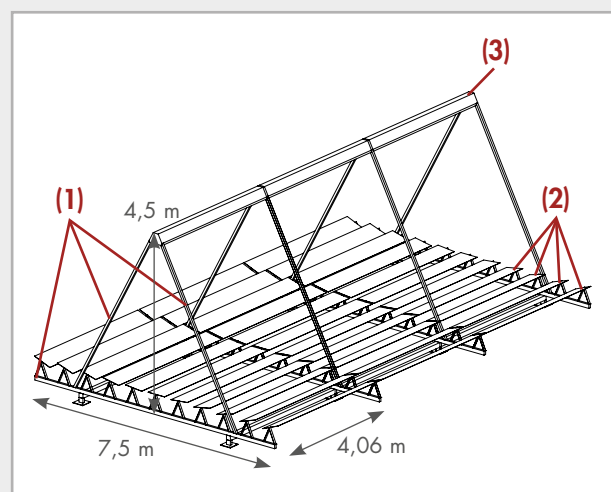
The lightweight, modular system, in combination with the high heat gain per installed area, makes it optimal for rooftop installation for industrial and utility facilities.

Main components of the system are:

- supporting structure ⁽¹⁾
- primary reflectors ⁽²⁾
- receiver, consisting of secondary reflectors and vacuum absorber tubes ⁽³⁾
- control systems for the primary reflector tracking and the solar array output.

Optional components are:

- package for monitoring of the collector performance
- hydraulic circuit designed to meet the customers' needs



Technical Data Industrial Solar LF-11

General description

The LF-11 process heat collector uses individually tracked reflector rows to concentrate direct solar irradiance on a stationary linear receiver.

Advantages are:

- simple power control
- optimized stow positions for various weather conditions, i.e. protection during hail and sand storms
- self-cleaning position in rain
- easy maintenance access to individual rows, thereby allowing continued operation of the plant

The basic module for the Industrial Solar LF-11 consists of 11 primary reflector units with a total mirror surface area of 22 m² and 1 receiver unit (= 1 Schott PTR absorber tube plus secondary mirrors).

The basic modules are combined in a longitudinal direction to form collector rows. These rows can be arranged in parallel to form a solar array of any size, with a maximum packing density (aperture area/ground area) of 67%.

Recommended minimum row length:

- 8 modules, 32.5 m in length

Standard row length:

- 16 modules, 65 m in length

Economically recommended array:

- multiple of 16 modules

Orientation:

- optimal orientation for maximum gain is north-south, but any orientation is possible
- foundation spacing adaptable to existing infrastructure (e.g. roof trusses spacing)

General data of the basic module

Module width	7.5 m
Module length	4.06 m
Aperture surface of primary reflectors	22 m ²
Receiver height above primary reflector	4.0 m
Height of primary reflector above ground level	0.5 m
Recommended minimum clearance between parallel rows	0-0.5 m
Specific weight (related to installation surface area)	27 kg/m ²
Maximum operational wind speed	100 km/h
Maximum wind speed stowed	180 km/h
Life expectancy	+20 years

Thermal performance characteristics

Due to the vacuum absorber, thermal performance is independent of wind speed.

Maximum operating temperature: 400°C

Thermal loss per m² of primary reflector:

$$u_1 = 0.00043 \text{ W}/(\text{m}^2\text{K}^2)$$

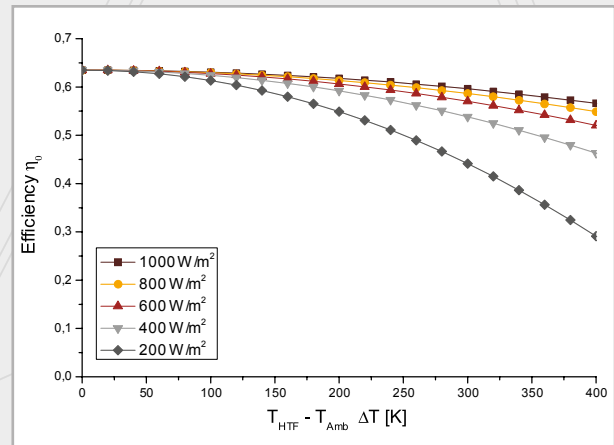
(according to DLR)

Thermal output (under reference conditions*)

12.3 kW per standard module

562 W/m² in terms of aperture surface area of primary reflectors

377 W/m² in terms of total installation surface area



Characteristic collector curve

***reference conditions:**

30°C ambient temperature

160°C inflow temperature

180°C outflow temperature

900 W/m² direct normal radiation

Azimuth angle 90°

Zenith angle 30°

Optical performance characteristics

Angle-independent optical efficiency

(with 100% clean primary and secondary reflectors and receiver glass tube)

$$\eta_0 = 0.635 \text{ (for sun in zenith)}$$

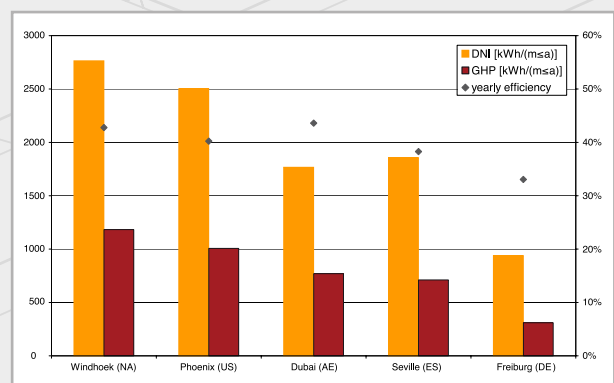
$$\eta_{max} = 0.663 \text{ (for sun at } 5^\circ \text{ transversal zenith angle)}$$

Mirror reflectivity 95%

Schott PTR[®]70 Receiver:

thermal emittance (@380°C): 9%

solar absorptance direct: 95%

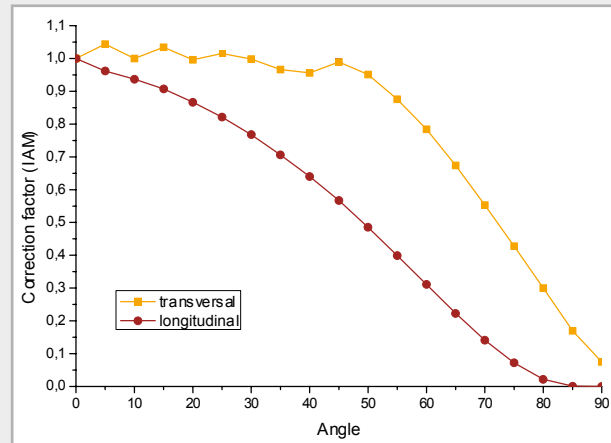


Yearly sum of direct normal irradiance (DNI), gross heat production (GHP) as well as the yearly efficiency for various locations.

Technical Data Industrial Solar LF-1 1

Correction factor (IAM)

Angle	Transversal	Longitudinal
00	1.000	1.000
05	1.044	0.962
10	1.000	0.937
15	1.034	0.907
20	0.996	0.867
25	1.015	0.821
30	0.998	0.768
40	0.956	0.640
50	0.951	0.485
60	0.784	0.311
70	0.553	0.141
80	0.300	0.022
90	0.075	0.000



Correction factor

Control

The individual control of each mirror row allows perfect stow and cleaning positions, integrated maximum temperature protection and shutdown procedures.

A touch-screen with graphical user interface allows comfortable operation and easy monitoring.

Remote control via internet is possible.

External piping and hydraulic system

Stainless steel hydraulic components are recommended, but other steel types are possible, too.

Pressure class PN16 - PN160.

Piping diameter optimised for individual field size requirements.

Electrical

Electrical connection: 220/110 VAC

Electrical peak consumption (16 Modules): < 600 W

Typical electrical consumption:

Touch-screen and switchboard: 200W

Tracking system per 8 Modules: 50 W

Monitoring package

Temperature sensors, 2 per row, PT100

Mass flow measurement

Pressure sensors

Irradiance measurement

Webcam

Appendix B

Therminol 66 Datasheet



THERMINOL® 66

heat transfer fluid

Proven performance
for high-temperature,
low-pressure applications

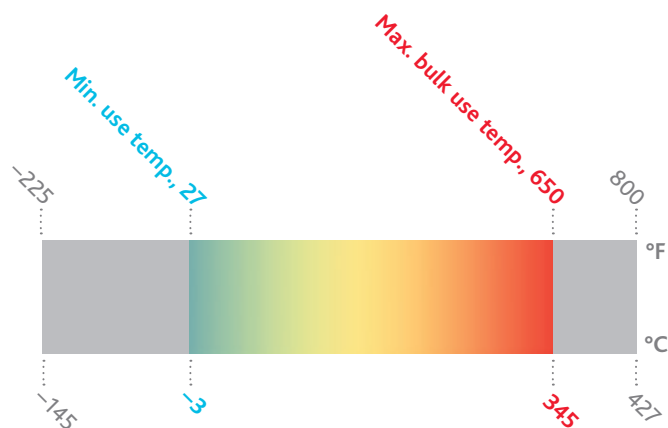
-3° to 345°C
(27° to 650°F)

THERMINOL

Heat Transfer Fluids by Eastman

THERMINOL® 66

heat transfer fluid



Eastman Therminol® 66 heat transfer fluid offers outstanding high-temperature performance to 345°C (650°F), including excellent thermal stability and low vapor pressure. These properties result in reliable, consistent performance of heat transfer systems over long periods of time. Therminol 66 performance is proven through many years of industrial experience under a wide range of operating conditions. No heat transfer fluid material in the world has had more success than Therminol 66.

Therminol 66 is available globally. Contact your local Eastman Therminol sales representative for more information.

Physical and chemical characteristics

Therminol 66 fluid is designed for use in nonpressurized/ low-pressure, indirect heating systems. It delivers efficient, dependable, uniform process heat with no need for high pressures. The high boiling point of Therminol 66 helps reduce the volatility and fluid leakage problems associated with other fluids.

The recommended maximum bulk (345°C/650°F) and film (375°C/705°F) temperatures are based on industry-standard thermal studies. Operation at or below these temperature maximums can provide long service life under most operating conditions.

Actual fluid life is dependent on the total system design and operation and can vary by heat transfer fluid chemistry. As fluid ages, the formation of low- and high-boiling compounds may result. Low-boiling compounds should be vented from the system as necessary to a safe location away from personnel and sources of ignition and in compliance with applicable regulations and laws. The high-boiling compounds can be very soluble in the fluid. Significant overheating or fluid contamination will accelerate decomposition and may result in increased high-boiler and solids concentrations. Excess solids can typically be filtered for removal.

Eastman recommends that systems utilizing Therminol 66 fluid should be blanketed with an atmosphere of inert gas to protect against the effects of fluid oxidation on its performance and life expectancy. Pressure relief device(s) should be installed where required.

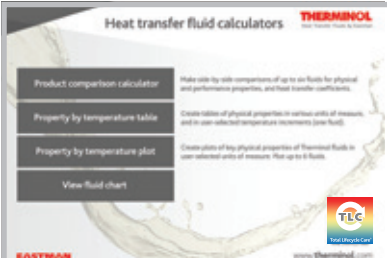
Therminol 66 is noncorrosive to metals commonly used in the construction of heat transfer systems.

While Therminol 66 has a relatively high flash point, it is not classified as a fire-resistant heat transfer fluid. Consequently, the use of protective devices may be required to minimize fire risk, and users of Therminol 66 should check with their safety and risk management experts for specific instructions.

Typical properties^a

Appearance	Clear, pale yellow liquid
Composition	Modified terphenyl
Maximum bulk temperature	345°C (650°F)
Maximum film temperature	375°C (705°F)
Normal boiling point	359°C (678°F)
Pumpability, at 300 mm ² /s (cSt)	11°C (52°F)
Pumpability, at 2000 mm ² /s (cSt)	-3°C (27°F)
Flash point, COC (ASTM D-92)	184°C (363°F)
Flash point, PMCC (ASTM D-93)	170°C (338°F)
Autoignition temperature (ASTM E-659)	374°C (705°F)
Autoignition temperature (DIN 51794)	399°C (750°F)
Pour point (ASTM D-97)	-32°C (-25°F)
Minimum liquid temperatures for fully developed turbulent flow ($N_{Re} > 10,000$)	
10 ft/sec, 1-in. tube (3.048 m/s, 2.54-cm tube)	72°C (162°F)
20 ft/sec, 1-in. tube (6.096 m/s, 2.54-cm tube)	53°C (128°F)
Minimum liquid temperatures for transitional region flow ($N_{Re} > 2000$)	
10 ft/sec, 1-in. tube (3.048 m/s, 2.54-cm tube)	35°C (96°F)
20 ft/sec, 1-in. tube (6.096 m/s, 2.54-cm tube)	26°C (78°F)
Coefficient of thermal expansion at 200°C	0.000819/°C (0.000455/°F)
Total acidity (ASTM D-664)	<0.2 mg KOH/g
Average molecular weight	252
Pseudocritical temperature	569°C (1056°F)
Pseudocritical pressure	24.3 bar (353 psia)
Pseudocritical density	317 kg/m ³ (19.8 lb/ft ³)
Chlorine content, ppm (DIN 51577)	<10 ppm
Copper corrosion (ASTM D-130)	<< 1a
Moisture content, maximum (ASTM E-203)	150 ppm
Dielectric constant @ 23°C (ASTM D-924)	2.61

^aThese data are based on samples tested in the laboratory and are not guaranteed for all samples. Contact us for complete sales specifications for Therminol 66 fluid. Does not constitute an express warranty. See disclaimer on the back page of this bulletin.



To create your own customized table

with preferred properties, units of measure,
and temperature intervals, visit

Therminol.com/resources

and download the Therminol heat transfer fluid calculator.

For technical service, visit the contact page of our website, **Therminol.com**.

Liquid properties of Therminol® 66 heat transfer fluid by temperature^a (SI units)

Temperature		Liquid density	Liquid heat capacity	Heat of vaporization	Liquid enthalpy ^b	Liquid thermal conductivity	Liquid viscosity ^c		Vapor pressure ^d
°C	°F	kg/m ³	kJ/(kg·K)	kJ/kg	kJ/kg	W/(m·K)	cP (mPa·s)	cSt (mm ² /s)	kPa
-3	27	1023	1.49	415.6	22.0	0.1180	2050	2000	—
0	32	1021	1.49	414.3	26.0	0.1183	1320	1300	—
10	50	1015	1.53	409.6	41.2	0.1179	344	339	—
20	68	1008	1.56	405.0	56.6	0.1176	123	122	—
30	86	1002	1.60	400.5	72.4	0.1172	55.6	55.5	—
40	104	995	1.63	396.1	88.5	0.1167	29.5	29.6	—
50	122	989	1.66	391.8	105.0	0.1163	17.6	17.8	—
60	140	982	1.70	387.5	121.8	0.1158	11.5	11.7	—
70	158	975	1.73	383.3	139.0	0.1152	8.06	8.26	0.011
80	176	969	1.77	379.2	156.5	0.1147	5.93	6.12	0.018
90	194	962	1.80	375.1	174.4	0.1141	4.55	4.73	0.030
100	212	955	1.84	371.1	192.6	0.1135	3.60	3.77	0.048
110	230	948	1.87	367.1	211.1	0.1128	2.92	3.08	0.077
120	248	941	1.91	363.2	230.0	0.1121	2.42	2.57	0.119
130	266	934	1.94	359.4	249.3	0.1114	2.05	2.19	0.181
140	284	928	1.98	355.5	268.9	0.1107	1.75	1.89	0.271
150	302	921	2.01	351.7	288.8	0.1099	1.52	1.65	0.400
160	320	914	2.05	347.9	309.1	0.1091	1.33	1.46	0.579
170	338	907	2.09	344.2	329.8	0.1083	1.18	1.30	0.827
180	356	899	2.12	340.4	350.9	0.1074	1.06	1.17	1.17
190	374	892	2.16	336.7	372.3	0.1065	0.950	1.06	1.62
200	392	885	2.19	332.9	394.0	0.1056	0.860	0.972	2.23
210	410	878	2.23	329.1	416.1	0.1046	0.784	0.893	3.02
220	428	870	2.27	325.3	438.6	0.1036	0.718	0.825	4.06
230	446	863	2.30	321.5	461.5	0.1026	0.661	0.766	5.39
240	464	856	2.34	317.7	484.7	0.1015	0.611	0.714	7.10
250	482	848	2.38	313.7	508.3	0.1004	0.567	0.669	9.25
260	500	840	2.42	309.8	532.3	0.0993	0.529	0.629	12.0
270	518	832	2.45	305.8	556.7	0.0982	0.495	0.594	15.3
280	536	825	2.49	301.7	581.4	0.0970	0.464	0.563	19.5
290	554	817	2.53	297.5	606.5	0.0958	0.437	0.535	24.5
300	572	809	2.57	293.2	632.0	0.0946	0.413	0.510	30.7
310	590	800	2.61	288.8	657.9	0.0933	0.391	0.488	38.2
320	608	792	2.65	284.3	684.2	0.0920	0.371	0.468	47.2
330	626	783	2.69	279.7	710.8	0.0906	0.353	0.450	57.9
340	644	775	2.73	274.9	737.9	0.0893	0.336	0.434	70.7
350	662	766	2.77	270.0	765.4	0.0879	0.321	0.420	85.7
360	680	757	2.81	264.9	793.2	0.0865	0.308	0.406	103
370	698	748	2.85	259.6	821.5	0.0850	0.295	0.395	124

^aMaximum recommended bulk temperature 345°C (650°F). These data are based on samples tested in the laboratory and are not guaranteed for all samples. Contact us for complete sales specifications for Therminol 66 fluid. ^bLiquid enthalpy basis is -17.8°C (0°F). ^c1 cSt = 1 mm²/s and 1 mPa·s = 1 cP. ^d100 kPa = 1 bar

Liquid properties of Therminol® 66 heat transfer fluid by temperature^a (English units)

Temperature		Liquid density		Liquid heat capacity	Heat of vaporization	Liquid enthalpy ^b	Liquid thermal conductivity	Liquid viscosity ^c		Vapor pressure ^d
°F	°C	lb/gal	lb/ft ³	Btu/(lb·°F)	Btu/lb	Btu/lb	Btu/(ft·h·°F)	lb/(ft·h)	cSt (mm ² /s)	psia
27	-3	8.54	63.9	0.355	178.8	9.4	0.0684	5020	2000	—
40	4	8.50	63.6	0.361	177.3	14.1	0.0683	1680	681	—
60	16	8.44	63.1	0.370	175.1	21.4	0.0681	456	186	—
80	27	8.38	62.7	0.379	173.0	28.9	0.0678	172	70.8	—
100	38	8.32	62.2	0.388	170.8	36.5	0.0675	81.2	33.7	—
120	49	8.26	61.8	0.397	168.7	44.4	0.0672	44.9	18.8	—
140	60	8.19	61.3	0.406	166.7	52.4	0.0669	27.9	11.7	—
160	71	8.13	60.8	0.415	164.7	60.6	0.0666	18.8	7.97	0.0016
180	82	8.07	60.4	0.424	162.7	69.0	0.0662	13.5	5.76	0.0029
200	93	8.01	59.9	0.434	160.8	77.6	0.0658	10.1	4.37	0.0051
220	104	7.94	59.4	0.443	158.9	86.4	0.0654	7.91	3.44	0.0086
240	116	7.88	59.0	0.452	157.0	95.3	0.0650	6.36	2.78	0.0142
260	127	7.82	58.5	0.462	155.2	104.5	0.0646	5.23	2.31	0.0229
280	138	7.75	58.0	0.471	153.3	113.8	0.0641	4.39	1.95	0.0360
300	149	7.69	57.5	0.480	151.5	123.3	0.0636	3.74	1.68	0.0556
320	160	7.62	57.0	0.490	149.7	133.0	0.0631	3.23	1.46	0.0840
340	171	7.56	56.5	0.499	147.9	142.9	0.0625	2.82	1.29	0.125
360	182	7.49	56.1	0.509	146.1	153.0	0.0620	2.49	1.15	0.182
380	193	7.43	55.6	0.519	144.3	163.3	0.0614	2.22	1.03	0.262
400	204	7.36	55.1	0.528	142.5	173.7	0.0608	2.00	0.935	0.370
420	216	7.29	54.5	0.538	140.7	184.4	0.0602	1.80	0.854	0.517
440	227	7.22	54.0	0.548	138.9	195.2	0.0595	1.64	0.784	0.712
460	238	7.15	53.5	0.558	137.0	206.3	0.0588	1.50	0.725	0.969
480	249	7.08	53.0	0.568	135.2	217.6	0.0581	1.38	0.674	1.30
500	260	7.01	52.5	0.578	133.3	229.0	0.0574	1.28	0.629	1.73
520	271	6.94	51.9	0.588	131.3	240.7	0.0567	1.19	0.591	2.28
540	282	6.87	51.4	0.598	129.4	252.5	0.0559	1.11	0.557	2.97
560	293	6.79	50.8	0.608	127.4	264.6	0.0551	1.04	0.527	3.84
580	304	6.72	50.2	0.618	125.3	276.8	0.0543	0.974	0.500	4.92
600	316	6.64	49.7	0.628	123.2	289.3	0.0535	0.918	0.477	6.24
620	327	6.56	49.1	0.639	121.0	302.0	0.0527	0.867	0.456	7.85
640	338	6.48	48.5	0.649	118.7	314.9	0.0518	0.822	0.438	9.81
660	349	6.40	47.9	0.660	116.4	327.9	0.0509	0.781	0.421	12.2
680	360	6.32	47.3	0.671	113.9	341.3	0.0500	0.744	0.406	15.0
700	371	6.23	46.6	0.682	111.4	354.8	0.0491	0.711	0.393	18.4

TLC Total Lifecycle Care[®]

Eastman's TLC Total Lifecycle Care[®] program is designed to support Therminol customers throughout their systems' life cycle. This comprehensive program includes system design support, start-up assistance, training, sample analysis, flush and refill fluids, and our fluid trade-in program. In North America, call our hotline at 1-800-433-6997 or contact your local sales or technical representative.



In-service heat transfer fluid sample analysis

When Therminol heat transfer fluids are used within suggested temperature limits, they may provide years of trouble-free service. To help users get maximum life, Eastman offers testing of in-service heat transfer fluids to detect contamination, moisture, thermal degradation, and other conditions that may impact system performance. This comprehensive analysis includes acid number, kinematic viscosity, insoluble solids, low boilers, high boilers, and moisture content. Additional special analyses are available on request. Sample analysis includes sample collection kits that are easy to use. Most systems should be sampled annually. Users should also sample anytime a fluid-related problem is suspected.

myTHERMINOL

Results of the test are presented in a detailed report that provides suggestions for corrective action. Test results are stored in a database for future reference. Customers can access their specific test information via my.therminol.com.

Technical service hotline

Experienced technical service specialists can help answer your questions regarding heat transfer fluid selection, system start-ups, system design, and operational issues.

System design support

Eastman regularly assists some of the world's largest engineering, chemical, and equipment manufacturing companies on the design and operation of heat transfer systems. Our liquid phase and vapor phase design guide information and system design data have been field tested in numerous installations. Eastman also conducts engineering seminars for customers, engineering firms, and equipment manufacturers to cover a wide range of heat transfer fluid system design and operation issues. Customers can request a technical service visit to audit heat transfer systems for fluid loss and leak prevention opportunities.

Operational training

Eastman believes that by sharing our experience with customers, we can help improve system design, promote safety, and reduce overall cost. Customers can take advantage of Eastman's heat transfer system operation and product training programs. These programs are customized to suit the varied needs of frontline technicians, operations supervisors, and maintenance technicians to design engineers. Customers can also receive training assistance for dealing with important topics like fluid safety and handling.

Safety awareness training

At Eastman, we're "All in for Safety." We provide our customers safety awareness training that focuses on the design, start-up, operation, and maintenance of heat transfer fluid systems.

Start-up assistance

Eastman provides start-up assistance by reviewing procedures and offering suggestions to reduce typical problems. Customers can also receive help by calling their local Eastman technical specialist or through on-site assistance.

Flush fluid and fluid refill

Liquid phase heat transfer systems can be cleaned with Therminol® FF flushing fluid. After the system is flushed, the appropriate liquid phase Therminol heat transfer fluid can be added.

Fluid trade-in program*

As part of our commitment to sustainability and the environment, Eastman offers a trade-in program for used Therminol and competitive heat transfer fluids. Depending on the fluid and its condition, it may be turned in for potential credit towards the purchase of new Therminol heat transfer fluid.

*Available in North America. Contact your local sales representative for more information.

For more information, visit our website, Therminol.com.

North America
Solutia Inc.
A subsidiary of Eastman Chemical Company
575 Maryville Centre Drive
St. Louis, MO 63141 U.S.A.
Telephone:
Customer Service, 800-426-2463
Technical Service, 800-433-6997

Latin America
Solutia Brasil Ltda.
A subsidiary of Eastman Chemical Company
Rua Alexandre Dumas, 1711—Birmann 12—
7º Andar 04717-004
São Paulo, SP, Brazil
Telephone:
Brazil, 0800 55 9989
Other Locations, +55 11 3579 1800

Europe/Middle East/Africa
Eastman Chemical B.V.
Watermanweg 70
3067 GG Rotterdam
The Netherlands
Telephone: +31 10 2402 111

Asia Pacific
Eastman (Shanghai) Chemical
Commercial Company Ltd.
Building 3, Yaxin Science & Technology Park
Lane 399 Shengxia Road
Pudong New District
201210, Shanghai, P.R. China
Telephone: +86 21 6120 8700

EASTMAN
The results of insight™

Eastman Corporate Headquarters
P.O. Box 431
Kingsport, TN 37662-5280 U.S.A.

U.S.A. and Canada, 800-EASTMAN (800-327-8626)
Other Locations, +(1) 423-229-2000

www.eastman.com/locations

Although the information and recommendations set forth herein are presented in good faith, Eastman Chemical Company ("Eastman") and its subsidiaries make no representations or warranties as to the completeness or accuracy thereof. You must make your own determination of its suitability and completeness for your own use, for the protection of the environment, and for the health and safety of your employees and purchasers of your products. Nothing contained herein is to be construed as a recommendation to use any product, process, equipment, or formulation in conflict with any patent, and we make no representations or warranties, express or implied, that the use thereof will not infringe any patent. NO REPRESENTATIONS OR WARRANTIES, EITHER EXPRESS OR IMPLIED, OF MERCHANTABILITY, FITNESS FOR A PARTICULAR PURPOSE, OR OF ANY OTHER NATURE ARE MADE HEREUNDER WITH RESPECT TO INFORMATION OR THE PRODUCT TO WHICH INFORMATION REFERS AND NOTHING HEREIN WAIVES ANY OF THE SELLER'S CONDITIONS OF SALE.

Safety Data Sheets providing safety precautions that should be observed when handling and storing our products are available online or by request. You should obtain and review available material safety information before handling our products. If any materials mentioned are not our products, appropriate industrial hygiene and other safety precautions recommended by their manufacturers should be observed.

© 2019 Eastman. Eastman brands referenced herein are trademarks of Eastman or one of its subsidiaries or are being used under license. The ® symbol denotes registered trademark status in the U.S.; marks may also be registered internationally. Non-Eastman brands referenced herein are trademarks of their respective owners.